

**РЕДАКЦИОННАЯ КОЛЛЕГИЯ**

**ГЛАВНЫЙ РЕДАКТОР**

*Ватин Н.И.*, д-р техн. наук, проф., РУДН, Москва, Россия

**ЗАМЕСТИТЕЛИ ГЛАВНОГО РЕДАКТОРА**

*Ерофеев В.Т.*, акад. РААСН, д-р техн. наук, проф., МГУ им. Н.П. Огарева, Саранск, Россия

*Колчунов В.И.*, акад. РААСН, д-р техн. наук, проф., НИУ МГСУ, Москва, Россия

**ОТВЕТСТВЕННЫЙ РЕДАКТОР**

*Мамиева И.А.*, РУДН, Москва, Россия

**ЧЛЕНЫ РЕДАКЦИОННОЙ КОЛЛЕГИИ:**

*Агапов В.П.*, д-р техн. наук, проф., НИУ МГСУ, Москва, Россия

*Адилодждаев А.И.*, д-р техн. наук, проф., ТГТУ, Ташкент, Узбекистан

*Андреев В.И.*, акад. РААСН, д-р техн. наук, проф., НИУ МГСУ, Москва, Россия

*Базаров Д.Р.*, д-р техн. наук, проф., ТИИМ, Ташкент, Узбекистан

*Ванин В.В.*, д-р техн. наук, проф., КПИ им. Игоря Сикорского, Киев, Украина

*Варум У.*, д-р философии, проф., Университет Порту, Порту, Португалия

*Войццкий З.*, проф., Вроцлавский научно-технический университет, Вроцлав, Польша

*Волосухин В.А.*, д-р техн. наук, проф., Кубанский ГАУ, Краснодар, Россия

*Галишикова В.В.*, д-р техн. наук, проф., НИУ МГСУ, Москва, Россия

*Дуцев М.В.*, д-р архитектуры, проф., ННГАСУ, Нижний Новгород, Россия

*Евкин А.Ю.*, д-р техн. наук, проф., независимый исследователь, Торонто, Канада

*Какоеи С.*, д-р философии, проф., Технологический университет ПЕТРОНАС, Перак, Малайзия

*Карпенко Н.И.*, акад. РААСН, д-р техн. наук, проф., НИИСФ РААСН, Москва, Россия

*Козлов Д.В.*, д-р техн. наук, проф., НИУ МГСУ, Москва, Россия

*Красич С.*, канд. техн. наук, Нишский университет, Ниш, Сербия

*Кудрявцев С.А.*, чл.-корр. РААСН, д-р техн. наук, проф., ДВГУПС, Хабаровск, Россия

*Курбачкий Е.Н.*, д-р техн. наук, проф., МИИТ, Москва, Россия

*Лазарев Ю.Г.*, д-р техн. наук, проф., СПбПУ, Санкт-Петербург, Россия

*Магул Ф.*, проф., Высшая инженерная школа «Централь Сюпелек», Университет Париж-Сакли, Париж, Франция

*Мендонка П.*, д-р философии, Архитектурная школа, Университет Минью, Брага, Португалия

*Перькова М.В.*, д-р архитектуры, доцент, СПбПУ, Санкт-Петербург, Россия

*Сантос Р.*, исследователь, Национальная лаборатория строительной техники, Лиссабон, Португалия

*Травуш В.И.*, акад. РААСН, д-р техн. наук, проф., ЭНПИ, Москва, Россия

*Федюк Р.С.*, д-р техн. наук, доцент, ДВФУ, Владивосток, Россия

*Якулов Н.М.*, чл.-корр. РИА, д-р техн. наук, проф., ИММ ФИЦ КазНЦ РАН, Казань, Россия

**СОДЕРЖАНИЕ**

**ЧИСЛЕННЫЕ МЕТОДЫ РАСЧЕТА ОБОЛОЧЕК**

*Косицын С.Б., Акулич В.Ю.* Численный анализ НДС ортогонально пересекающихся цилиндрических оболочек, взаимодействующих с основанием, с учетом изменения расчетной модели во времени ..... 303

*Merkulov V.V., Ulyeva G.A., Yepaneshnikova A.A., Volokitina I.E.* Preparation of Polymer Coatings for Protection of Metal Structures from Corrosive Effects (Подготовка полимерных покрытий для защиты металлических конструкций от коррозионного воздействия) ..... 311

**РАСЧЕТ И ПРОЕКТИРОВАНИЕ СТРОИТЕЛЬНЫХ КОНСТРУКЦИЙ**

*Rimshin V.I., Suleymanova L.A., Amelin P.A.* Strength of Normal Sections of Flexural Reinforced Concrete Elements Damaged by Corrosion and Strengthened with External Composite Reinforcement (Прочность нормальных сечений изгибаемых железобетонных элементов, поврежденных коррозией и усиленных внешним композитным армированием) ..... 331

*Морозов Ю.А., Белелобский Б.Ф.* Проектирование тонкостенных деталей одинарной кривизны для использования в облегченных конструкциях ... 342

**СЕЙСМОСТОЙКОСТЬ СООРУЖЕНИЙ**

*Mkrtychev O.V., Mingazova S.R.* Behavior of Reinforced Concrete Buildings with Sliding Belt Seismic Isolation and Elastic Limiter of Horizontal Displacements (Работа железобетонных зданий с сейсмоизолирующим скользящим поясом с упругим ограничителем горизонтальных перемещений) ..... 355

**ТЕОРИЯ ПЛАСТИЧНОСТИ**

*Morozov E.M., Kurbanmagomedov A.K.* Is It Possible to Determine the Whole Crack Path at Once? (Возможно ли определение траектории трещины сразу и в целом?) ..... 364

**ДИНАМИКА КОНСТРУКЦИЙ И СООРУЖЕНИЙ**

*Кбейли Д., Чернов Ю.Т.* Расчет виброизолирующей системы здания с нелинейными характеристиками при кинематическом воздействии (смещении основания) ..... 374

Редактор И.Л. Панкратова  
Редактор англоязычных текстов Е.Ф. Шалеева  
Дизайн обложки Ю.Н. Ефремовой  
Компьютерная верстка Н.В. Маркеловой

**Адрес редакции:**

Российский университет дружбы народов имени Патриса Лумумбы  
Российская Федерация, 117198, Москва, ул. Миклухо-Маклая, д. 6; тел./факс: +7 (495) 955-08-28; e-mail: stmj@rudn.ru, i\_mamieva@mail.ru

Подписано в печать 19.08.2024. Выход в свет 31.08.2024. Формат 60x84/8.

Бумага офсетная. Печать офсетная. Гарнитура «Times New Roman». Усл. печ. л. 10,23 Тираж 250 экз. Заказ № 1075. Цена свободная.

Федеральное государственное автономное образовательное учреждение высшего образования «Российский университет дружбы народов имени Патриса Лумумбы»  
Российская Федерация, 117198, Москва, ул. Миклухо-Маклая, д. 6

Отпечатано в типографии ИПК РУДН  
Российская Федерация, 115419, Москва, ул. Орджоникидзе, д. 3

# STRUCTURAL MECHANICS OF ENGINEERING CONSTRUCTIONS AND BUILDINGS

2024 VOLUME 20 No. 4

DOI: 10.22363/1815-5235-2024-20-4

<http://journals.rudn.ru/structural-mechanics> (Open Access)

Founded in 2005

by Peoples' Friendship University of Russia named after Patrice Lumumba

ISSN 1815-5235 (Print), 2587-8700 (Online)

Published 6 times a year.

Languages: Russian, English.

Indexed by RSCI, Russian Index of Science Citation, Cyberleninka, DOAJ, Google Scholar, Ulrich's Periodicals Directory, WorldCat, Dimensions.

The journal has been included in the list of the leading review journals and editions of the Highest Certification Committee of Ministry of Education and Science of Russian Federation in which the basic results of PhD and Doctoral Theses are to be published.

International scientific-and-technical peer-reviewed journal "Structural Mechanics of Engineering Constructions and Buildings" shows the readers round the achievements of Russian and foreign scientists in the area of geometry of spatial structures, strength of materials, structural mechanics, theory of elasticity and analysis of building and machine-building structures, illumines the problems of scientific-and-technic progress in building and machine-building, publishes analytic reviews on the aims and scope of the journal.

The journal website contains full information about the journal, editorial policy and ethics, requirements for the preparation and publication of the articles, etc., as well as full-text issues of the journal since 2008 (Open Access).

## EDITORIAL BOARD

### EDITOR-IN-CHIEF

*Nikolai I. Vatin*, DSc, Professor, RUDN University, Moscow, Russia

### ASSISTANT EDITORS-IN-CHIEF

*Vladimir T. Erofeev*, member of the RAACS, DSc, Professor, Ogarev Mordovia State University, Saransk, Russia

*Vitaly I. Kolchunov*, member of the RAACS, DSc, Professor, NRU MGSU, Moscow, Russia

### MANAGING EDITOR

*Iraida A. Mamieva*, RUDN University, Moscow, Russia

### MEMBERS OF EDITORIAL BOARD:

*Anvar I. Adylkhodzhaev*, DSc, Professor, TSTU, Tashkent, Uzbekistan

*Vladimir P. Agapov*, DSc, Professor, NRU MGSU, Moscow, Russia

*Vladimir I. Andreev*, chairman, member of the RAACS, DSc, Professor, NRU MGSU, Moscow, Russia

*Dilshod R. Bazarov*, DSc, Professor, TIAME, Tashkent, Uzbekistan

*Mikhail V. Dutsev*, Dr. of Architecture, NNGASU, Nizhny Novgorod, Russia

*Alexander Yu. Evkin*, DSc, Professor, independent scientist, Toronto, Canada

*Roman S. Fedyuk*, DSc, Associate Professor, FEPU, Vladivostok, Russia

*Vera V. Galishnikova*, DSc, Professor, MGSU, Moscow, Russia

*Saeid Kakooei*, PhD, senior lecturer, Universiti Teknologi PETRONAS, Seri Iskandar, Malaysia

*Nikolay I. Karpenko*, member of the RAACS, DSc, Professor, NIISF RAACS, Moscow, Russia

*Dmitriy V. Kozlov*, DSc, Professor, MGSU, Moscow, Russia

*Sonja Krasic*, PhD of Technical Science, University of Nis, Nis, Serbia

*Sergey A. Kudryavtsev*, corresponding member of the RAACS, DSc, Professor, FESTU, Khabarovsk, Russia

*Evgeniy N. Kurbatskiy*, DSc, Professor, MIIT, Moscow, Russia

*Yuriy G. Lazarev*, DSc, Professor, SPbPU, St. Petersburg, Russia

*Fredéric Magoulès*, DSc, Professor, Centrale Supélec, Université Paris-Saclay, Paris, France

*Paulo Mendonca*, Associate Professor, Architecture School, University of Minho, Braga, Portugal

*Margarita V. Perkova*, Dr. of Architecture, SPbPU, St. Petersburg, Russia

*Ricardo Santos*, PhD in Civil Engineering, Laboratório Nacional de Engenharia Civil, Lisbon, Portugal

*Vladimir I. Travush*, member of the RAACS, DSc, Professor, ENPI, Moscow, Russia

*Vladimir V. Vanin*, DSc, Professor, NTUU KPI, Kiev, Ukraine

*Humberto Varum*, Full Professor, University of Porto, Porto, Portugal

*Viktor A. Volosukhin*, DSc, Professor, KubSAU, Krasnodar, Russia

*Zbigniew Wójcicki*, Professor, Wrocław University of Science and Technology, Wrocław, Poland

*Nukh M. Yakupov*, corresponding member of the Russian Academy of Engineering, DSc, Professor, IME of FIC KazanSC of RAS, Russia

## CONTENTS

### NUMERICAL METHODS OF SHELL ANALYSIS

- Kosytsyn S.B., Akulich V.Yu.* Numerical Stress Analysis of Orthogonally Intersecting Cylindrical Shells Interacting with Soil Considering Stages of Construction ..... 303
- Merkulov V.V., Ulyeva G.A., Yepaneshnikova A.A., Volokitina I.E.* Preparation of Polymer Coatings for Protection of Metal Structures from Corrosive Effects ..... 311

### ANALYSIS AND DESIGN OF BUILDING STRUCTURES

- Rimshin V.I., Suleymanova L.A., Amelin P.A.* Strength of Normal Sections of Flexural Reinforced Concrete Elements Damaged by Corrosion and Strengthened with External Composite Reinforcement ..... 331
- Morozov Yu.A., Beleyubskiy B.F.* Design of Thin-Walled Single-Curvature Parts for Use in Lightweight Structures ..... 342

### SEISMIC RESISTENCE

- Mkrtychev O.V., Mingazova S.R.* Behavior of Reinforced Concrete Buildings with Sliding Belt Seismic Isolation and Elastic Limiter of Horizontal Displacements ..... 355

### THEORY OF PLASTICITY

- Morozov E.M., Kurbanmagomedov A.K.* Is It Possible to Determine the Whole Crack Path at Once? ..... 364

### DYNAMICS OF STRUCTURES AND BUILDINGS

- Qbaily J., Chernov Yu.T.* Calculation of a Vibration-Isolated Building System with Non-Linear Characteristics Under Kinematic Action (Base Displacement) ..... 374

Copy Editor I.L. Pankratova

English Texts' Editor E.F. Shaleeva

Graphic Designer Iu.N. Efremova

Layout Designer N.V. Markelova

### Address of the Editorial Board:

Peoples' Friendship University of Russia named after Patrice Lumumba  
6 Miklukho-Maklaya St, Moscow, 117198, Russian Federation; tel./fax: +7 (495) 955-08-28; e-mail: [stmj@rudn.ru](mailto:stmj@rudn.ru), [i\\_mamieva@mail.ru](mailto:i_mamieva@mail.ru)

Printing run 250 copies. Open price

Peoples' Friendship University of Russia named after Patrice Lumumba  
6 Miklukho-Maklaya St, Moscow, 117198, Russian Federation

Printed at Publishing House of RUDN University  
3 Ordzhonikidze St, Moscow, 115419, Russian Federation

## ЧИСЛЕННЫЕ МЕТОДЫ РАСЧЕТА ОБОЛОЧЕК NUMERICAL METHODS OF SHELL ANALYSIS

DOI: 10.22363/1815-5235-2024-20-4-303-310

УДК 69.04

EDN: TVXXYV

Научная статья / Research article

### Численный анализ НДС ортогонально пересекающихся цилиндрических оболочек, взаимодействующих с основанием, с учетом изменения расчетной модели во времени

С.Б. Косицын<sup>id</sup>, В.Ю. Акулич<sup>id</sup>✉

Российский университет транспорта, Москва, Россия

✉ 79859670635@yandex.ru

Поступила в редакцию: 12 апреля 2024 г.

Принята к публикации: 30 июня 2024 г.

**Аннотация.** Объектом исследования являются ортогонально пересекающиеся цилиндрические оболочки и окружающий их грунт. Основная цель расчета состоит в определении напряженно-деформированного состояния цилиндрических оболочек и влияния учета стадий строительства на результаты расчета. Численный анализ выполнен в универсальном программном комплексе ANSYS Mechanical. Узел ортогонально пересекающихся цилиндрических оболочек расположен на глубине 30 м от верхней поверхности основания. Размеры грунтового массива выбраны из условия затухания напряженно-деформированного состояния грунта и приняты по 5 диаметров большой оболочки слева и справа от нее. При решении задачи учтены физическая и контактная нелинейности. Контактная нелинейность обусловлена совместной работой узла ортогонально пересекающихся цилиндрических оболочек с окружающим грунтовым массивом в процессе деформирования системы и при активации элементов оболочек на стадиях расчета. Контакт между телами выполнен с помощью контактных пар. Составлены расчетные случаи с 8, 4, 2 и 1 стадиями возведения тройникового соединения (в каждом случае дополнительно одна стадия (нулевая) отводилась на определение бытового состояния основания) и без учета стадий. По результатам видно, что стадийный расчет дает значительное изменение величин напряжений по Мизесу в тройниковом соединении по сравнению с расчетным случаем без учета стадий. Перспективы дальнейших исследований связаны с применением нелинейных материалов оболочки и различными вариантами контактного взаимодействия оболочки и основания.

**Ключевые слова:** строительная механика, метод конечных элементов, тройниковое соединение, пространственный расчет, стадийный расчет, подземные сооружения, тоннелестроение

**Заявление о конфликте интересов.** Авторы заявляют об отсутствии конфликта интересов.


**Вклад авторов.** Косицын С.Б. — научное руководство; концепция исследования; развитие методологии; итоговые выводы. Акулич В.Ю. — концепция исследования; развитие методологии; реализация численных моделей, написание статьи. Все авторы сделали эквивалентный вклад в подготовку публикации

**Для цитирования:** Косицын С.Б., Акулич В.Ю. Численный анализ НДС ортогонально пересекающихся цилиндрических оболочек, взаимодействующих с основанием, с учетом изменения расчетной модели во времени // Строительная механика инженерных конструкций и сооружений. 2024. Т. 20. № 4. С. 303–310. <http://doi.org/10.22363/1815-5235-2024-20-4-303-310>

Косицын Сергей Борисович, советник Российской академии архитектуры и строительных наук, доктор технических наук, профессор, заведующий кафедрой теоретической механики, Российский университет транспорта, Москва, Россия; eLIBRARY SPIN-код: 9390-7610, ORCID: 0000-0002-3241-0683; e-mail: kositsyn-s@yandex.ru

Акулич Владимир Юрьевич, кандидат технических наук, доцент кафедры теоретической механики, Российский университет транспорта, Москва, Россия; eLIBRARY SPIN-код: 8428-4636, ORCID: 0000-0002-9467-5791; e-mail: 79859670635@yandex.ru

© Косицын С.Б., Акулич В.Ю., 2024

 This work is licensed under a Creative Commons Attribution 4.0 International License  
<https://creativecommons.org/licenses/by-nc/4.0/legalcode>

# Numerical Stress Analysis of Orthogonally Intersecting Cylindrical Shells Interacting with Soil Considering Stages of Construction

Sergey B. Kosytsyn<sup>ID</sup>, Vladimir Yu. Akulich<sup>ID</sup>✉

Russian University of Transport, *Moscow, Russia*

✉ 79859670635@yandex.ru

Received: April 12, 2024

Accepted: June 30, 2024

**Abstract.** The objects of research are orthogonally intersecting cylindrical shells and the surrounding soil. A numerical stress analysis of the shells has been conducted the effect of taking into account the stages of construction has been evaluated. The analysis was performed in ANSYS Mechanical software. The joint of orthogonally intersecting cylindrical shells is located at a depth of 30 m from the ground surface. The dimensions of the soil body are selected from the condition of stress release and are adopted as 5 diameters of the larger shell to the left and to the right of it. The problem takes into account the physical and contact nonlinearities. Contact nonlinearity is associated with the interaction of the joint of the orthogonally intersecting cylindrical shells and the soil body in the process of deformation and as a result of shell element activation at calculation stages. The contact between the bodies is modelled using contact pairs. The cases of 8, 4, 2 and 1 stages of the construction of the T-connection were designed (in each case an additional stage (zeroth) was allocated for determining the initial state of the soil). The case without taking into account the construction stages was also considered. The results showed that the stage analysis leads to significant changes in the values of the von Mises stresses in the T-connection compared to the case without taking into account construction stages. The potential for further research is associated with the use of nonlinear materials for the shell and various alternatives for the contact interaction of the shell and the soil.

**Keywords:** structural mechanics, finite element method, T-connection, three-dimensional analysis, construction stages, underground structures, tunnel construction

**Conflicts of interest.** The authors declare that there is no conflict of interest.

**Authors' contribution.** *Kosytsyn S.B.* — scientific guidance, research concept, development of methodology, final conclusions. *Akulich V.Yu.* — research concept, development of methodology, implementation of numerical models, writing an article. *All authors have made an equivalent contribution to the publication*

**For citation:** Kosytsyn S.B., Akulich V.Yu. Numerical stress analysis of orthogonally intersecting cylindrical shells interacting with soil considering stages of construction. *Structural Mechanics of Engineering Constructions and Buildings*. 2024;20(4):303–310. (In Russ.) <http://doi.org/10.22363/1815-5235-2024-20-4-303-310>

## 1. Введение

Важным направлением развития строительной механики является численное моделирование напряженно-деформированного состояния пространственных систем сложной геометрии, в том числе ортогонально пересекающихся цилиндрических оболочек, взаимодействующих с окружающим основанием [1–3]. Численное моделирование таких систем имеет ряд особенностей, которые необходимо учитывать, а именно контактное взаимодействие между цилиндрической оболочкой и окружающим основанием, а также учет стадийного возведения оболочки. Современные программные комплексы позволяют реализовать учет этих особенностей.

Объектом исследования являются ортогонально пересекающиеся цилиндрические оболочки и окружающий их грунт. Основная цель расчета состоит в определении напряженно-деформированного состояния цилиндрических оболочек и влияния учета стадий строительства на результаты расчета. Разработанная модель ортогонально пересекающихся цилиндрических оболочек, взаимодействующих с окружающим основанием, с учетом перечисленных выше особенностей обеспечива-

*Sergey B. Kosytsyn*, Advisor of the Russian Academy of Architecture and Construction Sciences, Dr. in Tech. Sc., Professor, Head of Department of Theoretical Mechanics, Russian University of Transport, Moscow, Russia; eLIBRARY SPIN-code: 9390-7610, ORCID: 0000-0002-3241-0683; e-mail: kosytsyn-s@yandex.ru

*Vladimir Yu. Akulich*, Candidate of Technical Sciences, Associate professor of Department of Theoretical Mechanics, Russian University of Transport, Moscow, Russia; eLIBRARY SPIN-code: 8428-4636, ORCID: 0000-0002-9467-5791; e-mail: 79859670635@yandex.ru

ет новый, востребованный современной практикой уровень расчетного обоснования подобных систем. Например, при строительстве метрополитена, помимо перегонных тоннелей и станций всегда есть необходимость в притоннельных сооружениях (тоннельных сбойках), которые являются вспомогательными сооружениями, необходимыми для функционирования основных.

Численный анализ выполнен в универсальном программном комплексе ANSYS Mechanical [4–8], который позволяет выполнять расчет статического напряженно-деформированного состояния произвольных пространственных комбинированных конструкций, зданий и сооружений с учетом эффектов физической, геометрической, контактной и генетической (стадийность возведения и нагружения) нелинейностей на основе метода конечных элементов. Библиотека конечных элементов программного комплекса ANSYS содержит более шестидесяти типов элементов для задач статического и динамического анализа. С использованием команд на языке APDL возможности программного комплекса могут быть расширены (например, для решения связанных задач) [9–10].

## 2. Метод расчета

Пространственная расчетная модель состоит из узла ортогонально пересекающихся цилиндрических оболочек (тройникового соединения) и окружающего основания: основная цилиндрическая оболочка диаметром  $D_1 = 5,50$  м и толщиной  $t_1 = 0,25$  м; примыкающая оболочка диаметром  $D_2 = 3,85$  м и толщиной  $t_2 = 0,20$  м. Материал оболочек [11–13] задан идеально упругой моделью со следующими параметрами: модуль упругости  $E_{sh} = 30\,000$  МПа, коэффициент Пуассона  $\mu_{sh} = 0,2$ , плотность  $\rho_{sh} = 2300$  кг/м<sup>3</sup>. Материал основания задан упругопластической моделью Мора — Кулона (O. Mohr, C.A. Coulomb) [14–15] со следующими параметрами: модуль деформации  $E_{soil} = 30$  МПа, коэффициент поперечной деформации  $\mu_{soil} = 0,3$ , плотность  $\rho_{soil} = 2000$  кг/м<sup>3</sup>, сцепление  $C_{soil} = 10$  кПа, угол внутреннего трения  $\varphi_{soil} = 25^\circ$ .

Узел ортогонально пересекающихся цилиндрических оболочек расположен на глубине 30 м от верхней поверхности основания. Размеры грунтового массива выбраны из условия затухания напряженно-деформированного состояния грунта и приняты по 5 диаметров большой оболочки слева и справа от нее. На рис. 1 показан общий вид расчетной модели (рис. 1, а) и вид тройникового соединения (рис. 1, б), которое состоит из четырех частей основной цилиндрической оболочки и четырех частей примыкающей оболочки.

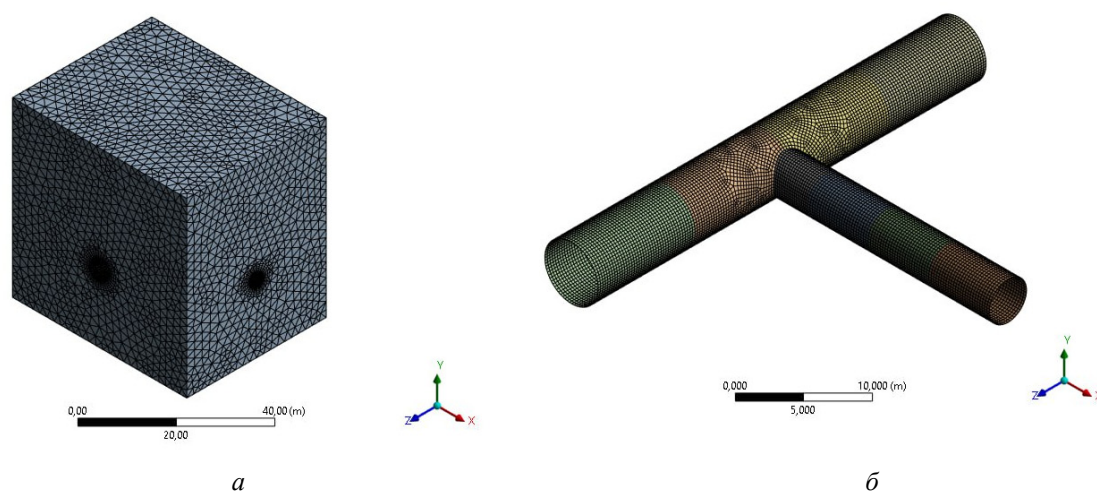


**Рис. 1.** Расчетная модель: а — общий вид; б — вид тройникового соединения  
И с т о ч н и к: выполнено В.Ю. Акуличем в программном комплексе ANSYS Mechanical

**Figure 1.** Finite element model: а — general view; б — T-connection  
S o u r c e: made by V.Yu. Akulich in ANSYS Mechanical software

Нижней и боковым поверхностям грунтового массива и краям тройникового соединения заданы граничные условия, которые обеспечивают геометрическую неизменяемость и корректную работу рассматриваемой системы. К телам приложена нагрузка только от собственного веса.

При решении задачи учтена контактная нелинейность, которая обусловлена совместной работой узла ортогонально пересекающихся цилиндрических оболочек с окружающим грунтовым массивом в процессе деформирования системы и при активации элементов оболочек на стадиях расчета [16–18]. Контакт между телами выполнен с помощью контактных пар, расположенных на внешней стороне тройникового соединения и на массиве основания. Зона контакта до решения задачи неизвестна. В зависимости от нагрузок, свойств материала, граничных условий и других факторов поверхности могут входить в контакт друг с другом и выходить из него. Расчет контактного взаимодействия выполнен с использованием метода штрафов, который реализован в программном комплексе ANSYS Mechanical [19–20]. В данных расчетных моделях возможность отлипания тройникового соединения от окружающего основания учтена, но контактное трение между объектами не рассмотрено.

Составлены расчетные случаи с 8, 4, 2 и 1 стадиями возведения тройникового соединения (в каждом случае дополнительно одна стадия (нулевая) отводилась на определение бытового состояния основания) и без учета стадий. Первой активировалась вся основная цилиндрическая оболочка диаметром  $D_1$  (за 4, 2 и 1 стадии в зависимости от расчетного случая), затем примыкающая оболочка диаметром  $D_2$  (за 4, 2 и 1 стадии в зависимости от расчетного случая).

### 3. Результаты и обсуждение

По результатам расчета проведен сравнительный анализ максимальных эквивалентных напряжений по Мизесу [21–23] в ортогонально пересекающихся цилиндрических оболочках. Кривые изменения напряжений в оболочке в зависимости от количества стадий в расчетном случае показаны на рис. 2. Дополнительно маркером на графике указано максимальное эквивалентное напряжение в тройниковом соединении без учета стадийности возведения.

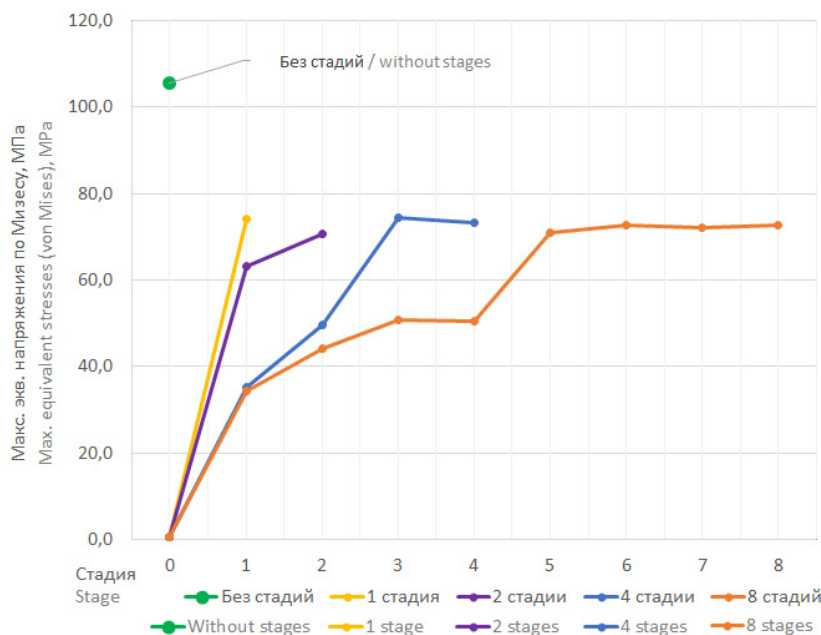


**Рис. 2.** Максимальные эквивалентные напряжения по Мизесу в ортогонально пересекающихся цилиндрических оболочках

И с т о ч н и к: выполнено В.Ю. Акуличем в программном комплексе ANSYS Mechanical  
**Figure 2.** Maximum equivalent stresses (von Mises) in orthogonally intersecting cylindrical shells  
 S o u r c e: made by V.Yu. Akulich in ANSYS Mechanical software

По результатам видно, что стадийный расчет дает значительное изменение величин напряжений по Мизесу в тройниковом соединении по сравнению с расчетным случаем без учета стадий [24–25]. В случае с 8 стадиями возведения максимальные эквивалентные напряжения по Мизесу в оболочке составляют 75,2 МПа, в то время как без учета стадийности максимальные эквивалентные напряжения в оболочке составляют 105,6 МПа.

Напряжения по Мизесу  $\sigma_e$  определяются по формуле

$$\sigma_e = \sqrt{\frac{1}{2} \left[ (\sigma_1 - \sigma_2)^2 + (\sigma_2 - \sigma_3)^2 + (\sigma_3 - \sigma_1)^2 \right]},$$

где  $\sigma_1, \sigma_2, \sigma_3$  — главные напряжения.

Распределение максимальных эквивалентных напряжений по Мизесу в теле цилиндрических оболочек в случае с 8 стадиями возведения показано на рис. 3. Максимальные значения напряжений возникают в месте сопряжения оболочек.

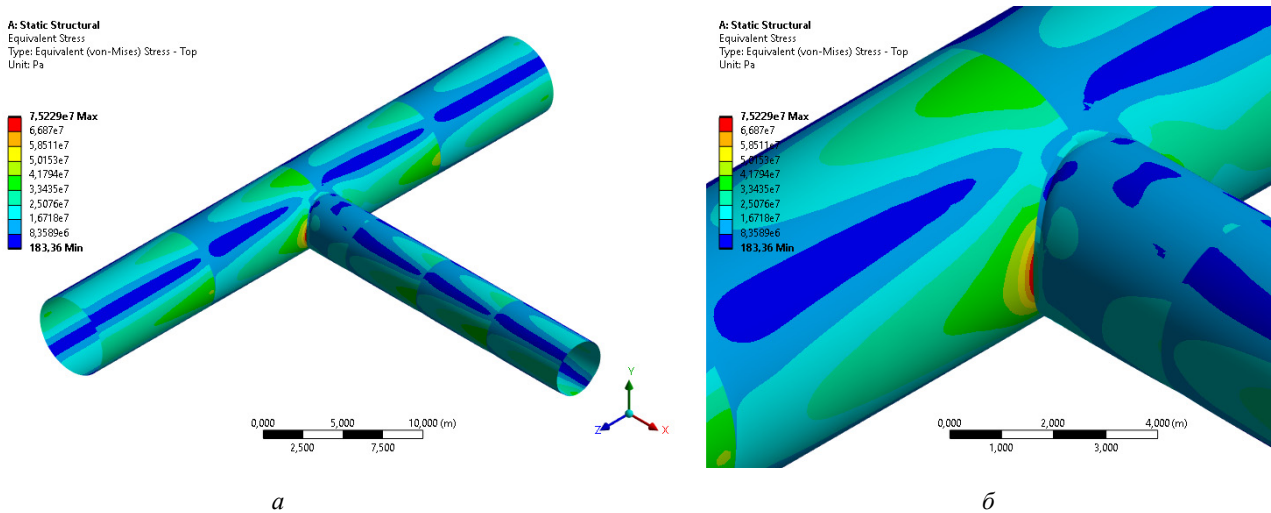


**Рис. 3.** Распределение максимальных эквивалентных напряжений по Мизесу в теле цилиндрических оболочек (справа показан увеличенный вид места сопряжения оболочек)  
И с т о ч н и к: выполнено В.Ю. Акуличем в программном комплексе ANSYS Mechanical

**Figure 3.** Distributions of maximum equivalent stresses (von Mises) in the body of cylindrical shells (the connection of the shells is shown on the right)  
S o u r c e: made by V.Yu. Akulich in ANSYS Mechanical software

В таблице представлены максимальные эквивалентные напряжения по Мизесу в теле тройникового соединения для каждого из 8 расчетных случаев.

**Максимальные эквивалентные напряжения по Мизесу в теле тройникового соединения**

№	Количество стадий возведения	Максимальные эквивалентные напряжения по Мизесу, МПа
1	Без учета стадий	105,6
2	1	78,2
3	2	72,5
4	4	77,4
5	8	75,2

И с т о ч н и к: выполнено В.Ю. Акуличем в программном комплексе ANSYS Mechanical

**Maximum equivalent stresses (von Mises) in a T-connection**

№	Number of stages	Maximum equivalent stresses (von Mises), MPa
1	Disregarding stages	105.6
2	1	78.2
3	2	72.5
4	4	77.4
5	8	75.2

Source: made by V.Yu. Akulich in ANSYS Mechanical software

**4. Заключение**

1. Рассмотрено влияние учета последовательности возведения тройникового соединения на его напряженно-деформированное состояние. В случае с 8 стадиями возведения максимальные эквивалентные напряжения по Мизесу в оболочке составляют 75,2 МПа, в то время как без учета стадийности максимальные эквивалентные напряжения в оболочке составляют 105,6 МПа.

2. Полученные результаты показали, что учет последовательности возведения существенно влияет на напряженно-деформированное состояние ортогонально пересекающихся цилиндрических оболочек и окружающего основания.

3. Перспективы дальнейших исследований связаны с применением нелинейных материалов оболочки и различными вариантами контактного взаимодействия оболочки и основания.

**Список литературы**

1. Белостоцкий А.М., Потапенко А.Л. Реализация и верификация методов субмоделирования и динамического синтеза подконструкций в универсальных и специализированных программных комплексах // Международный журнал по расчету гражданских и строительных конструкций. 2011. Т. 7. № 1. С. 76–84. EDN: PZEWIF
2. Клочков Ю.В., Николаев А.П., Киселева Т.А. Сравнение напряжений, вычисленных на основе скалярной и векторной интерполяций МКЭ в сочлененных оболочках из разнородных материалов // Строительная механика и расчет сооружений. 2013. № 5 (250). С. 70–76. EDN: REACMJ
3. Косицын С.Б., Чан Суан Линь. Численный анализ напряженно-деформированного состояния ортогонально пересекающихся цилиндрических оболочек без учета и с учетом их одностороннего взаимодействия с окружающим массивом грунта // International Journal for Computational Civil and Structural Engineering. 2014. Т. 10. № 1. С. 72–78. EDN: SXXAQJ
4. Бате К., Вилсон Е. Численные методы анализа и метод конечных элементов. М.: Стройиздат, 1982. 446 с. URL: <https://dwg.ru/dnl/4071> (дата обращения: 02.03.2024).
5. Зенкевич О.К. Метод конечных элементов в технике. М.: Мир, 1975. 542 с. URL: <https://djvu.online/file/DtUw9VqXrtZCc> (дата обращения: 02.03.2024).
6. Золотов А.Б., Акимов П.А., Сидоров В.Н., Мозгалева М.Л. Численные и аналитические методы расчета строительных конструкций. М.: Издательство АСВ, 2009. 336 с.
7. Галлагер Р. Метод конечных элементов. Основы. М.: Мир, 1984. 429 с.
8. Трушин С.И. Метод конечных элементов. Теория и задачи. М.: Издательство АСВ, 2008. 256 с.
9. Басов К.А. ANSYS: справочник пользователя. М.: ДМК Пресс, 2005. 640 с.
10. Theory Reference for the Mechanical APDL and Mechanical Applications / ed. by P. Kohnke; ANSYS, Inc. 2009. 1226 p.
11. Зверьяев Е.М. Выделение согласованных уравнений классической теории оболочек из трехмерных уравнений теории упругости // Строительная механика инженерных конструкций и сооружений. 2019. Т. 15. № 2. С. 135–148. <https://doi.org/10.22363/1815-5235-2019-15-2-135-148>
12. Зверьяев Е.М., Макаров Г.И. Итерационный метод построения НДС тонкой оболочки // Строительная механика и расчет сооружений. 2012. № 3 (242). С. 55–60. EDN: OYZEXJ
13. PISAČIĆ K., HORVAT M., BOTAK Z. Finite difference solution of plate bending using Wolfram Mathematica // Tehnički glasnik. 2019. Vol. 13. Issue 3. P. 241–247. <https://doi.org/10.31803/tg-20190328111708>
14. Косицын С.Б., Чан Суан Линь. Сравнительный анализ различных моделей грунтового основания, окружающего цилиндрическую оболочку, с учетом возможности его отлипания от оболочки // International Journal for Computational Civil and Structural Engineering. 2013. Vol. 9. Issue 1. P. 65–71. EDN: PZEXRZ



15. Kosytsyn S.B., Akulich V.Yu. Influence of Stage-By-Stage Construction of a Cylindrical Shell on Stress-Strain States of an Existing Nearby Shell in a Soil Body // *International Journal for Computational Civil and Structural Engineering*. 2022. Vol. 18. Issue 2. P. 112–120. <http://doi.org/10.22337/2587-9618-2022-18-2-112-120>.
16. Rodrigues L., Silva F.M.A., Gonçalves P.B. Effect of geometric imperfections and circumferential symmetry on the internal resonances of cylindrical shells // *International Journal of Non-Linear Mechanics*. 2022. Vol. 139. <http://doi.org/10.1016/j.ijnonlinmec.2021.103875>
17. Перельмутер А.В., Сливкер В.И. Расчетные модели сооружений и возможности их анализа. М.: Склад Софт, 2017. 736 с.
18. Голованов А.И. Моделирование больших упругопластических деформаций оболочек. Теоретические основы конечно-элементных моделей // *Проблемы прочности и пластичности*. 2010. № 72. С. 5–17. EDN: NCVHZV
19. Zhao W., Zhang J., Zhang W., Yuan X. Internal resonance characteristics of hyperelastic thin-walled cylindrical shells composed of Mooney-Rivlin materials // *Thin-Walled Structures*. 2021. Vol. 163. <http://doi.org/10.1016/j.tws.2021.107754>
20. Semenov A.A. Strength and Stability of Geometrically Nonlinear Orthotropic Shell Structures // *Thin-Walled Structures*. 2016. Vol. 106. P. 428–436. <https://doi.org/10.1016/j.tws.2016.05.018>
21. Бочкарев С.А. Исследование собственных колебаний композитных цилиндрических оболочек с жидкостью, лежащих на упругом основании // *Механика композиционных материалов и конструкций*. 2023. Т. 29. № 2. С. 149–166. <http://doi.org/10.33113/mkmk.ras.2023.29.02.01>
22. Баженов В.Г., Казаков Д.А., Кибец А.И., Нагорных Е.В., Самсонова Д.А. Постановка и численное решение задачи потери устойчивости упругопластических оболочек вращения с упругим наполнителем при комбинированных осесимметричных нагрузениях с кручением // *Вестник Пермского национального исследовательского политехнического университета. Механика*. 2022. № 3. С. 95–106. <http://doi.org/10.15593/perm.mech/2022.3.10>
23. Lalin V.V., Dmitriev A.N., Diakov S.F. Nonlinear deformation and stability of geometrically exact elastic arches // *Magazine Of Civil Engineering*. 2019. Issue. 5 (89). P. 39–51. <https://doi.org/10.18720/MCE.89.4>
24. Клочков Ю.В., Николаев А.П., Фомин С.Д., Соболевская Т.А., Андреев А.С. Расчет прочности оболочечных конструкций АПК бункерного типа // *Известия Нижневолжского агроуниверситетского комплекса: Наука и высшее профессиональное образование*. 2019. № 2 (54). С. 285–297. <http://doi.org/10.32786/2071-9485-2019-02-34>.
25. Кривошапко С.Н. Упрощенный критерий оптимальности для оболочек вращения // *Приволжский научный журнал*. 2019. № 4 (52). С. 108–116. EDN: CSTZXH

## References

1. Belostockij A.M., Potapenko A.L. Implementation and verification of methods of submodeling and dynamic synthesis of substructures in universal and specialized software complexes. *International Journal for Computational Civil and Structural Engineering*. 2011;7(1):76–84. (In Russ.) EDN: PZEWIF
2. Klochkov Yu.V., Nikolaev A.P., Kiseleva T.A. Comparison of stresses calculated on the basis of scalar and vector interpolation of FEM in articulated shells of dissimilar materials. *Construction mechanics and calculation of structures*. 2013;5(250):70–76. (In Russ.) EDN: REACMJ
3. Kosytsyn S.B., Chan Suan Lin. Numerical analysis of the stress-strain state of orthogonally intersecting cylindrical shells taking into account and not taking into account their unilateral interaction with the surrounding soil array. *International Journal for Computational Civil and Structural Engineering*. 2014;10(1):72–78. (In Russ.) EDN: SXXAQJ
4. Bate K., Wilson E. *Numerical methods of analysis and the finite element method*. Moscow: Strojizdat Publ.; 1982. (In Russ.) Available from: <https://dwg.ru/dnl/4071> (accessed: 02.03.2024).
5. Zenkevich O.K. *The finite element method in engineering*. Moscow: Mir Publ.; 1975. (In Russ.) Available from: <https://djuv.online/file/DtUw9BqXrtZCc> (accessed: 02.03.2024).
6. Zolotov A.B., Akimov P.A., Sidorov V.N., Mozgaleva M.L. *Numerical and analytical methods for calculating building structures*. Moscow: ACB Publ.; 2009. (In Russ.)
7. Gallager R. *The finite element method. Fundamentals*. Moscow: Mir Publ.; 1984. (In Russ.)
8. Trushin S.I. *Finite element method. Theory and problems*. Moscow: ACB Publ.; 2008. (In Russ.)
9. Basov K.A. *ANSYS: user reference*. Moscow: DMK Press; 2005. (In Russ.)
10. Kohnke P. (ed.). *Theory Reference for the Mechanical APDL and Mechanical Applications*. ANSYS, Inc. 2009.
11. Zverjaev E.M. Separation of the consistent equations of the classical theory of shells from the three-dimensional equations of the theory of elasticity. *Construction mechanics of engineering structures and structures*. 2019;15(2):135–148. (In Russ.) <https://doi.org/10.22363/1815-5235-2019-15-2-135-148>
12. Zverjaev E.M., Makarov G.I. Iterative method of constructing the stress-strain state of a thin shell. *Construction mechanics and calculation of structures*. 2012;3(3):55–60. (In Russ.) EDN: OYZEXJ
13. PISAČIĆ K., HORVAT M., BOTAK Z. Finite difference solution of plate bending using Wolfram Mathematica. *Tehnički glasnik*. 2019;13(3):241–247. <https://doi.org/10.31803/tg-20190328111708>

14. Kosytsyn S.B., Chan Suan Lin. Comparative analysis of various models of the soil surrounding the cylindrical shell, taking into account the possibility of its detachment from the shell. *International Journal for Computational Civil and Structural Engineering*. 2013;9(1):65–71. EDN: PZEXRZ (In Russ.)
15. Kosytsyn S.B., Akulich V.Yu. Influence of Stage-By-Stage Construction of a Cylindrical Shell on Stress-Strain States of an Existing Nearby Shell in a Soil Body. *International Journal for Computational Civil and Structural Engineering*. 2022;18(2):112–120. <http://doi.org/10.22337/2587-9618-2022-18-2-112-120>
16. Rodrigues L., Silva F.M.A., Gonçalves P.B. Effect of geometric imperfections and circumferential symmetry on the internal resonances of cylindrical shells. *International Journal of Non-Linear Mechanics*. 2022;(139):103875. <http://doi.org/10.1016/j.ijnonlinmec.2021.103875>
17. Perel'muter A.V., Slivker V.I. Design models of structures and the possibilities of their analysis. Moscow: Skad Soft Publ.; 2017. (In Russ.)
18. Golovanov A.I. Modeling of large elastic-plastic deformations of shells. Theoretical foundations of finite element models. *Problems of strength and plasticity*. 2010;(72):5–17. (In Russ.) EDN: NCVHZV
19. Zhao W., Zhang J., Zhang W., Yuan X. Internal resonance characteristics of hyperelastic thin-walled cylindrical shells composed of Mooney-Rivlin materials. *Thin-Walled Structures*. 2021;163107754. <http://doi.org/10.1016/j.tws.2021.107754>
20. Semenov A.A. Strength and Stability of Geometrically Nonlinear Orthotropic Shell Structures. *Thin-Walled Structures*. 2016;(106):428–436. <https://doi.org/10.1016/j.tws.2016.05.018>
21. Bochkarev S.A. Investigation of eigenmodes of composite cylindrical shells with liquid lying on an elastic soil. *Mechanics of composite materials and structures*. 2023;29(2):149–166. (In Russ.) <http://doi.org/10.33113/mkmmk.ras.2023.29.02.01>
22. Bazhenov V.G., Kazakov D.A., Kibec A.I., Nagornyh E.V., Samsonova D.A. Formulation and numerical solution of the problem of stability of elastic-plastic rotary shells with an elastic filler under combined axisymmetric torsion loads. *PNRPU Mechanics Bulletin*. 2022;(3):95–106. (In Russ.) <http://doi.org/10.15593/perm.mech/2022.3.10>
23. Lalin V.V., Dmitriev A.N., Diakov S.F. Nonlinear deformation and stability of geometrically exact elastic arches. *Magazine of Civil Engineering*. 2019;(5):39–51. <https://doi.org/10.18720/MCE.89.4>
24. Klochkov Yu.V., Nikolaev A.P., Fomin S.D., Sobolevskaya T.A., Andreev A.S. Strength calculation of shell structures of the bunker type agro-industrial complex. *Izvestia of the Lower Volga Agro-University Complex*. 2019;(2):285–297. (In Russ.) <http://doi.org/10.32786/2071-9485-2019-02-34>
25. Krivoshapko S.N. A simplified criterion of optimality for shells of revolution. *Privolzhsky Scientific Journal*. 2019;(4):108–116. (In Russ.) EDN: CSTZXH

DOI: 10.22363/1815-5235-2024-20-4-311-330

UDC 620.19

EDN: TYJZYZ

Research article / Научная статья

## Preparation of Polymer Coatings for Protection of Metal Structures from Corrosive Effects

Vladimir V. Merkulov<sup>1</sup>, Gulnara A. Ulyeva<sup>1,2</sup>, Anastasia A. Yepaneshnikova<sup>1</sup>, Irina E. Volokitina<sup>1</sup>✉<sup>1</sup> Karaganda Industrial University, Temirtau, Kazakhstan<sup>2</sup> Qarmet JSC, Temirtau, Kazakhstan

✉ irinka.vav@mail.ru

Received: May 16, 2024

Accepted: July 20, 2024

**Abstract.** Copolymers and the methodology for their synthesis are presented. In order to protect metal products and structures from the effects of corrosion processes, various fillers for polymer coating were selected: silicon production waste (microsilica) and titanium dioxide, as well as their combined mixtures. The obtained copolymers exhibit good adhesion required for composite protective coatings. An experiment was conducted to evaluate the corrosion resistance of metals subjected to aggressive environment, as well as to determine the hardness and thickness of the obtained polymer coatings. Thus, the corrosion score of the polymer coating with titanium dioxide filler is 2 in 5% NaCl and 5% KOH aggressive media and is 3–4 in acidic media with 10% KOH. Polymer coating with microsilica filler has a corrosion score of 2 in salt and acid aggressive media, but in alkaline media such coating performed worse and has a corrosion score of 4. The best corrosion resistance values are for the series 2 combination polymer coating consisting of methyl methacrylate, styrene and vinyl butyl ether, with a corrosion score of 2 in salt and acid media and a corrosion score of 4 in alkaline media. Series 1, methyl methacrylate, maleic anhydride, and vinyl butyl ether combined coating has the worst corrosion resistance: corrosion score of 4, 5, 6 in 10% H<sub>2</sub>SO<sub>4</sub> and in an alkaline media (5 and 10% KOH), respectively. At the same time, the developed polymer coatings exhibit satisfactory adhesion properties even after the exposure to aggressive media.

**Keywords:** copolymer synthesis, copolymer, polymer, polymer coating, protective coating, filler, microsilica, titanium dioxide, adhesion

**Conflicts of interest.** The authors declare that there is no conflict of interest.

**Authors' contribution.** Merkulov V.V. — supervision, project administration, conceptualization; Volokitina I.E. — methodology, text writing, reviewing and editing; Ulyeva G.A. — supervision, research; Yepaneshnikova A.E. — data processing, preparation of initial project.

**For citation:** Merkulov V.V., Ulyeva G.A., Yepaneshnikova A.A., Volokitina I.E. Preparation of polymer coatings for protection of metal structures from corrosive effects. *Structural Mechanics of Engineering Constructions and Buildings*. 2024;20(4): 311–330. <http://doi.org/10.22363/1815-5235-2024-20-4-311-330>


*Vladimir V. Merkulov*, Candidate of Chemical Sciences, Associate Professor of the Department of Chemical Technology and Ecology, Karaganda Industrial University, Temirtau, Kazakhstan; ORCID: 0000-0003-0368-3890; e-mail: smart-61@mail.ru

*Gulnara A. Ulyeva*, Candidate of Technical Sciences, Associate Professor, Leading Specialist of the Laboratory of Metallurgy and Flaw Detection of the Center for Analytical Control of Qarmet JSC, Temirtau, Kazakhstan; ORCID: 0000-0002-3600-1318; e-mail: g.ulyeva@mail.ru

*Anastasia A. Yepaneshnikova*, graduate student of the Department of Metallurgy and Materials Science of Karaganda Industrial University, Temirtau, Kazakhstan; ORCID: 0009-0004-8295-1367; e-mail: aae9909@mail.ru

*Irina E. Volokitina*, PhD, Professor of the Department of Metallurgy and Materials Science, Karaganda Industrial University (NPC KIU), Temirtau, Kazakhstan; eLIBRARY SPIN-code: 8965-4704; ORCID: 0000-0002-2190-5672; e-mail: irinka.vav@mail.ru

© Merkulov V.V., Ulyeva G.A., Yepaneshnikova A.A., Volokitina I.E., 2024

 This work is licensed under a Creative Commons Attribution 4.0 International License  
<https://creativecommons.org/licenses/by-nc/4.0/legalcode>

## Подготовка полимерных покрытий для защиты металлических конструкций от коррозионного воздействия

В.В. Меркулов<sup>1</sup>, Г.А. Ульева<sup>1,2</sup>, А.А. Епанешникова<sup>1</sup>, И.Е. Волокитина<sup>1</sup>

<sup>1</sup> Карагандинский индустриальный университет, Темиртау, Республика Казахстан

<sup>2</sup> АО «Qarmet», Темиртау, Республика Казахстан

✉ irinka.vav@mail.ru

Поступила в редакцию: 16 мая 2024 г.

Принята к публикации: 20 июля 2024 г.

**Аннотация.** Представлены сополимеры и разработана методика их синтеза. Для полимерного покрытия были выбраны различные наполнители — отходы производства кремния (микрокремнезем) и диоксид титана, а также их комбинированные смеси с целью защиты металлических изделий и конструкций от воздействия коррозионных процессов. Полученные сополимеры обладают хорошей адгезией, необходимой для создания композитных защитных покрытий. Проведен эксперимент по определению коррозионной стойкости металлов под воздействием агрессивных сред, а также по определению твердости и толщины полученных полимерных покрытий. Таким образом, коэффициент коррозии полимерного покрытия с наполнителем из диоксида титана составляет 2 в агрессивных средах с содержанием 5 % NaCl и 5 % KOH и 3–4 в кислых средах с содержанием 10 % KOH. Полимерное покрытие с микрокремнеземным наполнителем имеет показатель коррозии 2 в солевых и кислотных агрессивных средах, но в щелочных средах такое покрытие работает хуже и имеет показатель коррозии 4. Наилучшие показатели коррозионной стойкости имеют комбинированные полимерные покрытия серии 2, состоящие из метилметакрилата, стирола и винилбутилового эфира, с показателем коррозии 2 в соленой и кислой средах и 4 в щелочной среде. Комбинированное покрытие серии 1, состоящее из метилметакрилата, малеинового ангидрида и винилбутилового эфира, обладает наихудшей коррозионной стойкостью: показатель коррозии составляет 4, 5, 6 10 % H<sub>2</sub>SO<sub>4</sub> и щелочной среде (5 и 10 % KOH) соответственно. В то же время разработанные полимерные покрытия обладают удовлетворительными адгезионными свойствами даже после воздействия агрессивных сред.

**Ключевые слова:** синтез сополимера, сополимер, полимер, полимерное покрытие, защитное покрытие, наполнитель, микрокремнезем, диоксид титана, адгезия

**Заявление о конфликте интересов.** Авторы заявляют об отсутствии конфликта интересов.

**Вклад авторов.** Меркулов В.В. — руководство, администрирование проекта, концептуализация; Волокитина И.Е. — методология, написание, рецензирование и редактирование; Ульева Г.А. — руководство, исследование; Епанешникова А.Е. — обработка данных, подготовка первоначального проекта.

**Для цитирования:** Merkulov V.V., Ulyeva G.A., Yepaneshnikova A.A., Volokitina I.E. Preparation of polymer coatings for protection of metal structures from corrosive effects // *Строительная механика инженерных конструкций и сооружений*. 2024. Т. 20. № 4. С. 311–330. <http://doi.org/10.22363/1815-5235-2024-20-4-311-330>

### 1. Introduction

Concrete and reinforced concrete are the most common building materials, and therefore the problem of increasing the durability of various buildings and structures is particularly relevant. Corrosion protection is one of the most important scientific, environmental, social and economic challenges, since technical progress in many industries is hampered by a number of unresolved problems of corrosion control.

*Меркулов Владимир Витальевич*, кандидат химических наук, доцент кафедры химической технологии и экологии, Карагандинский индустриальный университет, Темиртау, Республика Казахстан; ORCID 0000-0003-0368-3890; e-mail: smart-61@mail.ru

*Ульева Гульнара Анатольевна*, кандидат технических наук, доцент, ведущий специалист лаборатории металловедения и дефектоскопии Центра аналитического контроля АО «Qarmet», Темиртау, Республика Казахстан; ORCID: 0000-0002-3600-1318; e-mail: g.ulyeva@mail.ru

*Епанешникова Анастасия Андреевна*, магистрант кафедры металлургии и материаловедения, Карагандинский индустриальный университет, Темиртау, Республика Казахстан; ORCID: 0009-0004-8295-1367; e-mail: aae9909@mail.ru

*Волокитина Ирина Евгеньевна*, доктор PhD, профессор кафедры металлургии и материаловедения, Карагандинский индустриальный университет, Темиртау, Республика Казахстан; eLIBRARY SPIN-код: 8965-4704, ORCID 0000-0002-2190-5672; e-mail: irinka.vav@mail.ru

The significance of corrosion processes is particularly evident in enterprises that use metal structures, equipment, machinery, tools and transportation with substantial wear and tear during their service life. According to open sources, annual direct global losses from corrosion are estimated at 1.8 trillion dollars.<sup>3</sup>

The importance of corrosion studies is determined by three aspects:

- economic — aims to reduce material losses as a result of corrosion of metallic and non-metallic structures and products;
- improving the equipment reliability, which as a result of corrosion can be destroyed with catastrophic consequences;
- metal stock preservation. The world's metal resources are limited, and metal losses due to corrosion lead to additional energy and water costs. Equally important, the human labor spent on the design and reconstruction of metal structures and equipment affected by corrosion can be directed to other socially useful tasks [1; 2].

This is most relevant in countries with a large metal stock due to the increasing use in the industry (construction, metallurgical, machine-building, etc.) not only of high-strength materials, but also of particularly aggressive media, high temperatures and pressures. Under these conditions, the specific weight of metal losses increased significantly.

Polymer coatings are widely used to protect metals from corrosion. They not only protect the metal from corrosive and other chemical influences, but also give the building structure or metal product excellent electrical insulation, decorative, antiseptic and other properties. Compared to paint and enamel, polymer coatings have a number of advantages. They are more durable, more elastic, better bonded to the metal; in the process of operation, they rub off and crack much less than enamels.

The requirements for polymer coatings are quite serious. First, they must exhibit very high surface adhesion as they bond to the metal base at the molecular level rather than just coating it. Polymer coatings not only protect metals from the effects of aggressive environments, but also increase their wear resistance, reducing the adhesion of various substances to the working surfaces, allow saving non-ferrous metals and other scarce materials [3; 4].

Scientists of many countries are engaged in the problem of corrosion of metal building structures or products, developing polymer coatings with the required complex of properties. Thus, in paper [5] the authors cite the technology of obtaining a composition for protective and decorative coating on a building material, including film-forming component (polyester resin 5.0–20.0% wt.), binding component (polyvinyl acetate emulsion 30.0–60.0% wt.), pigment 5.0–30.0% wt., plasticizer (diethylene glycol 2.0–15.0% wt. and butadiene-styrene copolymer in the form of “Bustilat” glue 5.0–10.0% wt.), polymerization initiator (ammonium persulfate 5.0–15.0% wt.) and water (rest). However, this protective coating is a complex composition including expensive functional additives.

The technology of obtaining the composition for the protection of steel structures and equipment made of carbon steel was developed by the authors of [6]: the obtained anticorrosive polymer coating consists of (part weight h): epoxy-diane resin (100), dibutyl phthalate, (10–20), highly dispersed silicon dioxide (1.5–3) with a specific surface area of 150–400 m<sup>2</sup>/g, acid hardener (30–50), mineral filler (100–550), accelerant, for example, dimethylaniline (0.1–0.5). Phthalic and maleic anhydrides can be used as acid hardener. The composition ensures increased corrosion and wear resistance. The developed protective polymer coating is difficult to prepare, is multi-component and belongs to hot curing coatings, which limits its application.

In papers [7; 8], a composition for anticorrosion coating used in various industrial fields is proposed, including film-forming agent — copolymer of trifluorochloroethylene with vinylidene fluoride F-32L, organic solvent — acetone, butyl acetate, additionally contains pigments — aluminum powder, or titanium dioxide, and/or blue phthalocyanine pigment, and/or yellow iron oxide pigment, and/or red iron oxide pigment, and/or technical carbon, and as an organic solvent additionally contains toluene and ethyl acetate.

<sup>3</sup> Corrosion is one of the main problems in the operation of metal structures (In Russ.). 2015. Available from: <https://1cert.ru/stati/korroziya-odna-iz-osnovnykh-problem-pri-ekspluatatsii-metallicheskikh-konstruktsiy> (accessed: 12.04.2023).

Combination of components in a certain ratio results in coatings with adhesion to steel of 75–810 N/m, impact strength of 12–15 J and drying time of 2.0–2.5 h, while maintaining the values of flexural strength and resistance to vapors of 30% HCl at 90 °C. However, the coating developed by this technology has low adhesion and negligible water resistance.

The authors of papers [9; 10] offer a technology for obtaining protective polymer coatings characterized by a composition based on copolymers, solvent, modifier, filler and hardener containing copolymers of vinyl-n-butyl ether (VBE), methyl methacrylate (MMA), maleic anhydride (MA) and low molecular weight dimethyldihexylbutyndiol as a modifier at the following ratio of components, % pts. wt.: copolymer VBE:MMA:MA 30–70, solvent 10–50, modifier 0.5–1.5, filler 20–60, and having corrosion properties of corrosion-resistant coatings.

A lot of scientific studies are aimed at obtaining composite protective polymer coating using silicon production wastes — microsilica (microsilicas, nanosilicas), as well as with zinc production wastes — zinc ashes [11–19].

The filler for polymer coatings is selected depending on the application. For example, for polymer coating of concrete floors, the composition may include silica sand, corundum and other substances that increase strength and resistance to abrasion. For metal surfaces it is steel, aluminum and other powder, as well as fibers. Products with such fillers are close in strength to the base material. The compositions may also include coloring agents [20].

Therefore, effective measures that can lead to the development of polymer protective coatings of new formulations are needed.

The authors of this article, having made a literature and patent analysis, offer a technology for creating a corrosion-resistant polymer coating, using various fillers (Figure 1).



**Figure 1.** Filler appearance: *a* — microsilica; *b* — titanium oxides  
Source: made by I. Volokitina

The purpose of this study is to develop a technology for obtaining a composition of protective coating based on copolymers with corrosion properties, as well as the possibility of using this coating to protect against the effects of aggressive environments of metal products.

The object of research is the obtained protective polymer coating with the use of various fillers.

The following tasks are set for fulfillment of the specified purpose:

- 1) development of the technology of copolymer production;
- 2) selection of formulation for a new polymer coating for protection of metal structures and products from the effect of aggressive media;
- 3) selection of fillers for making the polymer coating;
- 4) development of complex technology of obtaining protective polymer coating on the basis of copolymers;
- 5) determination of physical and mechanical properties of the obtained corrosion-resistant polymer coating.

In the course of the study, a copolymer based on vinyl butyl ether, styrene and methyl methacrylate was obtained. On the basis of the obtained copolymer, the composition of the protective coating was developed.

## 2. Methods

Methyl methacrylate and vinyl butyl ether were poured into a three-neck flask and maleic anhydride (copolymer 1) was loaded into the flask. 100 g of toluene was loaded after the maleic anhydride was dissolved. The heating temperature of the monomer mixture is about 60 °C. Then 0.2 g of dinitrilazoisobutyric acid polymerization initiator was added. Copolymerization occurs when slowly heated to a temperature of 70–80 °C for 1–2 hours. The reaction mixture was incubated for 24 hours (1 day) to mature the copolymer.

The synthesis of copolymer 2 (methyl methacrylate and vinyl butyl ether) with different ratios of initial components was carried out in a similar manner. The obtained copolymers were blended with fillers in order to change their technological and operational properties in a directed manner.

After preparation of copolymers (Figure 2–4) of different compositions, they were mixed with fillers — microsilica, titanium oxide and jointly titanium oxide and microsilica at the same copolymer to filler ratio of 3:1. During the mixing of the components, a solvation process occurred with vigorous bubbling lasting 15 min followed by a settling process. The drying time is 24 h after applying polymer coatings to the samples.

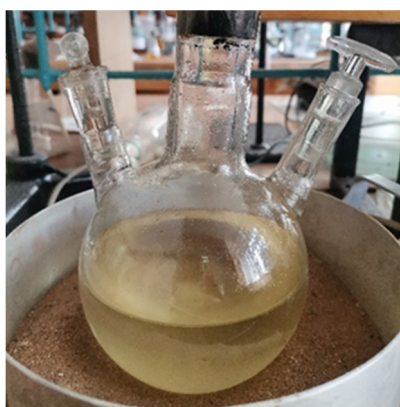


**Figure 2.** Copolymer preparation  
Source: photo by I. Volokitina



**Figure 3.** Finished copolymer materials for coating application  
Source: photo by I. Volokitina



**Figure 4.** Finished polymer coatings for metal samples  
Source: photo by I. Volokitina

Table 1 shows the formulation of the developed protective polymer coatings.

The method used was dip coating, a process in which a substrate is immersed in a liquid and then extracted under controlled environmental conditions, ultimately resulting in a coating.

Determination of hardness, adhesion, thickness of coatings was carried out according to state-approved methods. The microstructure was studied by electron microscopy on a Jeol microscope.

Table 1

Compositions of developed polymer coatings

No. of coverage	Composition			
	Polymers		Filling materials	
	Copolymer 1 MMA:VBE:MA	Copolymer 2 MMA:VBE	SiO <sub>2</sub>	TiO <sub>2</sub>
1	–	+	–	+
2	–	+	+	–
3	–	+	+	+
4	+	–	–	+
5	+	–	+	–
6	+	–	+	+

Note: MMA — methyl methacrylate; VBE — vinyl butyl ether;  
 MA — maleic anhydride; SiO<sub>2</sub> — microsilica powder; TiO<sub>2</sub> — titanium dioxide powder.  
 Source: made by I. Volokitina

### 3. Results and Discussion

The obtained polymer coatings were applied to metal plates (Figures 5–7).



**Figure 5.** Polymer coating with titanium oxide filler  
 Source: photo by A. Yepaneshnikova



**Figure 6.** Polymer coating with microsilica filler  
 Source: photo by A. Yepaneshnikova



**Figure 7.** Combined polymer coating  
 Source: photo by A. Yepaneshnikova

Plates with the studied coating and uncoated plates were placed in different aggressive media in order to determine the behavior of the obtained polymer coatings and to calculate their corrosion resistance. The composition of aggressive media is as follows: H<sub>2</sub>SO<sub>4</sub> acid — 5% and 10%; KOH base — 5% and 10%; NaCl salt — 10%. The plates were incubated in aggressive media for 24 hours (Figure 8).





a



b



c

**Figure 8.** Immersion of metal samples in aggressive media:

a — samples with titanium filler; b — samples with microsilica filler; c — samples with combined polymer coating

S o u r c e: photo by A. Yepaneshnikova

Table 2 describes the behavior of polymer coatings in contact with aggressive media.

According to the results of Table 2, it can be seen that the samples with titanium dioxide filler withstood the test in hydrochloric medium and in 10% KOH medium. Microsilica filled coating showed the best results after exposure to aggressive environments (5% H<sub>2</sub>SO<sub>4</sub>). Samples with combined polymer coating showed very good results when exposed to aggressive media: salt solution and sulfuric acid solutions.

The appearance of samples after exposure to aggressive media is shown in Figure 9.

The rate of corrosion of metals at their uniform destruction is determined by the depth index  $K_g$  (mm/year):

$$K_g = \frac{K_m^- \cdot 8760}{\rho \cdot 1000}, \quad (1)$$

where  $K_m^-$  — corrosion rate, g/(m<sup>2</sup>·h); 8760 — number of hours per year;  $\rho$  — density of metal, kg/cm<sup>3</sup>.

Mass loss per unit surface area  $\Delta m$ , kg/m<sup>2</sup>, is calculated by the formula:

$$\Delta_m = \frac{m_0 - m_1}{S}, \quad (2)$$

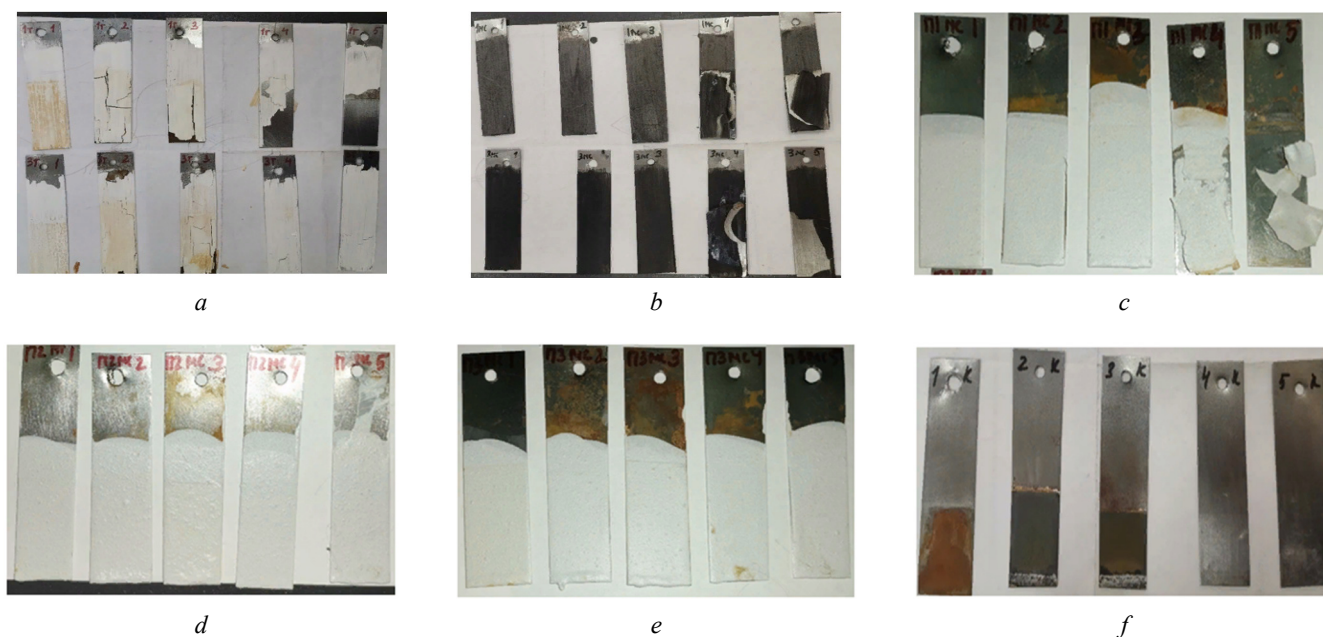
where  $m_0$  — mass of the specimen before testing, kg;  $m_1$  — mass of the sample after testing and removal of corrosion products, kg;  $S$  — surface area of the sample, m<sup>2</sup>.

Table 2

**Description of polymer coating behavior after exposure to aggressive media**

NaCl 1	H <sub>2</sub> SO <sub>4</sub> 5% 2	H <sub>2</sub> SO <sub>4</sub> 10% 3	KOH 5% 4	KOH 10% 5
<b>MMA+VBE+MA+TiO<sub>2</sub> 1TiO<sub>2</sub>1</b>				
Visually, the coating has not lost its integrity, i.e. it has withstood the effects of the aggressive environment. Corrosion products were isolated on the subcoating	Coating cracked on both sides, integrity damaged. Surface cracks are large and deep. In some areas the coating has peeled off. Corrosion products have also separated under the coating	The coating has peeled off completely on one side. Corrosion products are observed underneath the coating. There are also cracks on the surface of the coating	The coating on 2 sides is completely peeled off (loose from the backing), but there are no traces of corrosion products	The coating has peeled off on 2 sides. There are corrosion products under the coating in some areas
<b>VBE+MMA+TiO<sub>2</sub> 3TiO<sub>2</sub>1</b>				
The integrity of the coating is intact. Corrosion products have been released under the coating. Small, fine microcracks are observed on the coating	In some areas the coating has peeled off, but less than on the sample of series 1–2 (1TiO <sub>2</sub> sample No. 2), there are also corrosion products under the coating	The coating has bulged and, after drying, has almost completely peeled off on one side. There are corrosion products in a dense layer under the coating. The coating has a white tint	After exposure to the aggressive media, the weight of the sample increased, i.e. the coating swelled up. The coating has peeled off, but less than sample No. 4 of series 1. There are no traces of corrosion products under the coating. The coating has a white tint	After exposure to the aggressive media, the weight of the sample increased, i.e. the coating swelled up. The coating has peeled off, but less than sample No. 5 of series 1 and sample No. 4 of series 3. There are no traces of corrosion under the coating. The coating has a white tint
<b>MMA+VBE+MA+SiO<sub>2</sub> 1SiO<sub>2</sub>1</b>				
The coating has started to peel at the bottom. The coating itself is rough. There are localized corrosion products under the coating	The coating is rough. The surface has cracked, but the coating has not peeled off, it is tightly adhered to the base. There are no corrosion traces	The coating has peeled off from the base on one side, on the other side the coating is tightly adhered to the base. Roughness is observed	The coating has swollen and peeled off on both sides. The coating is rough	The coating has swollen and peeled off on both sides. The coating is rough
<b>VBE+MMA+SiO<sub>2</sub> 3SiO<sub>2</sub>1</b>				
The coating has preserved its integrity, is tightly adhered, has a uniform structure, and is rough. There are no traces of corrosion under the coating	Although the sample increased in weight after exposure to the aggressive media, the coating itself remained dense and kept its integrity. There are no traces of corrosion under the coating	The coating has preserved its integrity, is tightly adhered, has a uniform structure, and is rough. There are no traces of corrosion under the coating	The coating has swollen and peeled off completely. Corrosion products are observed locally	The coating has swollen and peeled off completely. Corrosion products are observed locally
<b>MMA+VBE+MA+TiO<sub>2</sub>+SiO<sub>2</sub> series 1 combined coating</b>				
The coating has preserved its integrity, is tightly adhered, has a smooth structure, and is rough. There are no traces of corrosion under the coating	The coating has maintained its integrity, adhering tightly to the base, but is beginning to peel off along the edges of the sample. The coating has a uniform rough structure. There are traces of corrosion under the coating	The coating has preserved its integrity, is tightly adhered, and has a uniform rough structure. There are localized corrosion products under the coating	The coating is swollen and cracked after drying, but there are no corrosion products under the coating	The coating has completely peeled off on both sides; there are also no corrosion products under the coating
<b>MMA+VBE+styrene+SiO<sub>2</sub>+TiO<sub>2</sub> series 2 combined coating</b>				
The coating has kept its integrity, is tight, has a smooth structure, and is rough. But under the coating there are traces of corrosion	The coating has maintained its integrity, is tightly adhered, has a uniform structure, and is rough. There are no traces of corrosion under the coating	The coating has maintained its integrity, is tightly adhered, has a uniform structure, and is rough, but locally slightly swollen; there are corrosion products under the coating	The coating has maintained its integrity, is tightly adhered, has a uniform structure, and is rough. There are no traces of corrosion under the coating	The coating has maintained its integrity, is tightly adhered, has a uniform structure, and is rough. Localized signs of corrosion are beginning to appear
<b>VBE+MMA+SiO<sub>2</sub>+TiO<sub>2</sub> series 3 combined coating</b>				
The coating has kept its integrity, is tightly adhered, has a smooth structure, is rough, but under the coating there are corrosion products in a continuous layer	The coating has maintained its integrity, is tightly adhered, has a uniform structure, and is rough. No traces of corrosion are under the coating	The coating has maintained its integrity, is tightly adhered, has a uniform structure, and is rough. There is delamination of the coating on the edges. But under the coating there are local traces of corrosion	The coating has maintained its integrity, is tightly adhered, has a uniform structure, and is rough. There are no corrosion traces under the coating	The coating has maintained its integrity, is tightly adhered, has a uniform structure, and is rough. There are no corrosion traces under the coating
<b>Check sample (uncoated)</b>				
The sample is fully corroded on both sides	Corrosion products are observed on the surface, but corrosion of the sample metal itself has not occurred	Both corrosion products and salt residues are observed on the surface. Corrosion products lie on the metal surface in a dense layer on both sides	There are no traces of corrosion, only roughness appeared in some areas after exposure to aggressive media	There are no traces of corrosion, only roughness appeared in some areas after exposure to aggressive media

Source: made by I. Volokitina



**Figure 9.** Appearance of samples after exposure to aggressive media:  
*a* — coating with titanium filler (series 1); *b* — coating with titanium filler (series 2);  
*c* — coating with microsilica filler (series 1); *d* — coating with microsilica filler (series 2);  
*e* — combined polymer coating (series 1, series 2, series 3); *f* — metal samples without coating  
 Source: photo by A. Yepaneshnikova

Table 3 shows the weight of coated samples before and after exposure to aggressive media and corrosion score according to Interstate standard GOST 9.908–85<sup>2</sup>.

Table 3

**Results of determination of corrosion weight score of polymer coatings with fillers (microsilica and titanium oxide)**

Parameter	Coating 1TiO <sub>2</sub>	Coating 3TiO <sub>2</sub>	Coating 1SiO <sub>2</sub>	Coating 3SiO <sub>2</sub>
<b>5% NaCl</b>				
<i>m</i> <sub>0</sub> , g	12.43	11.92	11.78	12.19
<i>m</i> <sub>к</sub> , g	12.45	11.88	11.81	12.16
<i>V</i> , g/m <sup>2</sup> *h	0.00083	0.00167	0.00125	0.00125
<i>C</i> <sub>м</sub> <sup>-</sup>	0.001	0.0019	0.0014	0.0014
<i>R</i> , %	quite resistant / 2	quite resistant / 2	quite resistant / 2	quite resistant / 2
$\Delta m$ , %	0.16	0.34	0.25	0.25
<b>5% H<sub>2</sub>SO<sub>4</sub></b>				
<i>m</i> <sub>0</sub> , g	11.94	11.60	11.11	11.56
<i>m</i> <sub>к</sub> , g	11.56	11.24	11.14	11.60
<i>V</i> , g/m <sup>2</sup> *h	0.0158	0.0150	0.00125	0.00167
<i>C</i> <sub>м</sub> <sup>-</sup>	0.0178	0.0169	0.0014	0.0019
<i>R</i> , %	resistant / 4	resistant / 4	quite resistant / 2	quite resistant / 2
$\Delta m$ , %	3.18	3.10	0.27	0.35

<sup>2</sup> GOST 9.908–85. Unified system of corrosion and ageing protection. Metals and alloys. Methods for determination of corrosion and corrosion resistance indices. 1989. (In Russ.)

Ending of the Table 3

Parameter	Coating 1TiO <sub>2</sub>	Coating 3TiO <sub>2</sub>	Coating 1SiO <sub>2</sub>	Coating 3SiO <sub>2</sub>
<b>10% H<sub>2</sub>SO<sub>4</sub></b>				
$m_o, g$	11.90	11.86	13.02	15.76
$m_k, g$	11.72	11.68	13.06	15.73
$V, g/m^2 \cdot h$	0.0750	0.0750	0.00167	0.00125
$C_m^-$	0.0084	0.0084	0.0019	0.0014
$R, \%$	quite resistant / 3	quite resistant / 3	quite resistant / 2	quite resistant / 2
$\Delta m, \%$	1.51	1.52	0.31	0.19
<b>5% KOH</b>				
$m_o, g$	11.33	11.45	11.89	12.14
$m_k, g$	11.42	11.49	12.30	11.10
$V, g/m^2 \cdot h$	0.0038	0.00167	0.01708	0.04333
$C_m^-$	0.0042	0.0019	0.0192	0.0487
$R, \%$	quite resistant / 2	quite resistant / 2	resistant / 4	resistant / 4
$\Delta m, \%$	0.79	0.35	3.45	8.57
<b>10% KOH</b>				
$m_o, g$	12.50	12.15	12.08	16.37
$m_k, g$	12.17	12.63	12.67	15.39
$V, g/m^2 \cdot h$	0.0138	0.0200	0.0246	0.0408
$C_m^-$	0.0154	0.0225	0.0276	0.0459
$R, \%$	resistant / 4	resistant / 4	resistant / 4	resistant / 4
$\Delta m, \%$	2.64	3.95	4.88	6.00

Source: made by I. Volokitina

The results of Table 3 show that the introduction of maleic anhydride into the composition of polymer coating significantly increases corrosion processes, i.e. decreases their corrosion resistance. Effect of aggressive media: the series samples with TiO<sub>2</sub> filler withstood the effect of aggressive media better in hydrochloric and alkaline solutions, and the series samples with SiO<sub>2</sub> filler can perform well, on the contrary, in acidic media.

Table 4 shows the weight of samples with combined polymer coating before and after exposure to aggressive media and the corrosion score.

The results of Table 4 show that the combined polymer coating of series 2 performed well in hydrochloric and acidic solutions, worse in alkaline solutions. This is probably due to the presence of styrene in the composition of the combined coating, which has good resistance to aggressive media. Series 1 combined polymer coating has good resistance to salt solution and 5% H<sub>2</sub>SO<sub>4</sub> solution. Series 3 combined polymer coating has average values of corrosion resistance in all presented aggressive media (score not higher than 4). The combined polymer coating with microsilica filler performed the worst in aggressive media; it has the highest corrosion rate, weight loss and corrosion scores.

Figure 10 shows a comparative plot of the change in corrosion rate of polymer coatings after exposure to aggressive media.

Figure 11 shows a comparative analysis of the weight change of the polymer coatings after exposure to aggressive media, and Figure 12 shows the score of the polymer coatings.

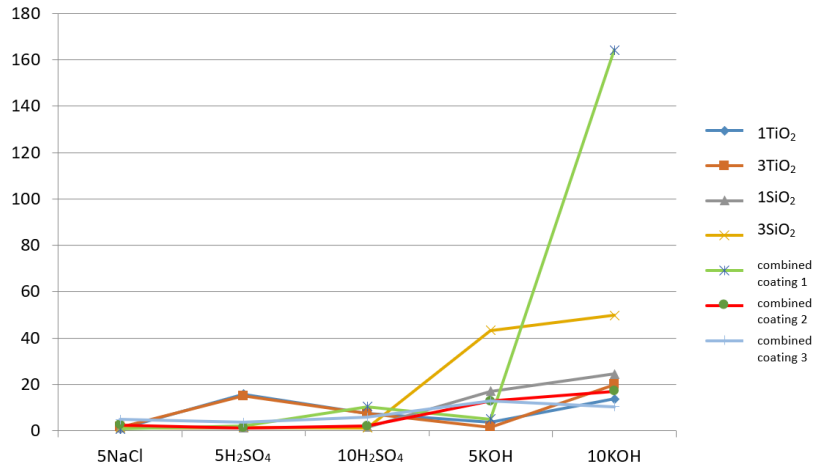
Figures 10–12 show that the combined polymer coating with microsilica filler performed the worst in aggressive media; it has the highest corrosion rate, mass loss and corrosion score.

Table 4

## Results of determining the corrosion weight score of the combined polymer coating

Parameter	1Methyl methacrylate + Maleic anhydride + Vinyl butyl ether +TiO <sub>2</sub> (titanium oxide) + SiO <sub>2</sub> (microsilica) series 1	2Methyl methacrylate + Vinyl butyl ether + styrene + TiO <sub>2</sub> (titanium oxide) + SiO <sub>2</sub> (microsilica) series 2	3Methyl methacrylate + Vinyl butyl ether + TiO <sub>2</sub> (titanium oxide) + SiO <sub>2</sub> (microsilica) series 3
<b>5% NaCl</b>			
$m_o, g$	12.87	12.53	16.78
$m_k, g$	12.85	12.47	16.66
$V, g/m^2 \cdot h$	0.0008	0.0250	0.0050
$C_m^-$	0.001	0.0028	0.0056
$R, \%$	quite resistant / 2	quite resistant / 2	quite resistant / 3
$\Delta m, \%$	0.16	0.48	0.71
<b>5% H<sub>2</sub>SO<sub>4</sub></b>			
$m_o, g$	12.68	12.98	12.52
$m_k, g$	12.63	12.95	12.43
$V, g/m^2 \cdot h$	0.0021	0.0013	0.0038
$C_m^-$	0.0023	0.0014	0.0042
$R, \%$	quite resistant / 2	quite resistant / 2	quite resistant / 2
$\Delta m, \%$	0.39	0.23	0.72
<b>10% H<sub>2</sub>SO<sub>4</sub></b>			
$m_o, g$	17.11	17.26	16.95
$m_k, g$	16.86	17.21	17.09
$V, g/m^2 \cdot h$	0.0104	0.0021	0.0058
$C_m^-$	0.0117	0.0023	0.0066
$R, \%$	resistant / 4	quite resistant / 2	quite resistant / 3
$\Delta m, \%$	1.46	0.29	0.83
<b>5% KOH</b>			
$m_o, g$	11.65	12.42	12.55
$m_k, g$	12.87	12.73	12.86
$V, g/m^2 \cdot h$	0.0508	0.0129	0.0129
$C_m^-$	0.0571	0.0145	0.0145
$R, \%$	resistant / 5	resistant / 4	resistant / 4
$\Delta m, \%$	10.47	2.50	2.47
<b>10% KOH</b>			
$m_o, g$	16.53	13.61	12.34
$m_k, g$	12.59	13.20	12.59
$V, g/m^2 \cdot h$	0.1642	0.0171	0.0104
$C_m^-$	0.1844	0.0192	0.0117
$R, \%$	low-resistant / 6	resistant / 4	resistant / 4
$\Delta m, \%$	23.84	3.01	0.36

Source: made by A. Yepaneshnikova



**Figure 10.** Graph of change in corrosion rate of polymer coatings after exposure to aggressive media  
 Source: made by G. Ulyeva

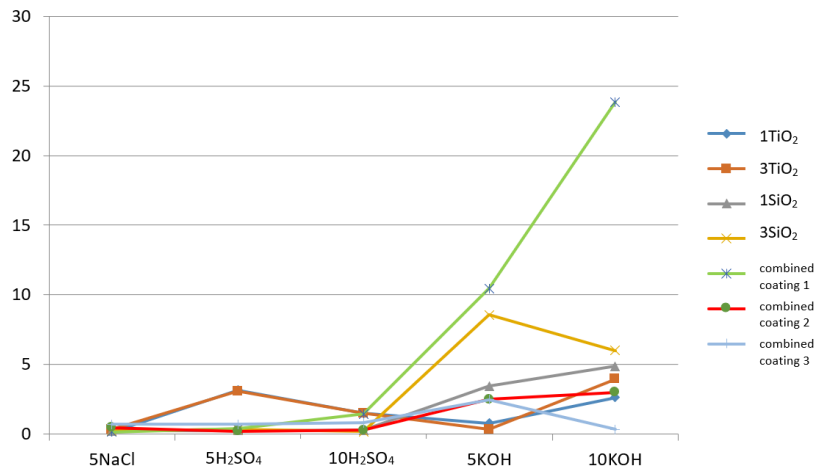


**Figure 11.** Graph of change in weight of polymer coatings after exposure to aggressive media  
 Source: made by G. Ulyeva

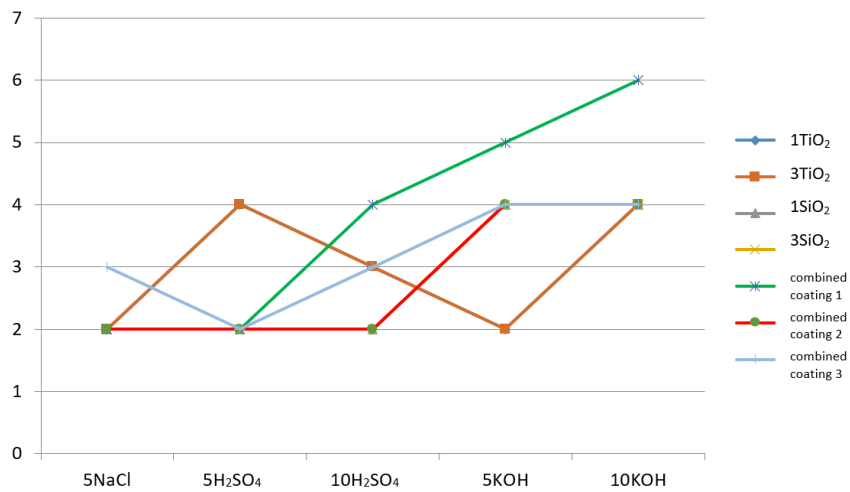


**Figure 12.** Score of polymer coatings  
 Source: made by G. Ulyeva

The photo shows microstructures of polymer coatings (Figure 13–19) obtained from the scanning electron microscope “Zeiss” in laboratory of metal science and defectoscopy of the Analytical Control Center of “Qarmet” JSC.

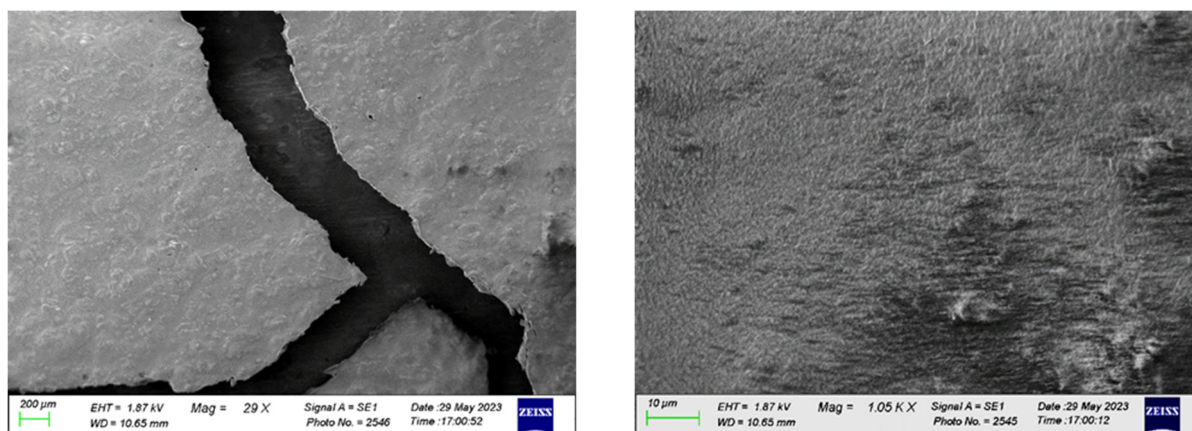


Figure 13. 1SiO<sub>2</sub> polymer coating after exposure to aggressive media  
Source: made by G. Ulyeva

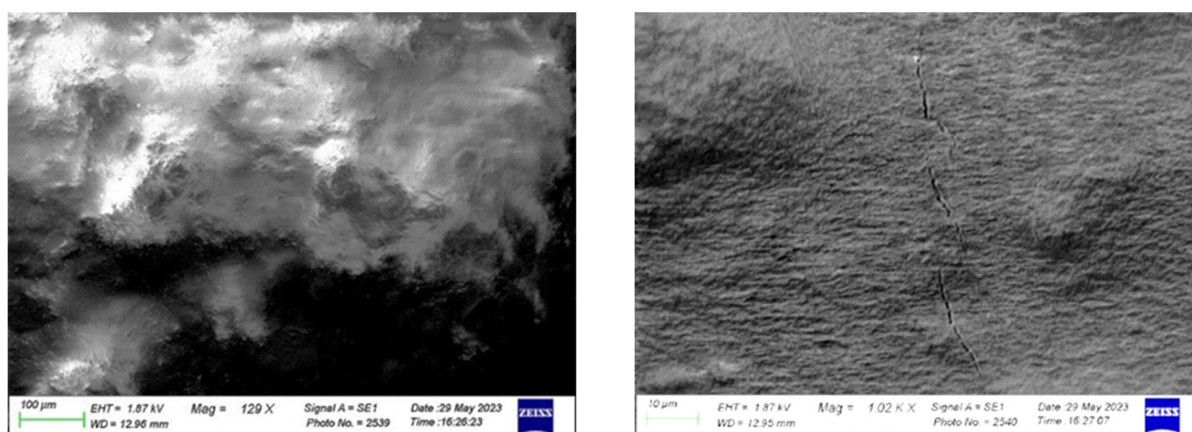


Figure 14. 3SiO<sub>2</sub> polymer coating after exposure to aggressive media  
Source: made by G. Ulyeva

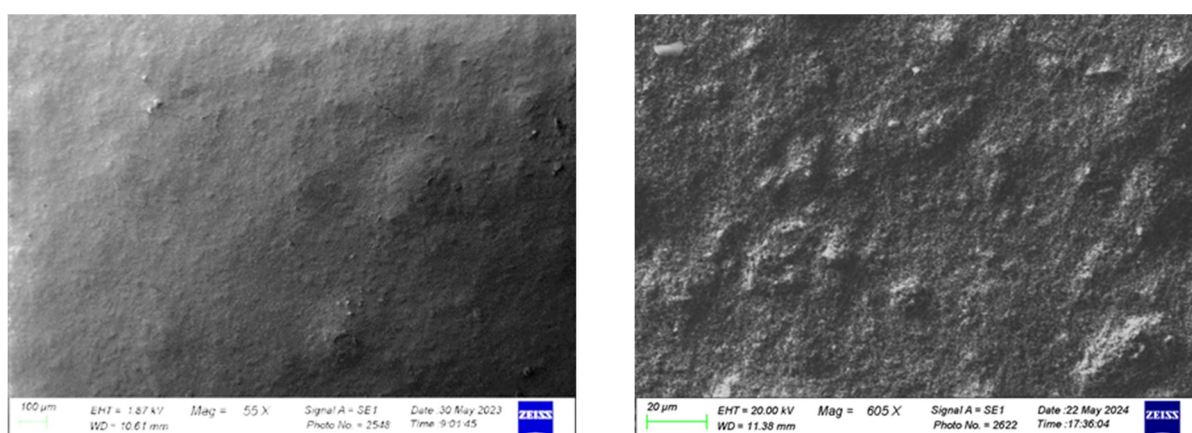
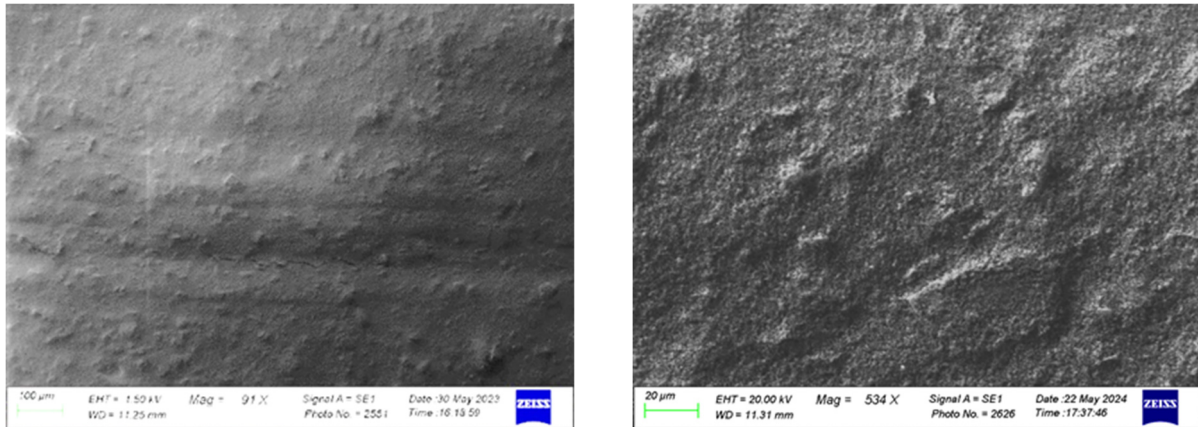


Figure 15. 1TiO<sub>2</sub> polymer coating after exposure to aggressive media  
Source: made by G. Ulyeva



**Figure 16.** 3TiO<sub>2</sub> polymer coating after exposure to aggressive media  
S o u r c e: made by G. Ulyeva

Figure 13 shows that the 1SiO<sub>2</sub> polymer coating has a uniform homogeneous structure after exposure to the aggressive media. The 3SiO<sub>2</sub> polymer coating after exposure to aggressive media is also uniform and homogeneous, but local microcracks are observed at high magnification (Figure 14). 1TiO<sub>2</sub> polymer coating has a similar structure after exposure to aggressive media (Figure 15). In polymer coating 3TiO<sub>2</sub> after exposure to aggressive media microcracks are observed in some places already at low magnification, the coating itself has a uniform homogeneous structure (Figure 16).

Combined polymer coating of series 1 after exposure to aggressive media has a uniform homogeneous structure, microcracks are also observed in some areas at low magnifications (Figure 17).

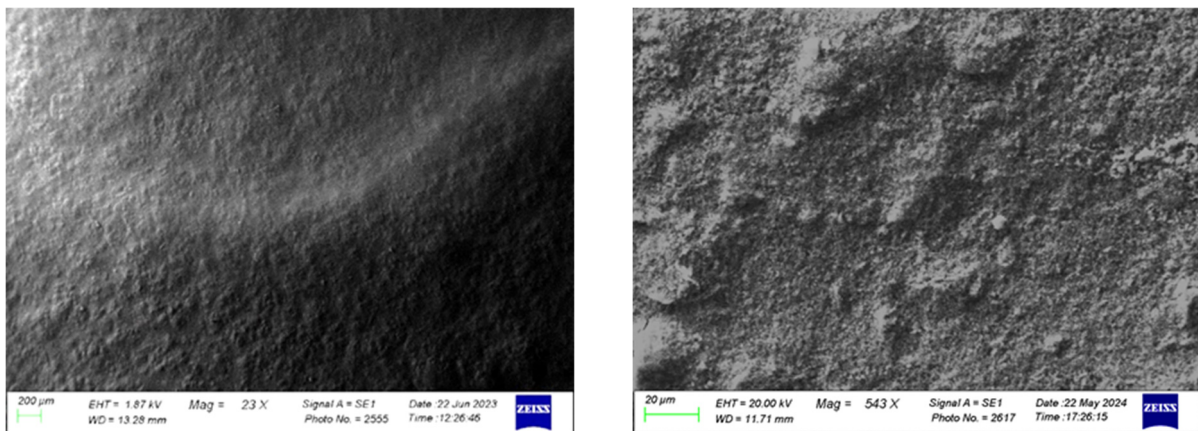


**Figure 17.** Combined polymer coating of series 1 after exposure to aggressive media  
S o u r c e: made by G. Ulyeva

Combined polymer coating of series 2 after exposure to aggressive media is characterized by a somewhat heterogeneous structure, there is a local swelling of the coating, but there are no microcracks (Figure 18).

Combined polymer coating of series 3 after exposure to aggressive media is characterized by a uniform, homogeneous structure, there is an interesting pattern of “crystallization”, and there are no microcracks (Figure 19).

Further, the adhesion of the polymer coating to the metal base was analyzed by scratch grid method according to Interstate standard GOST 15140–78<sup>3</sup>. The scratch grid method consists in that four-six parallel

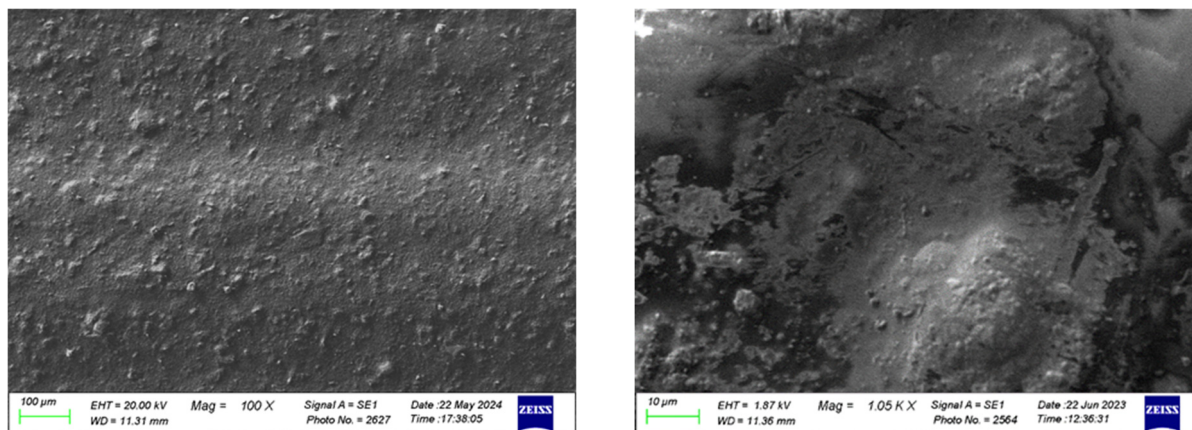
<sup>3</sup> GOST 15140–78. *Paintwork materials. Methods for determination of adhesion*. Standartinform Publ.; 2009. (In Russ.)



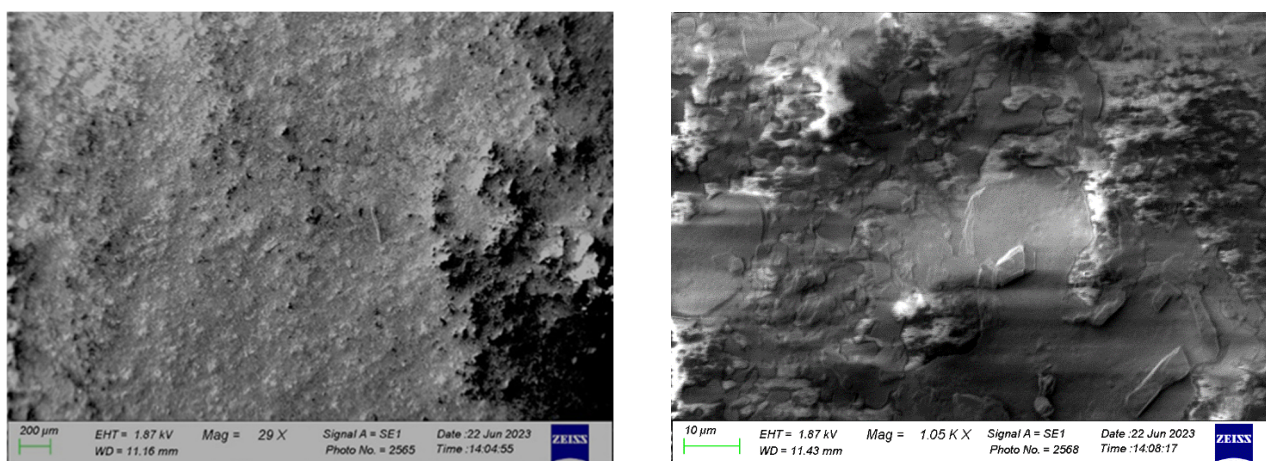
lines with depth to the base metal at a distance of 2–3 mm from each other and four-six parallel lines perpendicular to the first ones are drawn on the surface of the controlled coating with a steel point. No peeling should be observed on the controlled surface of the coating<sup>4</sup>.

Figure 20 shows the applied scratch grid on the polymer coating.

Table 5 shows the test results of polymer coatings with different filler for adhesion properties.



**Figure 18.** Combined polymer coating of series 2 after exposure to aggressive media  
Source: made by G. Ulyeva



**Figure 19.** Combined polymer coating of series 3 after exposure to aggressive media  
Source: made by G. Ulyeva



**Figure 20.** Example of scratch grid application  
Source: made by V. Merkulov

<sup>4</sup> Hardness testers. Available from: <http://www.tverdomer.ru/products/portable-hardness-testers> (accessed: 25.02.2024).

Table 5

**Determination of adhesion of polymer coatings on metal samples**

NaCl	H <sub>2</sub> SO <sub>4</sub> 5%	H <sub>2</sub> SO <sub>4</sub> 10%	KOH 5%	KOH 10%
1	2	3	4	5
<b>MMA+VBE+MA+TiO<sub>2</sub> (1TiO<sub>2</sub>)</b>				
No delamination of the coating during scratch application	The coating crumbled when the scratch grid was applied	The coating crumbled when the scratch grid was applied	The coating crumbled when the scratch grid was applied	The coating crumbled when the scratch grid was applied
<b>VBE+MMA+TiO<sub>2</sub>(3TiO<sub>2</sub>)</b>				
When applying the scratch grid, the coating peeled off locally (in one place), but overall withstood the test	The coating generally has good adhesion but crumbles at the intersections of the scratch grid	The coating adheres tightly to the base; there is no peeling in all the scratch grid crosshairs	The coating has completely peeled off when the scratch grid was applied	The coating has completely peeled off when the scratch grid was applied
<b>MMA+VBE+MA+SiO<sub>2</sub> (1SiO<sub>2</sub>)</b>				
The coating did not peel off when the scratch grid was applied	The coating did not peel off when the scratch grid was applied	The coating has completely peeled off when the scratch grid was applied	The coating has completely peeled off when the scratch grid was applied	The coating has completely peeled off when the scratch grid was applied
<b>VBE+MMA+SiO<sub>2</sub> (3SiO<sub>2</sub>)</b>				
When applying the scratch grid, the coating did not peel off, tightly adheres to the base	When applying the scratch grid, the coating did not peel off, tightly adheres to the base	When applying the scratch grid, the coating did not peel off, tightly adheres to the base	The coating has completely peeled off when the scratch grid was applied	The coating has completely peeled off when the scratch grid was applied
<b>MMA+VBE+MA+TiO<sub>2</sub>+SiO<sub>2</sub> (1 series combined)</b>				
When applying the scratch grid, the coating did not peel off, tightly adheres to the base	When applying the scratch grid, the coating did not peel off, tightly adheres to the base	When the scratch grid was applied, the coating did not peel off, leaving scratches in the coating but still adhering tightly to the base	The coating has completely peeled off after exposure to aggressive media	The coating has completely peeled off after exposure to aggressive media
<b>MMA+VBE+styrene+TiO<sub>2</sub>+SiO<sub>2</sub> (2 series combined)</b>				
When applying the scratch grid, the coating did not peel off, tightly adheres to the base	When applying the scratch grid, the coating did not peel off, tightly adheres to the base	When applying the scratch grid, the coating did not peel off, tightly adheres to the base	When applying the scratch grid, the coating did not peel off, tightly adheres to the base	When applying the scratch grid, the coating did not peel off, tightly adheres to the base
<b>VBE+MMA+SiO<sub>2</sub>+TiO<sub>2</sub> (3 series combined)</b>				
When applying the scratch grid, the coating did not peel off, tightly adheres to the base	When applying the scratch grid, the coating did not peel off, tightly adheres to the base	When applying the scratch grid, the coating did not peel off, tightly adheres to the base	When applying the scratch grid, the coating did not peel off, tightly adheres to the base	When applying the scratch grid, the coating did not peel off, tightly adheres to the base

Source: made by V. Merkulov

According to the results of Table 5, it can be seen that samples No. 1 of 1TiO<sub>2</sub> and 3TiO<sub>2</sub> series have good adhesion properties with the base. Samples Nos. 1–2 of 1SiO<sub>2</sub> series and samples Nos. 1–3 of 3SiO<sub>2</sub> series have the best adhesion properties with the base. Series 2 and 3 combined polymer coatings have the best adhesion properties.

Series 1 combined polymer coating has good adhesion properties except for the samples exposed to aggressive media (5 and 10% KOH).

The authors decided to determine the hardness of the coatings in order to evaluate the effect of coating composition and aggressive media on this mechanical characteristic. Hardness was determined using a MET-UD portable combination hardness tester. Hardness was determined on a selected Brinell scale. This hardness tester determines hardness electronically by measuring the change in ultrasonic frequency and by determining the ratio of the velocity of the striker inside the transducer before and after impact.

The striker, located in the dynamic sensor, has a carbide ball at the end, which is directly connected to the controlled surface at the moment of impact. There is a permanent magnet inside the striker. After the trigger is pressed, the striker is ejected onto the surface to be measured by means of a preloaded spring. In this case, the striker moves inside the inductance coil and induces EMF in it by its magnetic field. The signal from the output of inductance coil is fed to the input of the electronic unit, where it is converted to the value of hardness of the selected scale and displayed on the screen.

Table 6 shows the average Brinell hardness results of the samples after exposure to aggressive media.

Table 6

**Results of hardness measurements of polymer coating samples on metal**

Solution	Hardness, HB				
	Coating 1TiO <sub>2</sub>	Coating 3TiO <sub>2</sub>	Coating 1SiO <sub>2</sub>	Coating 3SiO <sub>2</sub>	Uncoated sample
5% NaCl	244.6	219.4	210.6	214.8	204.4
5% H <sub>2</sub> SO <sub>4</sub>	233.2	233.8	182.4	195.4	211.6
10% H <sub>2</sub> SO <sub>4</sub>	272.2	239.0	247.0	175.4	200.4
5% KOH	310.6	227.0	232.0	264.4	192.0
10% KOH	221.5	228.6	192.6	230.4	203.4
Medium	254.4	229.6	212.9	216.1	202.4

Source: made by G. Ulyeva

According to Table 6, the highest hardness values are found in titanium filled coatings of both series. Accordingly, the uncoated sample has the lowest values, indicating exposure to aggressive media and metal corrosion. It can be concluded that both titanium-filled and microsilica-filled coatings have protective properties against corrosion, since the hardness of the polymer-coated samples is greater than that of the uncoated sample.

Table 7 shows the average hardness results of the combined polymer coating samples after exposure to aggressive media according to the Brinell method.

Table 7

**Results of hardness measurements of combined polymer coating samples on metal**

Solution	Hardness, HB		
	Series 1 coating	Series 2 coating	Series 3 coating
5% NaCl	133.7	253.7	187.7
5% H <sub>2</sub> SO <sub>4</sub>	156.7	182.8	239.7
10% H <sub>2</sub> SO <sub>4</sub>	150.0	143.0	168.8
5% KOH	233.3	206.0	248.0
10% KOH	204.0	233.0	231.3
Medium	175.5	203.7	215.1
Not covered	213.0	214.5	203.5

Source: made by G. Ulyeva

According to Table 7, the hardness of metal samples with combined polymer coating is less than that of polymer coated samples with different fillers individually. However, the combined polymer coating of series 3 has the highest hardness value compared to series 1 and 2.

The thickness of coatings was also determined in accordance with National standard of the Russian Federation GOST R52146-2003<sup>5</sup> “Polymer-coated rolled products”. Table 8 shows the results of determining the thickness of the polymer coating using an electronic micrometer MK-25 (mechanical testing laboratory of the Analytical Control Center of “Qarmet” JSC) after exposure to aggressive media.

Table 8

**Results of thickness measurements of polymer coatings with titanium oxide and microsilica fillers,  $\mu\text{m}$** 

Solution	Coating 1TiO <sub>2</sub>	Coating 3TiO <sub>2</sub>	Coating 1SiO <sub>2</sub>	Coating 3SiO <sub>2</sub>
5% NaCl	0.096	0.152	0.217	0.687
5% H <sub>2</sub> SO <sub>4</sub>	0.093	0.093	0.267	0.197
10% H <sub>2</sub> SO <sub>4</sub>	0.059	0.103	0.338	0.256
5% KOH	0.875	0.113	0.159	0.179
10% KOH	0.119	0.091	0.220	0.277
Medium	0.249	0.111	0.241	0.320

Source: made by G. Ulyeva

According to the results of Table 8, it can be seen that the highest thickness values have the polymer coating with microsilica filler of series 3, but at the same time this coating has low hardness values. Conversely, the titanium filled polymer coating, especially series 3, having low thickness values, has higher hardness values.

Table 9 shows the results of the combined polymer coating thickness determination.

Table 9

**Thickness measurement results of combined polymer coatings,  $\mu\text{m}$** 

Solution	Series 1	Series 2	Series 3
5% NaCl	0.294	0.389	0.349
5% H <sub>2</sub> SO <sub>4</sub>	0.300	0.383	0.267
10% H <sub>2</sub> SO <sub>4</sub>	0.415	0.527	0.409
5% KOH	0.236	0.472	0.379
10% KOH	0.177	0.492	0.313
Medium	0.284	0.453	0.343

Source: made by A. Yepaneshnikova

According to Table 9, the combined polymer coating of series 2 has the maximum thickness values, which also performed well in aggressive media. Series 3 combined polymer coating with poor resistance to aggressive media has average thickness values. The combined polymer coatings of series 2 and 3 had higher thickness, which means that their initial formulation shall be taken into consideration. The combined polymer coating had a low viscosity when it was created, and initially already had a low thickness.

Thus, the technology of protective coatings of a new composition used for metallic and non-metallic products operating in aggressive media was developed. The new formulation of developed polymer protective coatings favorably distinguishes the proposed composition from the existing ones.

<sup>5</sup> GOST R52146–2003. Cold rolled and cold rolled hot-galvanized sheet with polymer coating, prepainted by the continuous coil-coating process. Moscow: Izdatel'stvo standartov Publ.; 2004.

#### 4. Conclusion

1. The formulation of corrosive polymer coating with various fillers for protection of metal structures and products from the harmful effects of corrosion was developed. The behavior of different polymer coatings in aggressive media (acidic, neutral, and alkaline) with fillers of microsilica, titanium dioxide and their combination were also considered.

2. It was found that the polymer coating with microsilica filler performed well in acidic environments (5 and 10% H<sub>2</sub>SO<sub>4</sub>), while the polymer coating with titanium dioxide filler performed well in hydrochloric (10% NaCl) and alkaline (5 and 10% KOH) environments.

3. The best performance was achieved by the combined polymer coating series 2, which performed well in hydrochloric and acid solutions, worse in alkaline solutions (corrosion score 2–4). This is due to the presence of styrene in the composition of the combined coating, which has good resistance to aggressive media.

4. The use of production waste as secondary raw materials coming from electrothermal, metallurgical, coke and chemical industries will serve as a basis for the creation of new production in order to strengthen and develop the economy and will reduce the environmental load, as well as reduce the area of storage of production waste.

#### References / Список литературы

1. Yakupov S.N., Gumarov G.G., Yakupov N.M. Experimental-theoretical method for assessing the stiffness and adhesion of the coating on a spherical substrate. *Structural Mechanics of Engineering Constructions and Buildings*. 2023; 19(6):577–582. <http://doi.org/10.22363/1815-5235-2023-19-6-577-582>
2. Zhangabay N., Baidilla I., Tagybayev A., Anarbayev Y., Kozlov P. Thermophysical indicators of elaborated sandwich cladding constructions with heat-reflective coverings and air gaps. *Case Studies in Construction Materials*. 2023;(18):e02161. <https://doi.org/10.1016/j.cscm.2023.e02161>
3. Kgabi N. A review of current and future challenges in paints and coatings chemistry. *J Progress Multidiscipl Res*. 2013;(3):75–76. Available from: <http://hdl.handle.net/10628/469> (accessed: 12.02.2024)
4. Khanna A.S. *High-Performance Organic Coatings*. Materials Science. Woodhead Publ.; 2008. <https://doi.org/10.1533/9781845694739>
5. Elnaggar E.M., Elsokkary T.M., Shohide M.A., El-Sabbagh B.A., Abdel-Gawwad H.A. Surface protection of concrete by new protective coating. *Construction and Building Materials*. 2019;(220):245–252. <https://doi.org/10.1016/j.conbuildmat.2019.117987>
6. Nikolaenko A.A., Djigiris D.D. Patent RU 2306325, *Polymer protective barrier coating*, Published on 20.09.2007. Bulletin No. 26.
7. Itsko E.F., Sidorova L.G., Gurvich R.Y., Mulin Y.A., Berzin V.I. Patent RU 2049100 C1, *Method of obtaining anticorrosive composition*, Published 27.11.1995.
8. Kuzmitsky G.E., Fedchenko N.N., Alikin V.N., Parakhin A.N., Mokretsov I.I., Mineeva O.I., Obodova T.N. Patent RU 2215763 C1, *Composition for anticorrosion coating*, Published 10.11.2003.
9. Merkulov V.V., Ulyeva G.A., Shishov J.D., Almazov A.I. Patent KZ 34563, *Composition for protection of metal and concrete structures*, Published 04.09.2020.
10. Merkulov V., Ulyeva G., Akhmetova G., Volokitin A. Synthesis of copolymers for protective coatings. *Journal Chemical technology and metallurgy*. 2024;59(3):639–646. <https://doi.org/10.59957/jctm.v59.i3.2024.18>
11. Bensalah W., Loukil N., Wery M.D.-P., Ayedi H.F. Assessment of automotive coatings used on different metallic substrates. *International Journal of Corrosion*. 2014: 838054. <https://doi.org/10.1155/2014/838054>
12. Sarkar P.K., Naik R.B., Mahato T.K., Naik R.S., Kandasubramanian B. Anticorrosive self-stratified PDMS-epoxy coating for marine structures. *Journal of the Indian Chemical Society*. 2023;100(1):100865. <https://doi.org/10.1016/j.jics.2022.100865>
13. Fernández-álvarez M., Velasco F., Bautista A., Lobo F.C.M., Fernandes E.M., Reis R.L. Manufacturing and characterization of coatings from polyamide powders functionalized with nanosilica. *Polymers*. 2020;12(10):2298. <https://doi.org/10.3390/polym12102298>
14. Pourjavadi A., Fakoorpoor S.M., Khaloo A., Hosseini P. Improving the performance of cement-based composites containing superabsorbent polymers by utilization of nano-SiO<sub>2</sub> particles. *Materials and Design*. 2012;42:94–101. <http://doi.org/10.1016/j.matdes.2012.05.030>

15. Fallah F., Khorasani M., Ebrahimi M. Improving the mechanical properties of waterborne nitrocellulose coating using nanosilica particles. *Progress in Organic Coatings*. 2017;109:110–116. <https://doi.org/10.1016/j.porgcoat.2017.04.016>
16. Malaki M., Hashemzadeh Y., Karevan M. Effect of nanosilica on the mechanical properties of acrylic polyurethane coatings. *Progress in Organic Coatings*. 2016;101:477–485. <https://doi.org/10.1016/j.porgcoat.2016.09.012>
17. Hosseinzadeh K., Ganji D.D., Ommi F. Effect of SiO<sub>2</sub> super-hydrophobic coating and self-rewetting fluid on two phase, closed thermosyphon heat transfer characteristics: An experimental and numerical study. *Journal of Molecular Liquids*. 2020;315:113748. <https://doi.org/10.1016/j.molliq.2020.113748>
18. Eduok U., Faye O., Szpunar J. Recent developments and applications of protective silicone coatings: A review of PDMS functional materials. *Progress in Organic Coatings*. 2017;111:124–163. <http://doi.org/10.1016/j.porgcoat.2017.05.012>
19. Jain R., Wasnik M., Sharma A., Kr Bhadu M., Rout T.K., Khanna A.S. Development of epoxy, based surface tolerant coating improvised with Zn Dust and SiO<sub>2</sub> on steel surfaces. *Journal of Coatings*. 2014:1–15. <https://doi.org/10.1155/2014/574028>
20. Ulyeva G.A., Fomina T.A. *Metal defects and quality control of metal products*. Temirtau: KGIU; 2009. (In Russ.)  
*Ульева Г.А., Фомина Т.А. Дефекты металлов и контроль качества металлопродукции*. Темиртау: ГИУ, 2009. 154 с.

## РАСЧЕТ И ПРОЕКТИРОВАНИЕ СТРОИТЕЛЬНЫХ КОНСТРУКЦИЙ ANALYSIS AND DESIGN OF BUILDING STRUCTURES

DOI: 10.22363/1815-5235-2024-20-4-331-341

UDC 69.059

EDN: TZOMCJ

Research article / Научная статья

### Strength of Normal Sections of Flexural Reinforced Concrete Elements Damaged by Corrosion and Strengthened with External Composite Reinforcement

Vladimir I. Rimshin<sup>1</sup>, Lyudmila A. Suleymanova<sup>2</sup>, Pavel A. Amelin<sup>2</sup><sup>1</sup> Moscow State University of Civil Engineering (National Research University), Moscow, Russia<sup>2</sup> Belgorod State Technological University named after V.G. Shukhov, Belgorod, Russia

✉ v.rimshin@niisf.ru

Received: April 10, 2024

Accepted: June 25, 2024

**Abstract.** The aim of the study is to develop a methodology for calculating the strength of normal sections of flexural reinforced concrete elements, which suffered corrosion damage and were strengthened with external composite reinforcement. The objects of the study are reinforced concrete elements used in various structures that are exposed to aggressive chloride environment that causes corrosion of concrete and rebars. The research method is based on the use of a diachronic model of deformation of corrosion-damaged elements. This model takes into account changes in the mechanical characteristics of concrete and reinforcement during corrosion and includes equations based on analytical relationships for determining the initial load-bearing capacity of intact structures. An important aspect of the method is taking into account external polymer composite reinforcement, which allows to increase the flexural rigidity and strength characteristics of damaged elements. The Picard's iterative method, which is designed for approximate solutions of differential equations, was used to ensure the accuracy of calculations. The results of the study showed that the proposed method allows to effectively assess the strength of normal sections of reinforced concrete elements subjected to corrosion. It was found that the methodology, which takes into account the changes in strength and deformation characteristics of materials, as well as the effect of aggressive chloride environment, ensures high accuracy and reliability of the analysis. The use of external polymer composite reinforcement significantly increases the stability and durability of structures. Thus, the developed methodology is an important tool for increasing operational reliability and extending the service life of reinforced concrete structures exposed to aggressive environments, which is a relevant problem in the construction industry.

**Keywords:** strength, reinforced concrete, chloride corrosion, composite materials, strengthening of building structures

**Conflicts of interest.** The authors declare that there is no conflict of interest.

**Authors' contribution.** Undivided co-authorship.

**For citation:** Rimshin V.I., Suleymanova L.A., Amelin P.A. Strength of normal sections of flexural reinforced concrete elements damaged by corrosion and strengthened with external composite reinforcement. *Structural Mechanics of Engineering Constructions and Buildings*. 2024;20(4):331–341. <http://doi.org/10.22363/1815-5235-2024-20-4-331-341>

**Vladimir I. Rimshin**, Corresponding Member of the Russian Academy of Architecture and Construction Sciences, Doctor of Technical Sciences, Professor of the Department of Housing and Utility Complex, Institute of Environmental Engineering and Mechanization, Moscow State University of Civil Engineering (National Research University), Moscow, Russia; eLIBRARY SPIN-code: 9629-5322; ORCID: 0000-0003-0209-7726; e-mail: v.rimshin@niisf.ru

**Lyudmila A. Suleymanova**, Doctor of Technical Sciences, Professor of the Department of Construction and Urban Management, Belgorod State Technological University named after V.G. Shukhov, Belgorod, Russia; eLIBRARY SPIN-code: 7156-3920; ORCID: 0000-0002-1180-558X; e-mail: ludmilasuleimanova@yandex.ru

**Pavel A. Amelin**, Assistant of the Department of Construction and Urban Management, Belgorod State Technological University named after V.G. Shukhov, Belgorod, Russia; eLIBRARY SPIN-code: 8237-9002; ORCID: 0000-0002-7104-3214; e-mail: p.amelin@inbox.ru

© Rimshin V.I., Suleymanova L.A., Amelin P.A., 2024

This work is licensed under a Creative Commons Attribution 4.0 International License  
<https://creativecommons.org/licenses/by-nc/4.0/legalcode>

# Прочность нормальных сечений изгибаемых железобетонных элементов, поврежденных коррозией и усиленных внешним композитным армированием

В.И. Римшин<sup>1</sup>✉, Л.А. Сулейманова<sup>2</sup>✉, П.А. Амелин<sup>2</sup>✉

<sup>1</sup> Национальный исследовательский Московский государственный строительный университет, Москва, Россия

<sup>2</sup> Белгородский государственный технологический университет им. В.Г. Шухова, Белгород, Россия

✉ v.rimshin@niisf.ru

Поступила в редакцию: 10 апреля 2024 г.

Принята к публикации: 25 июня 2024 г.

**Аннотация.** Исследование направлено на разработку методики расчета прочности нормальных сечений изгибаемых железобетонных элементов, подвергшихся коррозионным повреждениям и усиленных внешним композитным армированием. Объектом исследования являются железобетонные конструкции, используемые в различных сооружениях, которые подвергаются воздействию хлоридной агрессивной среды, вызывающей коррозию бетона и арматурных стержней. Метод исследования базируется на применении диахронной модели деформирования коррозионно-поврежденных элементов. Эта модель учитывает изменения механических характеристик бетона и арматуры в процессе коррозии и включает в себя расчеты, основанные на аналитических зависимостях для определения первоначальной несущей способности неповрежденных конструкций. Важным аспектом методики является учет внешнего полимеркомпозитного армирования, которое позволяет повысить изгибные жесткости и прочностные характеристики поврежденных элементов. Для обеспечения точности расчетов использован итерационный метод Пикара, предназначенный для аппроксимации решений дифференциальных уравнений. Результаты исследования показали, что предложенная методика позволяет эффективно оценивать прочность нормальных сечений железобетонных элементов, подверженных коррозии. Установлено, что методика, учитывающая изменения прочностных и деформационных характеристик материалов, а также воздействие хлоридной агрессивной среды, обеспечивает высокую точность и надежность расчетов. Применение внешнего полимеркомпозитного армирования значительно увеличивает устойчивость и долговечность конструкций. Таким образом, разработанная методика служит важным инструментом для повышения эксплуатационной надежности и продления срока службы железобетонных конструкций, подвергающихся воздействию агрессивных сред, что является актуальной задачей в строительной отрасли.

**Ключевые слова:** прочность, железобетон, хлоридная коррозия, композитные материалы, усиление строительных конструкций

**Заявление о конфликте интересов.** Авторы заявляют об отсутствии конфликта интересов.

**Вклад авторов.** Нераздельное соавторство.

**Для цитирования:** Rimshin V.I., Suleymanova L.A., Amelin P.A. Strength of normal sections of flexural reinforced concrete elements damaged by corrosion and strengthened with external composite reinforcement // *Строительная механика инженерных конструкций и сооружений*. 2024. Т. 20. № 4. С. 331–341. <http://doi.org/10.22363/1815-5235-2024-20-4-331-341>

## 1. Introduction

### 1.1. Problems of Corrosion of Reinforced Concrete Structures

Buildings and structures may contain flexural reinforced concrete elements that are exposed to aggressive corrosion loads, which leads to deterioration of concrete and reinforcement, causing premature onset of limit states [1–4]. Corrosion of reinforced concrete is a complex set of chemical processes, as a result of which the strength and deformation properties are significantly changed [5–7].

<sup>2</sup>Римшин Владимир Иванович, член-корреспондент Российской академии архитектуры и строительных наук, доктор технических наук, профессор кафедры жилищно-коммунального комплекса, Институт инженерно-экологического строительства и механизации, Национальный исследовательский Московский государственный строительный университет, Москва, Россия; eLIBRARY SPIN-код: 9629-5322; ORCID: 0000-0003-0209-7726; e-mail: v.rimshin@niisf.ru

Сулейманова Людмила Александровна, доктор технических наук, профессор кафедры строительства и городского хозяйства, Белгородский государственный технологический университет им. В.Г. Шухова, Белгород, Россия; eLIBRARY SPIN-код: 7156-3920; ORCID 0000-0002-1180-558X; e-mail: ludmilasuleymanova@yandex.ru

Амелин Павел Андреевич, ассистент кафедры строительства и городского хозяйства, Белгородский государственный технологический университет им. В.Г. Шухова, Белгород, Россия; eLIBRARY SPIN-код: 8237-9002; ORCID: 0000-0002-7104-3214; e-mail: p.amelin@inbox.ru



One of the key problems in construction is exposure to chloride environments, which is recognized as hazardous and is widespread in practice. Studies conducted by various methods, including expert surveys, analysis of project documentation and field observations, show that about 3/4 of enterprises in chemical, metallurgical and other industries, as well as in the field of transportation and in coastal areas, are exposed to aggressive environments containing chlorides [8–10].

### 1.2. Existing Models of Corrosion Damage

At the moment, the processes of determining the stress-strain state of structures damaged by corrosion under the combined action of service and environmental loads have been sufficiently investigated. The works of V.M. Bondarenko, V.I. Rimshin, N.K. Rosental, A.I. Popesko, I.G. Ovchinnikov, G.A. Smolyago, V.P. Selyaev, V.P. Chirkov, P.S. Mangat, G.C. Gaal, R. Al-Hammoud, C. Andrade and others [1–16] are devoted to this subject.

In the model of corrosion damage of concrete, it is possible to partially apply the dissipative resistance theory of V.M. Bondarenko [5], according to which the cross-section of the element is divided into three zones. The first zone represents the area of complete material failure of thickness  $Z^*$ . The second zone is a transitional zone of partial concrete damage of thickness  $\sigma$ . The third zone is the area of concrete undamaged by corrosion of thickness  $p$  (Figure 1).

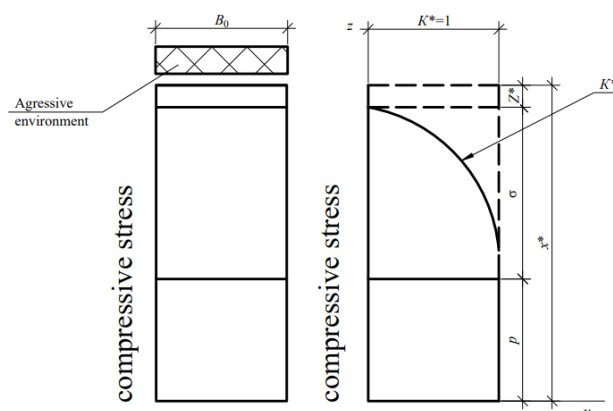


**Figure 1.** The change of strength characteristics of concrete along the cross section and the relationship between the depth of corrosion and stresses  
Source: made by V.I. Rimshin, L.A. Suleymanova, P.A. Amelin

According to the theory, the stress in corrosion-damaged concrete is described by the following relationship [4–6]:

$$\sigma_{\text{corr}} = \sigma_b(t) K(z), \quad (1)$$

where  $\sigma_b(t)$  is the stress-strain model of undamaged concrete;  $K(z)$  is the function of damage for layer of thickness  $z$ .

Coefficient  $K$  varies between 0 and 1 and is defined in general form as:

$$K(z) = \sum_{i=0}^{i=3} a_i z^i, \quad (2)$$

where  $z$  is the vertical coordinate measured from the stress axis of the corrosion-damaged concrete element;  $a_i$  are the coefficients of the power series, which are found at fixed values of  $K_i$ .

According to the model, the conditions for determining parameters  $a_i$  are the following:

$$\text{at } z = p \quad K(p) = 1 \quad \left. \frac{dk^*}{dz} \right|_{z=p} = 0, \tag{3}$$

$$\text{at } z > p \quad K^*(p + \delta) = K_1. \tag{4}$$

Given that  $z = p + \sigma \rightarrow K(p + \sigma) = 0$ , coefficients  $a_0, a_1, a_2$  are equal to:

$$a_0 = 1 - \left( \frac{p}{\delta} \right)^2; \tag{5}$$

$$a_1 = 2 \frac{p}{\delta^2}; \tag{6}$$

$$a_2 = -\frac{1}{\delta^2}. \tag{7}$$

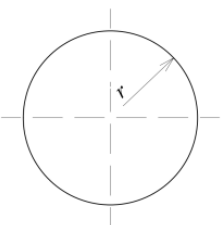
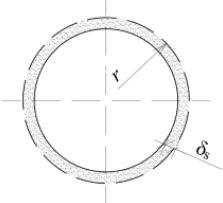
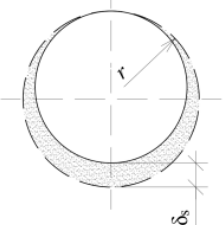
Rebar corrosion changes the geometric characteristics of reinforcement to a greater extent than the physical and mechanical characteristics of steel. The calculated cross-sectional area of damaged steel reinforcement is presented as [15]:

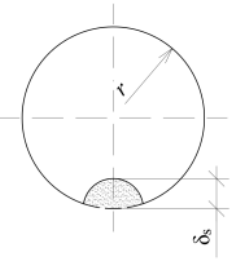
$$A_s^* = A_s - A_s, \tag{8}$$

where  $A_s$  is the cross-sectional area of rebar before corrosion;  $A_s^{cor}$  is the calculated area of corrosion damage of rebar cross-section determined from Table 1.

Table 1

**Models of corrosion development along the rebar cross-section and calculated area of corrosion damage**

Rebar corrosion type	Illustration	Function for determining the corrosion area of rebar, $A_s^{cor}$
Absence of critical concentration		0
Continuous uniform corrosion		$\pi \delta_s (2r - \delta_s)$
Continuous non-uniform corrosion		$r \delta_s - \frac{\delta_s^2}{4}$

Rebar corrosion type	Illustration	Function for determining the corrosion area of rebar, $A_s^{cor}$
Local and pitting corrosion		$\delta_s^2 \sqrt{m - m^2} + \delta_s^2 \arcsin \sqrt{m} - 2r\delta_s \sqrt{m} - 2r\delta_s \sqrt{m} +$ $+ \delta_s \sqrt{mr^2 - \delta_s^2 m^2} + r^2 \arcsin \frac{\delta_s \sqrt{m}}{r},$ <p>where <math>m = 1 - \frac{\delta_s^2}{4r^2} a</math></p>

Source: made by V.I. Rimshin, L.A. Suleymanova, P.A. Amelin  
 Note.  $r$  is the original radius of rebar,  $\delta_s$  is the depth of corrosion damage.

The depth of corrosion of steel reinforcement in the studies of I.G. Ovchinnikov is determined by the following relationship [16]:

$$\delta_s = \begin{cases} 0, & t \leq t_{inc} \\ \frac{\delta_{s,0} (t - t_{inc})}{T + (t - t_{inc})}, & t > t_{inc} \end{cases}, \tag{9}$$

where  $\delta_{s,0}$ ,  $T$  are experimental constants of damage;  $t_{inc}$  is the corrosion initiation time.

The time duration of the incubation period is determined based on the Fick's law [15]:

$$t_{inc} = \frac{1}{12D} \left( \frac{a}{1 - \frac{C_{cr}}{C_s}} \right)^2, \tag{10}$$

where  $D$  is the coefficient of chloride diffusion,  $a$  is the thickness of the protective layer of concrete,  $C_s$  is the chloride concentration at concrete surface.

### 1.3. Existing Prerequisites for Composite Strengthening of Reinforced Concrete Elements

A relevant problem in long-term operation of buildings and structures is the extension of the remaining service life of damaged reinforced concrete elements. In construction practice, the process of inspection of technical condition of reinforced concrete structures is performed simultaneously with the aim to increase the bearing capacity of the elements for resisting higher load values.

Along with the existing methods of strengthening of structures, such as increasing the cross-section and reinforcement, application of steel casings, the method of external polymer composite reinforcement is used. The development and application of strengthening methods for intact reinforced concrete structures with external composite reinforcement became possible owing to theoretical and experimental works of V.I. Rimshin, D.R. Mailyan, V.I. Morozov, S.I. Merkulov, P.P. Polsky, J.F. Bonacci, A.H. Al-Saidy and others [17–23].

The tensile behavior of composite materials is characterized by their elastic deformation up to fracture. Composite fibers differ from steel in that they are not ductile and their failure is brittle. The stress of composite materials depends on their strain according to Hooke's equation:

$$\sigma_f = E_f \varepsilon_f \delta_{s,0}, \quad (11)$$

where  $E_f$  is the elastic modulus of the composite material;  $\varepsilon_f$  is the fiber strain at a specific moment in time.

This affects the strengthening design of reinforced concrete structures with external reinforcement made of composites, as restrictions are imposed on the magnitude of elastic deformations of concrete and steel.

However, at the moment, the problem of determining the load-bearing capacity of previously damaged flexural reinforced concrete elements due to contact with aggressive chloride environment during operation is studied to a small extent. Which is the subject of this scientific study.

The objects of this study are flexural reinforced concrete elements damaged by aggressive chloride environment and strengthened with external composite reinforcement.

The aim of the study is to develop a methodology for calculating the strength of the normal sections of flexural reinforced concrete elements subjected to aggressive chloride environment and strengthened with external polymer composite reinforcement.

## 2. Methods

In this paper, a mathematical iterative method is used for determining the unknowns, which is reduced to the sequential application of the Picard's method.

The Picard's method, when used as a tool for partitioning the cross-section of a reinforced concrete element, is an iterative approach used for analysis and modeling of damaged structures. It involves successive refinement of the cross-section characteristics by dividing it into sub-elements and iteratively calculating their properties. In general, the formula of the iterative Picard's method is defined by the following relationship:

$$y(t) = y_0 + \int_{t_0}^t f(x, y(x)) dx. \quad (12)$$

Below is the solution algorithm:

- Initial conditions such as cross-sectional configurations of the reinforced concrete element, including dimensions, shape, position and number of rebars, geometric parameters of damage such as depth and length of cracks are specified.

- The cross-section is divided into several zones (sub-elements), taking into account both damaged and undamaged areas.

- An initial approximation of  $y$  is selected (adopted at first as a constant) and substituted in the right-hand side of the differential equation:  $dy / dx = f(x, y)$ .

- The equation is integrated with respect to  $x$ , which yields  $y$  in terms of  $x$  in the second approximation, and the specified numerical values are substituted into it. The result is rounded to the specified number of decimal places or significant digits. Initially, the mechanical properties of each sub-element are evaluated. Iterative calculation of the stress-strain state is performed for each sub-element, taking into account the interaction between them. The sub-element characteristics are updated based on the calculation results, gradually refining the model.

- The iterative process is repeated until convergence is achieved, when changes in the characteristics become insignificant. The results are verified to ensure that the model is adequate and the calculations are correct.

- Integral characteristics of the entire section, such as moment of inertia, static moment, stiffness and bearing capacity, are determined on the basis of the iterative calculations.

The Picard's method in this context provides accurate modeling and analysis, which is essential for assessing the condition of a structure and making decisions about its repair or strengthening.

### 3. Results and Discussion

The methodology of strength analysis of flexural elements assumes initial determination of flexural strength  $M$  of the undamaged structure using the following analytical relationships:

$$N + \sigma'_s A'_s + \sigma_s A_s + b \int_{-h/2}^{z_0} \sigma_p dz + b \int_{z_0}^{h/2} \sigma_c dz = 0; \quad (13)$$

$$M + \sigma'_s A'_s z_c + \sigma_s A_s z_p + b \int_{-h/2}^{z_0} \sigma_p z dz + b \int_{z_0}^{h/2} \sigma_c z dz = 0. \quad (14)$$

Further, to calculate the strength of normal sections damaged by corrosion and elements with cracks, a special case of the diachronic deformation model of V.V. Belov and S.Ye. Nikitin is used [24; 25]. This model takes into account:

- changes in strength and deformation characteristics of concrete in compression and tension;
- development of corrosion in rebars;

For the normal section, the resultant systems of equations of the diachronic model of deformation for corrosion-damaged reinforced concrete elements comprise the conditions of static equivalence  $\Sigma N_{cor} = 0$  and  $\Sigma M_{cor} = 0$ , as well as kinematic relationships under all-round aggression:

$$N_{cor} = b \int_{h/2}^{\delta_1} \sigma_b^{degr}(y) dy + 2\delta_2 \int_{\delta_1}^x \sigma_b^{degr}(y) dy + (b - 2\delta_2) \int_{\delta_1}^x \sigma_b(y) dy + A'_{s,cor} E_s \epsilon_b - A_{s,cor} E_s \epsilon_s; \quad (15)$$

$$M_{str} = b \int_{h/2}^{\delta_1} \sigma_b^{degr}(y) y dy + 2\delta_2 \int_{\delta_1}^x \sigma_b^{degr}(y) y dy + (b - 2\delta_2) \int_{\delta_1}^x \sigma_b(y) y dy + A'_{s,cor} E_s \epsilon_b \left( \frac{h}{2} - a \right) - A_{s,cor} E_s \epsilon_s \left( \frac{h}{2} - a \right); \quad (16)$$

$$\frac{\epsilon_b^m}{\epsilon_s^m} = \frac{x}{h - x - a}, \quad (17)$$

where  $h$  is the height of the rectangular section;  $b$  is the width of the rectangular section;  $\epsilon_b^m$  is the strain of the reinforcement in tension, in the middle section;  $E_s$  is the elastic modulus of the reinforcement;  $a$  is the distance from the resultant force in the reinforcement to the closest section edge;  $\epsilon_b^m$  is the concrete strain, in the middle section;  $\sigma_b^{degr}, \sigma_b$  are the concrete stresses in the damaged and undamaged zones respectively;  $\delta_1, \delta_2$  are the depths of damage of the concrete section in the compression zone and side edges.

The calculation methodology is based on a number of assumptions and hypotheses, including the assumption of constant external load on the element and concentration of aggressive environment around the section throughout the entire observation period. Corrosion of reinforcement by section reduction and polynomial stress-strain relationship of concrete are also taken into account. It is assumed that the axis of the center of gravity passes through the middle of the beam section height.

The contribution of external composite strengthening of flexural element is determined by adding the forces in the composite reinforcement at a distance  $h/2$  from the location of the axis of symmetry to the equilibrium equations (15) and (16), as shown in Figure 2.

As a result, the following relationships are obtained:

$$N_{str} = b \int_{h/2}^{\delta_1} \sigma_b^{degr}(y) dy + 2\delta_2 \int_{\delta_1}^x \sigma_b^{degr}(y) dy + (b - 2\delta_2) \int_{\delta_1}^x \sigma_b(y) dy + A'_{s,cor} E_s \epsilon_b - A_{s,cor} E_s \epsilon_s - A_f E_f \epsilon_f; \quad (18)$$

$$M_{str} = b \int_{h/2}^{\delta_1} \sigma_b^{degr}(y) y \partial y + 2\delta_2 \int_{\delta_1}^x \sigma_b^{degr}(y) y \partial y + (b-2\delta_2) \int_{\delta_1}^x \sigma_b(y) y \partial y + A_{s,cor} E_s \varepsilon_b \left(\frac{h-a}{2}\right) - A_{s,cor} E_s \varepsilon_s \left(\frac{h-a}{2}\right) - A_{s,cor} E_s \varepsilon_s \frac{h}{2}; \tag{19}$$

$$\frac{\varepsilon_b^m}{\varepsilon_f^m} = \frac{x}{h-x}, \tag{20}$$

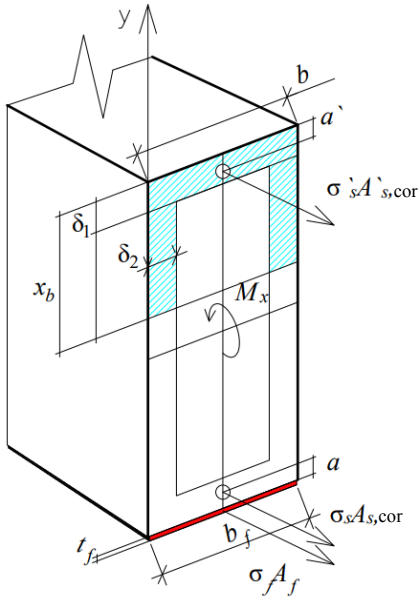


**Figure 2.** Model of the normal section of strengthened damaged rectangular element

S o u r c e: made by V.I. Rimshin, L.A. Suleymanova, P.A. Amelin

where  $A_f$  is the cross-sectional area of the composite material;  $E_f$  is the elastic modulus of the composite material;  $\varepsilon_f^m$  is the strain of the composite material, in the middle section.

In order to perform the iterative calculation, equations (17) and (18) defining axial force  $N_{str}$  and bending moment  $M_{x, str}$  are expressed in terms of flexural stiffness  $D$ , curvature  $\frac{1}{r_x}$  and fiber strain at the starting point  $\varepsilon_0$ :

$$N_{str} = D_{13} \frac{1}{r_x} + D_{33} \varepsilon_0; \tag{21}$$

$$M_{str} = D_{11} \frac{1}{r_x} + D_{13} \varepsilon_0. \tag{22}$$

Taking into account the forces of the polymer composite material, the flexural stiffness values are equal to:

$$D_{11} = b \int_{h/2}^{\delta_1} E_b^{degr}(y) v_b y^2 \partial y + 2\delta_2 \int_{\delta_1}^x E_b^{degr}(y) v_b y^2 \partial y + (b-2\delta_2) \int_{\delta_1}^x E_b(y) v_b y^2 \partial y + A_{s,cor} \alpha_s E_s v_s \left(\frac{h-a}{2}\right)^2 - A_{s,cor} \alpha_s E_s v_s \left(\frac{h-a}{2}\right)^2 - A_f \alpha_f E_f \left(\frac{h}{2}\right)^2; \tag{23}$$

$$D_{13} = b \int_{h/2}^{\delta_1} E_b^{degr}(y) v_b y \partial y + 2\delta_2 \int_{\delta_1}^x E_b^{degr}(y) v_b y \partial y + (b-2\delta_2) \int_{\delta_1}^x E_b(y) v_b y \partial y + A_{s,cor} \alpha_s E_s v_s \left(\frac{h-a}{2}\right) - A_{s,cor} \alpha_s E_s v_s \left(\frac{h-a}{2}\right) - A_f \alpha_f E_f \left(\frac{h}{2}\right); \tag{24}$$

$$D_{33} = b \int_{h/2}^{\delta_1} E_b^{degr}(y) v_b \partial y + 2\delta_2 \int_{\delta_1}^x E_b^{degr}(y) v_b \partial y + (b-2\delta_2) \int_{\delta_1}^x E_b(y) v_b \partial y + A_{s,cor} \alpha_s E_s v_s - A_{s,cor} \alpha_s E_s v_s - A_f \alpha_f E_f; \tag{25}$$

where  $E_b^{degr}, E_b$  are the elastic moduli of concrete in damaged and undamaged zones respectively;  $E_s, E_s'$  are the elastic moduli of reinforcement in tension and compression zones respectively;  $E_f$  is the elastic modulus of the polymer composite material;  $\alpha_s', \alpha_s, \alpha_f$  are the adjustment factors of geometrical characteristics of compressed, stretched and polymer composite reinforcement;  $v_b, v_s$  are the coefficients of the secant modulus of concrete and reinforcement of a particular region.

#### 4. Conclusion

In this study, the general relationships of stress-strain state changes in corrosion-damaged flexural reinforced concrete elements, which are strengthened with external polymer composite reinforcement, were determined. The results of the study allowed to formulate the following conclusions:

1. A methodology for calculating the strength of flexural reinforced concrete elements has been developed, including the initial determination of the load-bearing capacity of undamaged structure using analytical relationships.

2. To estimate the strength of normal sections of corrosion-damaged reinforced concrete elements, a diachronic deformation model was used, which takes into account the changes in strength and deformation characteristics of concrete and reinforcement due to corrosion.

3. The developed methodology includes stress-strain models of corrosion-damaged reinforced concrete elements and application of external polymer composite reinforcement, which makes it possible to accurately determine flexural stiffness and strength characteristics of structures.

4. The proposed methodology is based on a number of assumptions, including constant external load and concentration of aggressive environment around the cross-section throughout the observation period, which ensures the stability of the calculations.

5. It is established that exposure to aggressive chloride environment is a critical factor contributing to the corrosion of concrete and reinforcement, which leads to premature failure of reinforced concrete structures.

6. In order to obtain accurate results, the Picard's mathematical iterative method, designed for approximate solutions of differential equations, was applied, which provides high accuracy and reliability of the results.

These conclusions emphasize the significance of the developed methodology and its potential for improving practices of protection and strengthening of reinforced concrete structures in aggressive environments.

#### References

1. Smolyago G.A., Frolov N.V., Dronov A.V. Analysis of corrosion damages of reinforced concrete structures in operation. *Bulletin of BSTU named after V.G. Shukhov*. 2019;(1):52–57. (In Russ.) [https://doi.org/10.12737/article\\_5c506209065dd6.02007715](https://doi.org/10.12737/article_5c506209065dd6.02007715)
2. Ovchinnikov I.I. Current state of the calculation of reinforced structures that are exposed to aggressive medium. *Construction of unique buildings and structures*. 2012;2(2):46–60. (In Russ.) EDN: PCKXDB
3. Mangat P.S., Elgarf M.S. Flexural strength of concrete beams with corroding reinforcement. *ACI Structural Journal*. 1999;96(1):149–158. Available from: <https://shura.shu.ac.uk/id/eprint/1042> (accessed: 22.03.2024).
4. Bondarenko V.M., Rimshin V.I. Linear equations of force resistance and diagram  $\sigma - \varepsilon$  of concrete. *Structural Mechanics of Engineering Constructions and Buildings*. 2014;(6):40–44. (In Russ.) EDN: SYZJHL
5. Bondarenko V.M. The elements of dissipative theory of force resistance of concrete. *Structural Mechanics of Engineering Constructions and Buildings*. 2014;(2):47–57. (In Russ.) EDN: RZRQOF
6. Rimshin V.I., Suleymanova L.A., Amelin P.A., Kryuchkov A.A. Experimental studies of bent reinforced concrete elements with reinforcement damage due to contact with an aggressive chloride environment. *Expert: theory and practice*. 2023;3(22):138–146. (In Russ.) EDN: GATSZC
7. Feng G., Jin Z., Jiang Y., Wang X., Zhu D. Localized corrosion propagation of steel in cracked mortar and long-term corrosion of steel reinforcement in cracked concrete in seawater environment. *Corrosion Science*. 2024;228:111793. <https://doi.org/10.1016/j.corsci.2023.111793>
8. Chirkov V.P., Antropova E.A. Forecasting the service life of road bridges. *Proceedings of the International Scientific and Technical Conference "Reliability of building elements and systems."* Samara, 1997. p. 78–81. (In Russ.)
9. Al-Hammoud R., Soudki K., Topper T.H. Bond analysis of corroded reinforced concrete beams under monotonic and fatigue loads. *Cement Concrete Composites*. 2010;32(3):194–203.
10. Rozental N.K. Permeability and corrosion resistance of concrete. *Industrial and civil engineering*. 2013;(1):35–37. (In Russ.) EDN: PNQAJB

11. Gaal G.C., Veen C., Djourai M.H. Prediction of deterioration of concrete bridges in the Netherlands. *Proceedings of First International Conference on Bridge Maintenance, Safety and Management*. Barcelona, 2002. p. 111–118. ISBN 84-95999-05-6
12. Popesco A.I., Antsygin O.I., Danilov A.A. Numerical calculation of reinforced concrete rods under corrosive influences. *Concrete and reinforced concrete*. 2007;(3):25–27. (In Russ.) EDN: HZVULP
13. Selyaev V.P., Selyaev P.V., Sorokin E.V., Kechutkina E.L. Modeling of the reinforced concrete structure performance at joint influence of mechanical and chemical loads. *IOP Conference Series: Materials Science and Engineering*. 2018;456:012060. <https://doi.org/10.1088/1757-899X/456/1/012060>
14. Andrade C., Alonso C., Gulikers J. Test methods for on-site corrosion rate measurement of steel reinforcement in concrete by means of the polarization resistance method. *Materials and Structures*. 2004;37:623–643.
15. Frolov N.V., Smolyago G.A. Reinforced concrete beams strength under power and environmental influences. *Magazine of Civil Engineering*. 2021;(3):10303. <https://doi.org/10.34910/MCE.103.3>
16. Ovchinnikov I.I., Snezhkina O.V., Ovchinnikov I.G. Diffusion model of penetration of a chloride-containing environment in the volume of a constructive element. *AIP Conference Proceedings*. 2018;1973(1):020010. <https://doi.org/10.1063/1.5041394>
17. Rimshin V.I., Suleymanova L.A., Amelin P.A., Kryuchkov A.A. Composite strengthener of reinforced concrete bendable elements damaged under the influence of chloride aggressive environment. *Expert: theory and practice*. 2023; 1(20):29–34. (In Russ.) EDN: YUOKZK
18. Bonacci J.F., Maalej M. Externally bonded fiber-reinforced polymer for rehabilitation of corrosion damaged concrete beams. *ACI Structural Journal*. 2000;97(5):703–711. Available from: <http://scholarbank.nus.edu.sg/handle/10635/65577> (accessed: 11. 03.2024).
19. Yushin A.V., Morozov V.I. Experimental investigation of double-span beams with carbon fiber polymer reinforcement on the sloping section. *Bulletin of civil engineers*. 2014;(5):77–84. (In Russ.) EDN: TBPWWF
20. Merkulov S., Esipov S., Esipova D. Experimental studies of the cracking of reinforced concrete beams reinforced with composite materials. *Proceeding of the Donbas national academy of civil engineering and architecture*. 2019;(3):102–107. (In Russ.) EDN: MMDDMZ
21. Al-Saidy A.H., Saadatmanesh H., El-Gamal S., Al-Jabri K.S., Waris B.M. Structural behavior of corroded RC beams with/without stirrups repaired with CFRP sheets. *Materials and Structures*. 2016;49:3733–3747. <https://doi.org/10.1617/s11527-015-0751-y>
22. Mailyan D.R., Mihoub A., Polskoy P.P. Research questions of flexural reinforced concrete elements, strengthened with different types of composite materials. *Engineering journal of Don*. 2013;(2):99. (In Russ.) EDN: QLISLZ
23. Al-Saidy A.H., Al-Jabri K.S. Effect of damaged concrete cover on the behavior of corroded concrete beams repaired with CFRP sheets. *Composite Structures*. 2011;93(7):1775–1786. <https://doi.org/10.1016/j.compstruct.2011.01.011>
24. Belov V.V., Nikitin S.Ye. Diachronic deformation model of corrosion damaged reinforced concrete elements with cracks. *Bulletin of civil engineers*. 2011;(4):18–25. (In Russ.) EDN: OPBYHN
25. Nikitin S.E. Estimation of corrosion-damaged concrete construction durability based on diachronic deformation model. *Modern problems of science and education*. 2012;(2):242. (In Russ.) EDN: OXCNJX

### Список литературы

1. Смоляго Г.А., Фролов Н.В., Дронов А.В. Анализ коррозионных повреждений эксплуатируемых изгибаемых железобетонных конструкций зданий и сооружений // Вестник БГТУ им. В.Г. Шухова. 2019. № 1. С. 52–57. [https://doi.org/10.12737/article\\_5c506209065dd6.02007715](https://doi.org/10.12737/article_5c506209065dd6.02007715).
2. Овчинников И.И. Современное состояние проблемы расчета армированных конструкций, подвергающихся воздействию агрессивных сред // Строительство уникальных зданий и сооружений. 2012. № 2 (2). С. 46–60. EDN: PCKXDB
3. Mangat P.S., Elgarf M.S. Flexural strength of concrete beams with corroding reinforcement // *ACI Structural Journal*. 1999. Vol. 96. No. 1. P. 149–158. URL: <https://shura.shu.ac.uk/id/eprint/1042> (дата обращения: 22.03.2024).
4. Бондаренко В.М., Римшин В.И. Квазилинейные уравнения силового сопротивления и диаграмма  $\sigma - \varepsilon$  бетона // *Строительная механика инженерных конструкций и сооружений*. 2014. № 6. С. 40–44. EDN: SYZJHL
5. Бондаренко В.М. Элементы диссипативной теории силового сопротивления железобетона // *Строительная механика инженерных конструкций и сооружений*. 2014. № 2. С. 47–57. EDN: RZRQOF
6. Римшин В.И., Сулейманова Л.А., Амелин П.А., Крючков А.А. Экспериментальные исследования изгибаемых железобетонных элементов, имеющих повреждения арматуры вследствие контакта с хлоридной агрессивной средой // *Эксперт: теория и практика*. 2023. № 3 (22). С. 138–146. [https://doi.org/10.51608/26867818\\_2023\\_3\\_138](https://doi.org/10.51608/26867818_2023_3_138).



7. Feng G., Jin Z., Jiang Y., Wang X., Zhu D. Localized corrosion propagation of steel in cracked mortar and long-term corrosion of steel reinforcement in cracked concrete in seawater environment // *Corrosion Science*. 2024. Vol. 228. <https://doi.org/10.1016/j.corsci.2023.111793>
8. Чирков В.П., Антропова Е.А. Прогнозирование срока службы автодорожных мостов // Надежность строительных элементов и систем: труды Международной научно-технической конференции Самара, 1997. С. 78–81.
9. Al-Hammoud R., Soudki K., Topper T.H. Bond analysis of corroded reinforced concrete beams under monotonic and fatigue loads // *Cement Concrete Composites*. 2010. Vol. 32. No. 3. P. 194–203.
10. Розенталь Н.К. Проницаемость и коррозионная стойкость бетона // *Промышленное и гражданское строительство*. 2013. № 1. С. 35–37. EDN: PNQAJB
11. Gaal G.C., Veen C., Djorai M.H. Prediction of deterioration of concrete bridges in the Netherlands // *Proceedings of First International Conference on Bridge Maintenance, Safety and Management*. Barcelona, 2002. P. 111–118. ISBN 84-95999-05-6
12. Песекко А.И., Анцыгин О.И., Данилов А.А. Численный расчет железобетонных стержней при коррозионных воздействиях // *Бетон и железобетон*. 2007. № 3. С. 25–27. EDN: HZVULP
13. Selyaev V.P., Selyaev P.V., Sorokin E.V., Kechutkina E.L. Modeling of the reinforced concrete structure performance at joint influence of mechanical and chemical loads // *IOP Conference Series: Materials Science and Engineering*. 2018. Vol. 456. P. 012060. <https://doi.org/10.1088/1757-899X/456/1/012060>
14. Andrade C., Alonso C., Gulikers J. Test methods for on-site corrosion rate measurement of steel reinforcement in concrete by means of the polarization resistance method // *Materials and Structures*. 2004. No. 37. P. 623–643.
15. Frolov N.V., Smolyago G.A. Reinforced concrete beams strength under power and environmental influences // *Magazine of Civil Engineering*. 2021. No. 3 (103). P. 10303. <https://doi.org/10.34910/MCE.103.3>
16. Ovchinnikov I.I., Snezhkina O.V., Ovchinnikov I.G. Diffusion model of penetration of a chloride-containing environment in the volume of a constructive element // *AIP Conference Proceedings*. 2018. Vol. 1973. Iss. 1. Article no. 020010. <https://doi.org/10.1063/1.5041394>
17. Римшин В.И., Сулейманова Л.А., Амелин П.А., Фролов Н.В. Композитное усиление железобетонных изгибаемых элементов, поврежденных под воздействием хлоридной агрессивной среды // *Эксперт: теория и практика*. 2023. № 1 (20). С. 29–34. EDN: YUOKZK
18. Bonacci J.F., Maalej M. Externally bonded fiber-reinforced polymer for rehabilitation of corrosion damaged concrete beams // *ACI Structural Journal*. 2000. Vol. 97. No. 5. P. 703–711. URL: <http://scholarbank.nus.edu.sg/handle/10635/65577> (accessed: 11.03.2024).
19. Юшин А.В., Морозов В.И. Экспериментальные исследования двухпролетных железобетонных балок, усиленных композитными материалами по наклонному сечению // *Вестник гражданских инженеров*. 2014. № 5 (46). С. 77–84. EDN: ТВРWWF
20. Меркулов С.И., Есипов С.М., Есипова Д.В. Экспериментальные исследования трещинообразования железобетонных балок, усиленных композитными материалам // *Вестник Донбасской национальной академии строительства и архитектуры*. 2019. № 3. С. 102–107. EDN: MMDDMZ
21. Al-Saidy A.H., Saadatmanesh H., El-Gamal S., Al-Jabri K.S., Waris B.M. Structural behavior of corroded RC beams with/without stirrups repaired with CFRP sheets // *Materials and Structures*. 2016. Vol. 49. P. 3733–3747. <https://doi.org/10.1617/s11527-015-0751-y>
22. Маилян Д.Р., Польской П.П., Михуб А. Вопросы исследования прочности нормальных сечений балок, усиленных различными видами композитных материалов // *Инженерный вестник Дона*. 2013. № 2. С. 99. EDN: QLISLZ
23. Al-Saidy A.H., Al-Jabri K.S. Effect of damaged concrete cover on the behavior of corroded concrete beams repaired with CFRP sheets // *Composite Structures*. 2011. Vol. 93. No. 7. P. 1775–1786. <https://doi.org/10.1016/j.compstruct.2011.01.011>
24. Белов В.В., Никитин С.Е. Диахронная модель деформирования коррозионно-поврежденных железобетонных элементов с трещинами // *Вестник гражданских инженеров*. 2011. № 4 (29). С. 18–25. EDN: ОРВУНН
25. Никитин С.Е. Оценка долговечности коррозионно-поврежденных железобетонных конструкций на базе диахронной модели деформирования // *Современные проблемы науки и образования*. 2012. № 2. С. 242. EDN: ОХСНЈХ



DOI: 10.22363/1815-5235-2024-20-4-342-354

УДК 621.981.1

EDN: TCWWPU

Научная статья / Research article

## Проектирование тонкостенных деталей одинарной кривизны для использования в облегченных конструкциях

Ю.А. Морозов<sup>1</sup>, Б.Ф. Белелюбский<sup>2</sup><sup>1</sup> Московский государственный технический университет имени Н.Э. Баумана  
(национальный исследовательский университет), Москва, Россия<sup>2</sup> Московский политехнический университет (Московский Политех), Москва, Россия

✉ akafest@mail.ru

Поступила в редакцию: 26 февраля 2024 г.

Принята к публикации: 15 июня 2024 г.

**Аннотация.** Цель исследования — нахождение минимальной (критической) кривизны листового материала, допускающей гибку без разрушения гнutoго элемента (образование продольных трещин) и определяемой совокупной «игрой» двух деформационных параметров — утонение, приводящее к ослаблению сечения детали, и деформационное упрочнение материала, характеризуемое интенсивностью деформаций. Проанализирована существующая схема листовой гибки в совокупности с кинематикой деформационного изменения первоначальных радиусов детали ввиду неразрывности сжимающих (радиальная) и растягивающих (тангенциальная) деформаций. При допущении гипотезы плоских сечений в условиях листовой гибки разработана математическая модель, позволяющая оценить деформационные и геометрические (утонение) параметры при формообразовании торовой поверхности различной кривизны. Выявлен уровень радиальных напряжений с учетом деформационного упрочнения и утонения изгибаемого материала, приводящих к исчерпанию его несущей способности (разрушение), где критерием пластичности являются механические свойства конкретного материала, полученные в испытаниях на растяжение (пределы текучести и прочности, относительное удлинение), аппроксимированные степенной зависимостью. Полученные результаты найдут применение при проектировании силовых облегченных конструкций; в моделировании напряженно-деформированного состояния металла при разработке технологических процессов листовой штамповки (гибки) для вычисления величины утонения, оценки уровня радиальных напряжений гибки металла по торцевой кромке давящего пуансона, а также при проектировании гибочной оснастки.

**Ключевые слова:** листовая гибка, радиус кривизны, утонение, радиальное напряжение, пластическая потеря устойчивости, разрушение материала

**Заявление о конфликте интересов.** Авторы заявляют об отсутствии конфликта интересов.


**Вклад авторов.** Нераздельное соавторство.

**Для цитирования:** Морозов Ю.А., Белелюбский Б.Ф. Проектирование тонкостенных деталей одинарной кривизны для использования в облегченных конструкциях // Строительная механика инженерных конструкций и сооружений. 2024. Т. 20. № 4. С. 342–354. <http://doi.org/10.22363/1815-5235-2024-20-4-342-354>

**Морозов Юрий Анатольевич**, кандидат технических наук, доцент кафедры МТ-13 технологии обработки материалов, Московский государственный технический университет имени Н.Э. Баумана (национальный исследовательский университет), Москва, Россия; eLIBRARY SPIN-код: 3189-5426, ORCID: 0000-0001-9229-7398; e-mail: akafest@mail.ru

**Белелюбский Борис Феликсович**, кандидат технических наук, доцент кафедры металлургии, Московский политехнический университет (Московский Политех), Москва, Россия; eLIBRARY SPIN-код: 2007-1003, ORCID: 0000-0002-1702-707x; e-mail: alib@bk.ru

© Морозов Ю.А., Белелюбский Б.Ф., 2024

 This work is licensed under a Creative Commons Attribution 4.0 International License  
<https://creativecommons.org/licenses/by-nc/4.0/legalcode>

# Design of Thin-Walled Single-Curvature Parts for Use in Lightweight Structures

Yury A. Morozov<sup>1</sup>✉ Boris F. Beleyubskiy<sup>2</sup>✉

<sup>1</sup> Bauman Moscow State Technical University, Moscow, Russia

<sup>2</sup> Moscow Polytechnic University, Moscow, Russia

✉ akafest@mail.ru

Received: February 26, 2024

Accepted: June 15, 2024

**Abstract.** The aim of the study — the purpose of the study was to find the minimum (critical) curvature of sheet material, to which it can be bent without fracture (formation of longitudinal cracks) and which is determined by the combined «play» of two deformational parameters: thinning, responsible for cross-section weakening, and strain hardening of the material, characterized by the intensity of deformations. The existing sheet bending pattern is analyzed with regard to the kinematics of deformational changes in the initial radii of the part due to the continuity of compressive (radial) and tensile (tangential) deformations. Assuming the Bernoulli's hypothesis in sheet bending conditions, a mathematical model has been developed for estimating the deformational and geometric (thinning) parameters during the formation of a torus surface of various curvatures. The level of radial stresses has been identified taking into account strain hardening and thinning of the bent material, which lead to the exhaustion of its load-bearing capacity (fracture), where the plasticity criterion is the mechanical properties of a particular material obtained in tensile tests (yield and strength limits, relative elongation), approximated by a power law. The obtained results can be applied in the design of lightweight power structures; in modeling the stress-strain state of metal when developing technological processes of sheet stamping (bending) for calculating the magnitude of thinning, assessing the level of radial stresses in metal bending along the end edge of a pressing punch, as well as when designing bending equipment.

**Keywords:** sheet bending, radius of curvature, thinning, radial stress, plastic buckling, material failure

**Conflicts of interest.** The authors declare that there is no conflict of interest.

**Authors' contribution.** Undivided co-authorship.

**For citation:** Morozov Yu.A., Beleyubskiy B.F. Design of thin-walled single-curvature parts for use in lightweight structures. *Structural Mechanics of Engineering Constructions and Buildings*. 2024;20(4):342–354. (In Russ.). <http://doi.org/10.22363/1815-5235-2024-20-4-342-354>

## 1. Введение

Современное строительство зданий и сооружений предусматривает использование облегченных силовых элементов, среди них светопрозрачные фасадные или навесные системы, обрешеченные стеклянными панелями, упакованными каркасной обвязкой, которую чаще всего выполняют из алюминиевых сплавов или стали (в зависимости от интенсивности действующих нагрузок).

Изготовление алюминиевых профилей прессованием позволяет спроектировать любую их конфигурацию, но высокая стоимость инструментальной оснастки также отражается и на стоимости подобных изделий.

Производство стальных профилей не требует какого-то инструмента индивидуального исполнения и может осуществляться различными схемами формоизменения (гибка, профилирование и пр.). В этом отношении изготовление гнутых профилей является аналогичным производству тонкостенных деталей одинарной кривизны методами листовой штамповки, обеспечивающей требуемую конфигурацию деталей, которые широко применяются в авиа-, судо-, автопромышленности [1; 2].

---

**Yury A. Morozov**, PhD in Technical Sciences, Associate Professor of the Department of Materials Processing Technologies (MT-13), Bauman Moscow State Technical University, Moscow, Russia; eLIBRARY SPIN-code: 3189-5426, ORCID: 0000-0001-9229-7398; e-mail: akafest@mail.ru

**Boris F. Beleyubskiy**, PhD in Technical Sciences, Associate Professor of the Department of Metallurgy, Moscow Polytechnic University, Moscow, Russia; eLIBRARY SPIN-code: 2007-1003, ORCID: 0000-0002-1702-707X; e-mail: alib@bk.ru

При этом актуальным является вопрос определения минимально возможного радиуса изгиба согнутой детали, который в пределе стремится к нулю (рис. 1).

Иногда уменьшение предельно допустимого радиуса изгиба диктуется необходимостью снижения материалоемкости изделия, условиями монтажа и др. При этом использование чрезвычайно малых радиусов гибки приближает конфигурацию листовой профильной детали (уголки, швеллеры и др.) к сечению прессованных профилей, т.е. к показателям большей жесткости [3; 4].

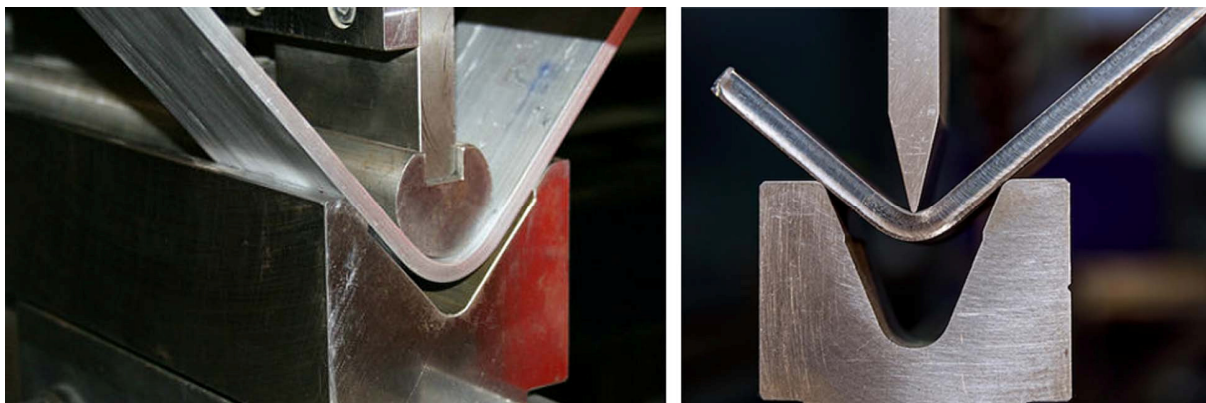


**Рис. 1.** Схема V-образной гибки в штампе

И с т о ч н и к: <https://ugselmash.ru/uslugi/gibka-metalla/gibka-stali;>  
<https://ipmet.ru/razd/metalloobrabotka/gibka-metalla>

**Figure 1.** V-die bending

S o u r c e: <https://ugselmash.ru/uslugi/gibka-metalla/gibka-stali;>  
<https://ipmet.ru/razd/metalloobrabotka/gibka-metalla>

Основной задачей в данном случае является предотвращение разрушения заготовки при ее изгибе, обычно происходящее на выпуклой поверхности радиуса  $R$  (по биссектрисе угла), вследствие больших деформаций растяжения и утонения материала (рис. 2)<sup>1</sup>.

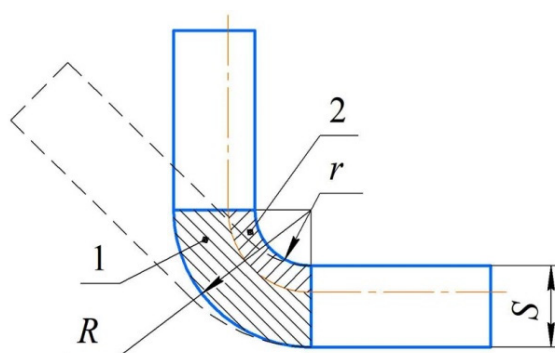


**Рис. 2.** Сечение изогнутой заготовки:

1, 2 — зоны тангенциальных напряжений растяжения и сжатия  
 И с т о ч н и к: выполнено Ю.А. Морозовым

**Figure 2.** Section of a curved workpiece:

1, 2 — zones of tangential tensile and compressive stresses  
 S o u r c e: made by Yu.A. Morozov

<sup>1</sup> Ершов В.И. Интенсификация формоизменяющих операций листовой штамповки. М.: Высшая школа, 1989. 85 с.

Утонение приводит к снижению прочности детали и является дополнительной причиной концентрации напряжений и усталостного разрушения (обычно допустимое утонение ограничивается 20 %).

Технологически процесс гибки (изменение кривизны листового материала) является весьма простой операцией, достаточно освященной в работах отечественных<sup>2</sup> и зарубежных авторов, предлагающих различные методики определения утонения материала и его деформационного упрочнения [5–9].

Однако решение задачи минимального радиуса изгиба требует комплексного рассмотрения кинематики процесса и анализа напряженно-деформированного состояния металла, обусловленного совокупной «игрой» двух деформационных параметров — утонение, приводящее к ослаблению сечения детали, и деформационное упрочнение материала, характеризующее интенсивностью деформаций [10–14].

Следует отметить, что современное программное обеспечение позволяет решать подобные задачи в диалоговом режиме компьютерного моделирования с использованием численных методов или метода конечных элементов [15; 16]. При этом следует учесть, что основой каждого подобного ПО является математический алгоритм, основанный на определенных моделях и допущениях. В связи с этим рассмотрим поведение металла в указанных условиях формирования.

## 2. Метод

Формоизменение гибкой приводит к появлению в материале двух противоположных деформационных процессов: растяжения и сжатия, обуславливающих деформационное изменение первоначальных радиусов  $R_1$  и  $R_2$  (рис. 3)<sup>3</sup> [17; 18].

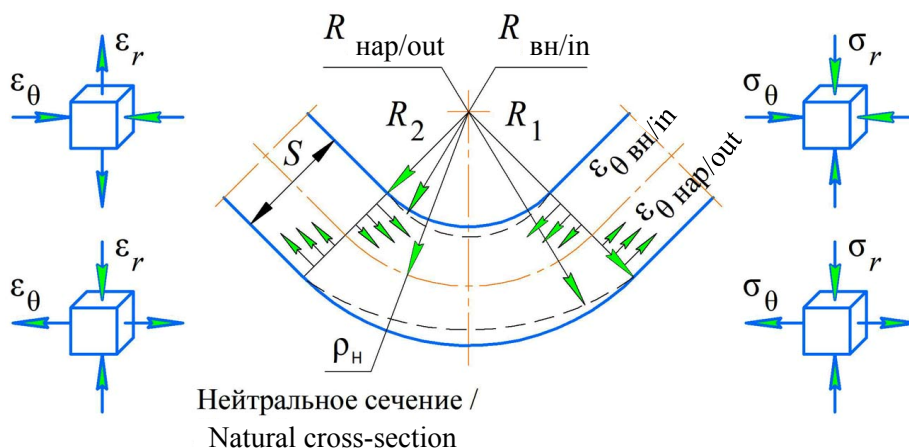


Рис. 3. Распределение тангенциальных деформаций по сечению полосы

И с т о ч н и к: выполнено Ю.А. Морозовым

Figure 3. Distribution of tangential deformations over the strip section

S o u r c e: made by Yu.A. Morozov

<sup>2</sup> Попов Е.А. Основы теории листовой штамповки. М.: Машиностроение, 1977. 278 с.; Зубцов М.Е. Листовая штамповка. Л.: Машиностроение, 1980. 432 с.; Аверкиев Ю.А., Аверкиев А.Ю. Технология холодной штамповки. М.: Машиностроение, 1989. 304 с.

<sup>3</sup> Кохан Л.С., Лебедев Н.Н., Морозов Ю.А., Мочалов Н.А. Проектирование калибров сортовых станков и операций листовой штамповки. М.: МГВМИ, 2007. 340 с.

Наружный радиус  $R_1$  под действием радиальной деформации  $\varepsilon_{r \text{ нар}} < 0$  уменьшается, принимая новое условное значение  $R_{\text{нар}}$ . Внутренний же радиус  $R_2$  увеличивается до  $R_{\text{вн}}$  под действием соответствующей радиальной деформации  $\varepsilon_{r \text{ вн}} > 0$

$$\left. \begin{aligned} R_{\text{нар}} &= R_1 + (R_1 - \rho_n) \varepsilon_{r \text{ нар}} \\ R_{\text{вн}} &= R_2 + (\rho_n - R_2) \varepsilon_{r \text{ вн}} \end{aligned} \right\} \quad (1)$$

Величина утонения будет определяться величиной тангенциальных деформаций, действующих в растянутых и сжатых слоях заготовки, вследствие чего первоначальные радиусы  $R_1$  и  $R_2$  принимают новые продеформированные значения — соответственно  $R_{\text{нар}}$  и  $R_{\text{вн}}$  с границей раздела в нейтральном сечении  $\rho_n$ , в котором тангенциальные деформации  $\varepsilon_\theta$  равны нулю:

$$\left. \begin{aligned} \varepsilon_{\theta \text{ нар}} &= \frac{R_{\text{нар}} - \rho_n}{\rho_n} = \frac{R_{\text{нар}}}{\rho_n} - 1 \\ \varepsilon_{\theta \text{ вн}} &= \frac{\rho_n - R_{\text{вн}}}{\rho_n} = 1 - \frac{R_{\text{вн}}}{\rho_n} \end{aligned} \right\} \quad (2)$$

Совместное решение (1) и (2) устанавливает выражения наружного и внутреннего радиусов (при допущении фиксированного внутреннего радиуса  $R_2 = R_{\text{вн}}$ ):

$$\frac{R_{\text{нар}}}{\rho_n} = \frac{(2 - Z_1) - \sqrt{4Z_1 - 3Z_1^2}}{\sqrt{4Z_1 - 3Z_1^2} - Z_1} + 1, \quad (3a)$$

$$\frac{R_{\text{вн}}}{\rho_n} = 1 + \frac{\frac{R_2}{R_1} - Z_1}{Z_1}, \quad (36)$$

где  $Z_1 = \rho_n/R_1$  — коэффициент, определяющий положение нейтральной поверхности.

Тогда из условия равенства по модулю тангенциальных деформаций в растянутых и сжатых слоях гнутого элемента получаем деформационную модель изгиба, позволяющую последовательно определить положение нейтральной поверхности  $Z_1$  в сечении и установить окончательную толщину полосы для разных значений первоначальных радиусов  $R_1/R_2$ :

$$\varepsilon_{\theta \text{ нар}} = -\varepsilon_{\theta \text{ вн}} \quad \text{или} \quad \frac{(2 - Z_1) - \sqrt{4Z_1 - 3Z_1^2}}{\sqrt{4Z_1 - 3Z_1^2} - Z_1} = \frac{\frac{R_2}{R_1} - Z_1}{Z_1}. \quad (4)$$

С использованием величины утонения при оценке радиальных напряжений изгибаемого материала по торцевой кромке давящего пуансона, можно рассчитать предельный и критический радиус кривизны, допускающий гибку без разрушения гнутого элемента (образование продольных трещин).

Рассмотрим гибку детали на кривизну  $R_1/R_2 = 1,1$ , определяющую следующий характер равновесия тангенциальных деформаций (4):

$$\frac{(2 - Z_1) - \sqrt{4Z_1 - 3Z_1^2}}{\sqrt{4Z_1 - 3Z_1^2} - Z_1} = \frac{1}{1,1} - Z_1$$

Итерационным перебором определяется коэффициент положения нейтральной поверхности  $Z_1 = 0,9535$  (рис. 4).

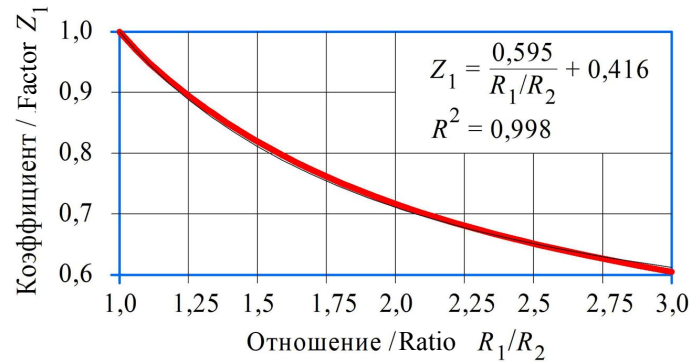


**Рис. 4.** Коэффициент нейтральной поверхности,  $Z_1$

И с т о ч н и к: выполнено Ю.А. Морозовым, Б.Ф. Белелюбским

**Figure 4.** Neutral surface factor,  $Z_1$

S o u r c e: made by Yu.A. Morozov, B.F. Belelyubskiy

Подставляя данное значение в выражения (3а) и (3б), устанавливается относительная величина деформированных радиусов:

$$\begin{aligned} \frac{R_{\text{нар}}}{\rho_n} &= \frac{(2 - Z_1) - \sqrt{4Z_1 - 3Z_1^2}}{\sqrt{4Z_1 - 3Z_1^2} - Z_1} + 1 = \\ &= \frac{(2 - 0,9535) - \sqrt{4 \cdot 0,9535 - 3 \cdot 0,9535^2}}{\sqrt{4 \cdot 0,9535 - 3 \cdot 0,9535^2} - 0,9535} + 1 = 1,0466; \end{aligned}$$

$$\frac{R_{\text{вн}}}{\rho_n} = 1 + \frac{\frac{R_2}{R_1} - Z_1}{Z_1} = 1 + \frac{1}{1,1} - 0,9535 = 0,9534.$$

При исходной толщине листового металла  $S = 0,8$  мм и фиксированном внутреннем радиусе гибки  $R_{\text{вн}}/\rho_n = \text{const}$  устанавливается радиус торового скругления давящего пуансона и радиус нейтральной поверхности

$$r_n = R_2 = R_{\text{вн}} = \frac{S}{\frac{R_1}{R_2} - 1} = \frac{0,8}{1,1 - 1} = 8 \text{ мм};$$

$$\rho_n = Z_1 R_1 = Z_1 \frac{R_1}{R_2} R_2 = 0,9535 \cdot 1,1 \cdot 8 = 8,39 \text{ мм}.$$

Наружный радиус торового скругления

$$R_{\text{нар}} = \frac{R_{\text{нар}}}{\rho_{\text{н}}} \rho_{\text{н}} = 1,0466 \cdot 8,39 = 8,78 \text{ мм.}$$

Коэффициент утонения (рис. 5) [19]

$$\frac{S'}{S} = \frac{Z_1}{1,0 - \frac{1}{R_1/R_2}} \left( \frac{R_{\text{нар}}}{\rho_{\text{н}}} - \frac{r_{\text{н}}}{\rho_{\text{н}}} \right) = \frac{0,9535}{1,0 - \frac{1}{1,1}} \left( 1,0466 - \frac{8}{8,39} \right) = 0,976.$$

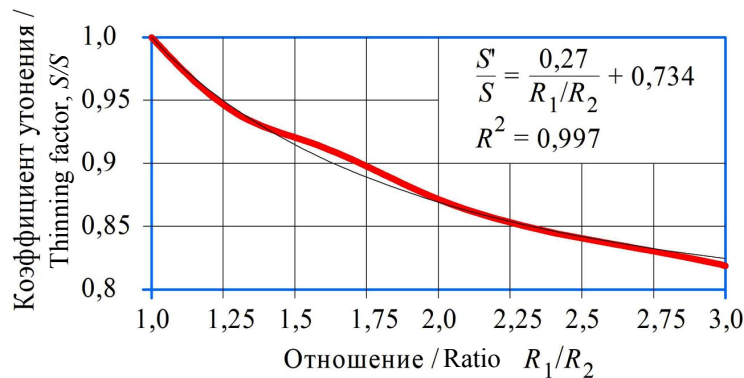


**Рис. 5.** Коэффициент утонения листового металла,  $S'/S$   
Источник: выполнено Ю.А. Морозовым, Б.Ф. Белелюбским  
**Figure 5.** Thinning factor of sheet metal,  $S'/S$   
Source: made by Yu.A. Morozov, B.F. Belelyubskiy

Упрочнение материала при гибке определяется интенсивностью деформаций, т.е. суммарным значением тангенциальных деформаций на наружной и внутренней поверхностях изгибаемой полосы

$$\varepsilon_i = \varepsilon_{\theta_{\text{нар}}} + \varepsilon_{\theta_{\text{вн}}} = \frac{R_{\text{нар}}}{\rho_{\text{н}}} - \frac{R_{\text{вн}}}{\rho_{\text{н}}} = 1,0466 - 0,9534 = 0,093 \text{ (9,3 \%)}.$$

Принимаем модельным материалом сталь  $20^4$  [20], пластичность которой будет устанавливаться механическими свойствами, полученными в испытаниях на растяжение и аппроксимированными степенной зависимостью

$$\sigma_T = \sigma_{0,2} + A \varepsilon_i^n = 245 + 22,4 \cdot 9,3^{0,62} = 334,3 \text{ МПа,}$$

где  $\sigma_{0,2} = 245 \text{ МПа}^5$  — условный предел текучести стали 20;  $A, n$  — коэффициенты упрочнения материала [21].

<sup>4</sup> Арзамасов Б.Н., Макарова В.И., Мухин Г.Г., Рыжов Н.М., Силаева В.И. Материаловедение. М.: МГТУ им. Н.Э. Баумана, 2008. 648 с.

<sup>5</sup> Сталь конструкционная // Марочник стали и сплавов. URL: [http://splav-kharkov.com/choose\\_type\\_class.php?type\\_id=3](http://splav-kharkov.com/choose_type_class.php?type_id=3) (дата обращения: 23.04.2024).



$$n = \frac{\sigma_B \delta}{\sigma_B - \sigma_{0,2}} = \frac{410 \cdot 0,25}{410 - 245} = 0,62;$$

$$A = \frac{\sigma_B - \sigma_{0,2}}{\delta^n} = \frac{410 - 245}{25^{0,62}} = 22,4,$$

где  $\sigma_B = 410$  МПа — предел прочности стали 20;  $\delta = 25$  % — относительное удлинение при разрыве.

Радиальное напряжение при V-образной гибке листового материала на угол 90 градусов ( $\alpha = \pi/2$ ) с использованием коэффициента контактного трения  $f = 0,2$  (табл. 1) [22]:

$$\sigma_{\rho \max} = \frac{\sigma_T}{2\rho_H} \frac{S}{S'/S} e^{f\alpha} = \frac{334,3}{2 \cdot 8,39} \frac{0,8}{0,976} e^{0,2 \cdot \frac{\pi}{2}} = 22,4 \text{ МПа},$$

где  $\sigma_T$  — сопротивление пластической деформации.

Таблица 1

**Напряженно-деформированное состояние металла при гибке**

Кривизна изогнутого элемента $R_1/R_2$	Коэффициент нейтральной поверхности $Z_1 = \rho_H/R_1$	Коэффициент утонения $S'/S$	Интенсивность деформаций $\epsilon_i, \%$	Радиальные напряжения $\sigma_{\rho \max}, \text{ МПа}$
1,1	0,9535	0,976	9,30	22,40
1,3	0,8779	0,938	24,8	78,50
1,5	0,8192	0,919	37,2	137,9
2,0	0,7171	0,871	60,6	290,0
2,5	0,6514	0,840	77,2	432,1
3,0	0,6055	0,819	89,9	558,2

И с т о ч н и к: выполнено Ю.А. Морозовым

Table 1

**The stress-strain state of the metal during bending**

Curvature of a curved element $R_1/R_2$	Neutral surface factor $Z_1 = \rho_H/R_1$	Thinning factor $S'/S$	Deformation intensity $\epsilon_i, \%$	Radial stresses $\sigma_{\rho \max}, \text{ МПа}$
1.1	0.9535	0.976	9.30	22.40
1.3	0.8779	0.938	24.8	78.50
1.5	0.8192	0.919	37.2	137.9
2.0	0.7171	0.871	60.6	290.0
2.5	0.6514	0.840	77.2	432.1
3.0	0.6055	0.819	89.9	558.2

S o u r c e: made by Yu.A. Morozov

Предельный радиус кривизны, допускающий гибку без разрушения гнутого элемента, будет при достижении радиальных напряжений начального предела текучести материала

$$\sigma_{\rho \max} \leq \sigma_{0,2} = 245 \text{ МПа}.$$

Критический радиус кривизны, характеризуемый началом разрушения гнutoго элемента (образование продольных трещин), будет при радиальных напряжениях, сравнимых с пределом прочности данного модельного материала (рис. 6):

$$\sigma_{p\max} < \sigma_B = 410 \text{ МПа.}$$

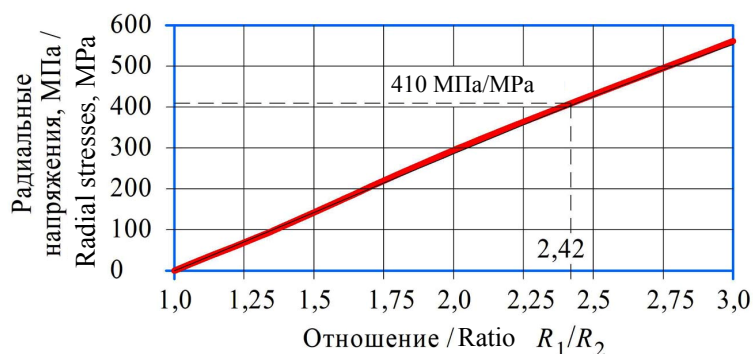


**Рис. 6.** Радиальные напряжения при изгибе листового материала (сталь 20)

И с т о ч н и к: выполнено Ю.А. Морозовым

**Figure 6.** Radial stresses during bending of sheet material (steel 20)

S o u r c e: made by Yu.A. Morozov

Аппроксимируя распределение радиальных напряжений (среднеквадратичная ошибка определения  $R^2 = 0,999$ ), устанавливается критический радиус кривизны  $R_1/R_2 \approx 2,42$ :

$$\begin{aligned} \sigma_{p\max} &= -10 \left( \frac{R_1}{R_2} \right)^2 + 324 \frac{R_1}{R_2} - 320,6 = \\ &= -10 \cdot 2,42^2 + 324 \cdot 2,42 - 320,6 \approx 405 \text{ МПа.} \end{aligned}$$

Для оценки влияния пластических свойств различных металлов ниже рассматриваются некоторые стали, используемые для производства листоштампованных изделий и имеющие различные характеристики прочности и пластичности (табл. 2).

Таблица 2

**Механические свойства материалов для листовой штамповки**

Параметр	Материал			
	Полоса, ГОСТ 1577–93 <sup>1</sup>		Прокат, ГОСТ 1050–88 <sup>2</sup>	
	Сталь 08	Сталь 40	Сталь 15	Сталь 20
Условный предел текучести $\sigma_{0,2}$ , МПа	196	335	225	245
Предел прочности $\sigma_B$ , МПа	320	570	370	410
Относительное удлинение $\delta$ , %	33	19	27	25
Коэффициенты упрочнения $A/n$	6,35/0,85	60,7/0,46	14,9/0,69	22,4/0,62

И с т о ч н и к: выполнено Ю.А. Морозовым

Table 2

**Mechanical properties of sheet stamping materials**

Parameter	Material			
	Strip, GOST 1577–93 <sup>6</sup>		Rolled steel, GOST 1050–88 <sup>7</sup>	
	Steel 08	Steel 40	Steel 15	Steel 20
Proof strength $\sigma_{0,2}$ , МПа / MPa	196	335	225	245
Tensile strength $\sigma_B$ , МПа	320	570	370	410
Relative elongation $\delta$ , %	33	19	27	25
Hardening factors, $A / n$	6.35/0.85	60.7/0.46	14.9/0.69	22.4/0.62

Source: made by Yu.A. Morozov

**3. Результаты и обсуждение**

Анализ интенсивности распределения радиальных напряжений с учетом пластических свойств рассмотренных материалов устанавливает практически одинаковые критические радиусы кривизны, граничащие с разрушением материала при  $R_1/R_2 \leq 2,41...2,45$  (рис. 7).

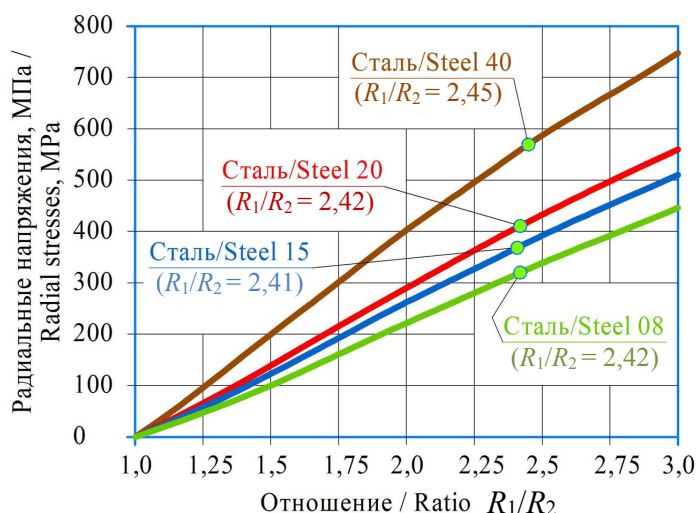


Рис. 7. Радиальные напряжения при изгибе листового материала  
Источники: выполнено Ю.А. Морозовым, Б.Ф. Белелюбским

Figure 7. Radial stresses during bending of sheet material  
Source: made by Yu.A. Morozov, B.F. Belelyubskiy

Найденное значение кривизны, также можно представить фактической величиной критического внутреннего радиуса

$$r_{кр} \geq R_2 = \frac{S}{R_1/R_2 - 1} = \frac{S}{(2,41...2,45) - 1} = (0,71...0,69) S .$$

<sup>6</sup> ГОСТ 1577–93. Прокат толстолистовой и широкополосный из конструкционной качественной стали. Минск: Изд-во стандартов, 2002. 24 с.

<sup>7</sup> ГОСТ 1050–88. Группа В32. Прокат сортовой, калиброванный, со специальной отделкой поверхности из углеродистой качественной. Конструкционной стали. Общие технические условия. М.: Изд-во стандартов, 2003. 33 с.

#### 4. Заключение

В статье проведено исследование минимального (критического) внутреннего радиуса кривизны гнутого элемента, допускающего гибку листового материала без разрушения (образование продольных трещин) на основе математической модели напряженно-деформированного состояния формоизменяемой заготовки. На основании проведенного исследования можно сформулировать следующие выводы:

1. На основе гипотезы плоских сечений представлен метод высчитывания критического радиуса, определяемый интенсивностью деформаций на наружной и внутренней поверхностях изгибаемой заготовки (полосы).

2. Численное моделирование, учитывающее деформационные процессы и механические характеристики прочности и пластичности материала, показало устойчивый рост радиальных напряжений, вызывающих разрушение материала при достижении определенной величины критического радиуса кривизны.

Таким образом, предложены математически обоснованные рекомендации для разработки технологических процессов листовой штамповки или проектирования гибочной оснастки с учетом пластических свойств конкретного материала, что позволит снизить материалоемкость изделия с повышением его жесткости.

Для исключения значительного объема итерационных расчетов, приводятся соответствующие аппроксимационные зависимости, позволяющие с высокой точностью 2...3 % определить положение нейтральной поверхности гнутого элемента и величину утонения материала.

#### Список литературы

1. Власов С.В., Елатонцев Н.А. Баланс напряжений и деформаций при холодной гибке листовой судостроительной стали // Вестник Инженерной школы Дальневосточного федерального университета. 2021. № 1 (46). С. 36–48. <http://www.doi.org/10.24866/2227-6858/2021-1-4>
2. Dang X., He K., Zhang F., Du R. A new flexible sheet metal forming method of incremental bending // *Procedia Manufacturing*. 2018. Vol. 15. P. 1298–1305. <https://doi.org/10.1016/j.promfg.2018.07.355>
3. Морозов Ю.А. Разработка конфигурации гнутых профилей при проектировании светопрозрачных конструкций // Информатика и технологии. Инновационные технологии в промышленности и информатике: сборник докладов Российской научно-технической конференции с международным участием. Москва, 12–13 апреля 2018 года: в 2 т. М.: РТУ МИРЭА, 2018. Т. 2. С. 733–7
4. Морозов Ю.А. Исследование деформированного состояния материала при производстве гнутых профилей // Информатика и технологии. Инновационные технологии в промышленности и информатике: сборник докладов Российской научно-технической конференции с международным участием. Москва, 11–12 апреля 2019 года: в 2 т. М.: РТУ МИРЭА, 2019. Т. 2. С. 288–295. EDN: IFOSTI
5. Ahn K. Plastic bending of sheet metal with tension/compression asymmetry // *International Journal of Solids and Structures*. 2020. Vol. 204–205. P. 65–80. <https://doi.org/10.1016/j.ijsolstr.2020.05.022>
6. Barnwal V.K., Lee S.-L., Jisik Choi, Kim J.-H., Barlat F. Fracture assessment in dual phase and transformation-induced plasticity steels during 3-point bending // *Theoretical and Applied Fracture Mechanics*. 2020. Vol. 110. Article no. 102834. <https://doi.org/10.1016/j.tafmec.2020.102834>
7. Zadpoor A.A., Campoli G., Sinke J., Benedictus R. Fracture in bending — The straining limits of monolithic sheets and machined tailor-made blanks // *Materials & Design*. 2011. Vol. 32. Issue 3. P. 1229–1241. <https://doi.org/10.1016/j.matdes.2010.10.005>
8. Yoshida M., Yoshida F., Konishi H., Fukumoto K. Fracture limits of sheet metals under stretch bending // *International Journal of Mechanical Sciences*. 2005. Vol. 47. Issue 12. P. 1885–1896. <https://doi.org/10.1016/j.ijmecsci.2005.07.006>
9. Романовский В.П. Справочник по холодной штамповке. М.; Л.: Машиностроение, 1979. 520 с.
10. Li F.F., Zhu J., Zhang W., Fang G. Investigation on the inhomogeneous deformation of magnesium alloy during bending using an advanced plasticity model // *Journal of Materials Research and Technology*. 2023. Vol. 25. P. 5064–5075. <https://doi.org/10.1016/j.jmrt.2023.06.264>

11. Li S., He J., Gu B., Zeng D., Xia Z.C., Zhao Y., Lin Z. Anisotropic fracture of advanced high strength steel sheets: Experiment and theory // *International Journal of Plasticity*. 2018. Vol. 103. P. 95–118. <https://doi.org/10.1016/j.ijplas.2018.01.003>
12. Soyarslan C., Malekipour Gharbi M., Tekkaya A.E. A combined experimental-numerical investigation of ductile fracture in bending of a class of ferritic-martensitic steel // *International Journal of Solids and Structures*. 2012. Vol. 49. Issue 13. P. 1608–1626. <https://doi.org/10.1016/j.ijsolstr.2012.03.009>
13. Thomas B. Stoughton, Jeong Whan Yoon. A new approach for failure criterion for sheet metals // *International Journal of Plasticity*. 2011. Vol. 27. Issue 3. P. 440–459. <https://doi.org/10.1016/j.ijplas.2010.07.004>
14. Levy B.S., Van Tyne C.J. Predicting breakage on a die radius with a straight bend axis during sheet forming // *Journal of Materials Processing Technology*. 2009. Vol. 209. Issue 4. P. 2038–2046. <https://doi.org/10.1016/j.jmatprotec.2008.04.053>
15. Bate K., Wilson E. Numerical methods in finite element analysis. Prentice-Hall Publ, 1976; 544 p. 1976. URL: <https://sciariium.com/file/268214/> (accessed: 02.03.2024).
16. Зенкевич О.К. Метод конечных элементов в технике. М.: Мир, 1975. 542 с. URL: <https://djvu.online/file/DtUw9BqXrtZSc> (дата обращения: 02.03.2024).
17. Лукашкин Н.Д., Кохан Л.С., Пунин В.И., Морозов Ю.А. Гибка профилей на прессах и станах. М.: МГВМИ, 2005. 140 с.
18. Кохан Л.С., Роберов И.Г., Морозов Ю.А. Исследование кинематических параметров при гибке листового материала // *Технология металлов*. 2008. № 10. С. 11–13. EDN: IVMCXK
19. Морозов Ю.А. Исследование предельных деформаций листовой вытяжки с учетом пластического утонения и разрушения материала // *Строительная механика инженерных конструкций и сооружений*. 2019. Т. 15. № 5. С. 353–359. <https://doi.org/10.22363/1815-5235-2019-15-5-353-359>
20. Арзамасов Б.Н., Соловьева Т.В., Герасимов С.А. Справочник по конструкционным материалам. М.: МГТУ им. Н.Э. Баумана, 2005. 640 с.
21. Третьяков А.В., Зюзин В.И. Механические свойства металлов и сплавов при обработке давлением: справочник. М.: Металлургия, 1973. 224 с.
22. Исаченков Е.И. Контактное трение и смазки при обработке металлов давлением. М.: Машиностроение, 1978. 208 с.

## References

1. Vlasov S.V., Yelatontsev N.A. Balans napryazheniy i deformatsiy pri kholodnoy gibke listovoy sudostroitel'noy stali. *FEFU: School of Engineering Bulletin*. 2021;(1):36–48. (In Russ.) <http://www.doi.org/10.24866/2227-6858/2021-1-4>
2. Dang X., He K., Zhang F., Du R. A new flexible sheet metal forming method of incremental bending. *Procedia Manufacturing*. 2018;15:1298–1305. <https://doi.org/10.1016/j.promfg.2018.07.355>
3. Morozov Yu.A. Development of the configuration of bent profiles in the design of translucent structures. *Informatics and technologies. Information technologies in industry and informatics. Proceedings of the conference*. Moscow, April 12–13, 2018. Moscow: RTU MIREA Publ.; 2018;2:733–737. (In Russ.) EDN: YWQWPB
4. Morozov Yu.A. Investigation of the deformed state of the material in the production of bent profiles. *Informatics and technologies. Information technologies in industry and informatics. Proceedings of the conference*. Moscow, April 11–12, 2019. Moscow: RTU MIREA Publ.; 2019;2:288–295. (In Russ.) EDN: IFOSTI
5. Ahn K. Plastic bending of sheet metal with tension/compression asymmetry. *International Journal of Solids and Structures*. 2020;204–205:65–80. <https://doi.org/10.1016/j.ijsolstr.2020.05.022>
6. Barnwal V.K., Lee S.-L., Jisik Choi, Kim J.-H., Barlat F. Fracture assessment in dual phase and transformation-induced plasticity steels during 3-point bending. *Theoretical and Applied Fracture Mechanics*. 2020;110:102834. <https://doi.org/10.1016/j.tafmec.2020.102834>
7. Zadpoor A.A., Campoli G., Sinke J., Benedictus R. Fracture in bending — The straining limits of monolithic sheets and machined tailor-made blanks. *Materials & Design*. 2011;32(3):1229–1241. <https://doi.org/10.1016/j.matdes.2010.10.005>
8. Yoshida M., Yoshida F., Konishi H., Fukumoto K. Fracture limits of sheet metals under stretch bending. *International Journal of Mechanical Sciences*. 2005;47(12):1885–1896. <https://doi.org/10.1016/j.ijmecsci.2005.07.006>
9. Romanovskiy V.P. *Handbook of Cold Forming*. Moscow. Leningrad: Mashinostroyeniye. Publ.; 1979. (In Russ.)
10. Li F.F., Zhu J., Zhang W., Fang G. Investigation on the inhomogeneous deformation of magnesium alloy during bending using an advanced plasticity model. *Journal of Materials Research and Technology*. 2023;25:5064–5075. <https://doi.org/10.1016/j.jmrt.2023.06.264>
11. Li S., He J., Gu B., Zeng D., Xia Z.C., Zhao Y., Lin Z. Anisotropic fracture of advanced high strength steel sheets: Experiment and theory. *International Journal of Plasticity*. 2018;103:95–118. <https://doi.org/10.1016/j.ijplas.2018.01.003>

12. Soyarslan C., Malekipour Gharbi M., Tekkaya A.E. A combined experimental-numerical investigation of ductile fracture in bending of a class of ferritic-martensitic steel. *International Journal of Solids and Structures*. 2012;49(13): 1608–1626. <https://doi.org/10.1016/j.ijsolstr.2012.03.009>
13. Stoughton T.B., Yoon J.W. A new approach for failure criterion for sheet metals. *International Journal of Plasticity*. 2011;27(3):440–459. <https://doi.org/10.1016/j.ijplas.2010.07.004>
14. Levy B.S., Van Tyne C.J. Predicting breakage on a die radius with a straight bend axis during sheet forming. *Journal of Materials Processing Technology*. 2009;209(4):2038–2046. <https://doi.org/10.1016/j.jmatprotec.2008.04.053>
15. Bate K., Wilson E. *Numerical methods in finite element analysis*. Prentice-Hall Publ.; 1976. Available from: <https://sciarium.com/file/268214/> (accessed: 02.03.2024).
16. Zenkevich O.K. *The finite element method in engineering*. Moscow: Mir Publ.; 1975. (In Russ.) Available from: <https://djvu.online/file/DtUw9BqXrtZCc> (accessed: 02.03.2024).
17. Lukashkin N.D., Kokhan L.S., Punin V.I., Morozov Yu.A. *Bending of profiles on presses and mills*. Moscow: MGVTI Publ.; 2005. (In Russ.)
18. Kokhan L.S., Roberov I.G., Morozov Yu.A. Investigation into kinematic parameters during bending the sheet materials. *Tekhnologiya metallov*. 2008;(10):11–13. (In Russ.) EDN: IVMCXX
19. Morozov Yu.A. The study of marginal deformations of the leaf extracts with regard to plastic thinning and destruction of the material. *Structural Mechanics of Engineering Constructions and Buildings*. 2019;15(5):353–359. (In Russ.) <https://doi.org/10.22363/1815-5235-2019-15-5-353-359>
20. Arzamasov B.N., Solovyova T.V., Gerasimov S.A. *Handbook of Structural Materials*. Moscow: MSTU named after N.E. Bauman Publ.; 2005. (In Russ.)
21. Tret'yakov A.V., Zyuzin V.I. *Mechanical properties of metals and alloys during pressure treatment. Directory*. Moscow: Metallurgiya Publ.; 1973. (In Russ.)
22. Isachenkov E.I. *Contact friction and lubrication in metal forming*. Moscow: Mashinostroyeniye Publ.; 1978. (In Russ.)

## СЕЙСМОСТОЙКОСТЬ СООРУЖЕНИЙ SEISMIC RESISTENCE

DOI: 10.22363/1815-5235-2024-20-4-355-363

UDC 624.012.4:624.92:699.841

EDN: UAZLMN

Research article / Научная статья

### Behavior of Reinforced Concrete Buildings with Sliding Belt Seismic Isolation and Elastic Limiter of Horizontal Displacements

Oleg V. Mkrtychev<sup>id</sup>, Salima R. Mingazova<sup>id</sup>✉

Moscow State University of Civil Engineering (National Research University), Moscow, Russia

✉ salima.mingazova@yandex.ru

Received: May 21, 2024

Accepted: July 5, 2024

**Abstract.** An effective way of ensuring seismic resistance of buildings and structures is the use of active seismic protection systems — seismic isolation. One known type of seismic isolation is a sliding belt at foundation level. However, the application of this seismic protection system is limited by the lack of necessary design justifications and studies. The behavior of a cast-in-situ reinforced concrete building with different number of storeys (5, 9, 16 floors) with sliding belt seismic isolation at foundation level containing fluoroplastic plates and an elastic limiter of horizontal displacements is considered. The main focus of the study is the effect of the size of the gap between the elastic limiter and the side faces of the upper foundation on the efficiency of the sliding belt. The analysis was carried out using the direct dynamic method. Comparative graphs of relative displacements and the stress intensity distributions for each calculation case are obtained. It is revealed that proximity of the elastic limiter to the foundation increases the likelihood of collision and the emergence of dangerous vibrations that can lead to the failure of the structure. The optimally selected gap size will allow the sliding belt to operate effectively, limiting excessive horizontal displacements, and reduce seismic loads on the superstructure.

**Keywords:** active seismic protection, seismic isolation, earthquake-resistant construction, fluoroplastic plates, direct dynamic method

**Conflicts of interest.** The authors declare that there is no conflict of interest.

**Authors' contribution.** *Mkrtychev O.V.* — scientific guidance, research concept, development of methodology, final conclusions. *Mingazova S.R.* — numerical analysis, evaluation of research results, preparation of text and infographics, final conclusions.

**For citation.** Mkrtychev O.V., Mingazova S.R. Behavior of reinforced concrete buildings with sliding belt seismic isolation and elastic limiter of horizontal displacements. *Structural Mechanics of Engineering Constructions and Buildings*. 2024; 20(4):355–363. <http://doi.org/10.22363/1815-5235-2024-20-4-355-363>

---

*Oleg V. Mkrtychev*, Doctor of Technical Sciences, Professor, Head of the Department of Strength of Materials, Moscow State University of Civil Engineering (National Research University) (MGSU), Moscow, Russia; eLIBRARY SPIN-code: 9676-4986, ORCID: 0000-0002-2828-3693; e-mail: mkrtychev@yandex.ru

*Salima R. Mingazova*, Postgraduate student of the Department of Strength of Materials, Moscow State University of Civil Engineering (National Research University) (MGSU), Moscow, Russia; eLIBRARY SPIN-code: 7506-5852, ORCID 0009-0009-3654-4038; e-mail: salima.mingazova@yandex.ru

© Mkrtychev O.V., Mingazova S.R., 2024

This work is licensed under a Creative Commons Attribution 4.0 International License  
<https://creativecommons.org/licenses/by-nc/4.0/legalcode>

# Работа железобетонных зданий с сейсмоизолирующим скользящим поясом с упругим ограничителем горизонтальных перемещений

О.В. Мкртычев<sup>ID</sup>, С.Р. Мингазова<sup>ID</sup>✉

Национальный исследовательский Московский государственный строительный университет, Москва, Россия  
✉ salima.mingazova@yandex.ru

Поступила в редакцию: 21.05.2024 г.

Принята к публикации: 05.07.2024 г.

**Аннотация.** Эффективным способом обеспечения сейсмостойкости зданий и сооружений является использование активной системы сейсмозащиты — сейсмоизоляции. Известна сейсмоизоляция в виде сейсмоизолирующего скользящего пояса в уровне фундамента. Однако применение данной системы сейсмозащиты ограничивается отсутствием необходимых расчетных обоснований и исследований. Рассмотрена работа монолитного железобетонного здания различной этажности (5, 9, 16 этажей) с сейсмоизолирующим скользящим поясом в уровне фундамента с фторопластовыми пластинами и упругим ограничителем горизонтальных перемещений. Основное внимание уделено влиянию зазора между упругим ограничителем и боковыми гранями верхнего фундамента на эффективность работы скользящего пояса. Расчет проведен с использованием прямого динамического метода. Получены сравнительные графики относительных перемещений и изополя интенсивности напряжений для каждой расчетной ситуации. Выявлено, что близкое расположение упругого ограничителя к фундаменту увеличивает вероятность столкновения и возникновения опасных колебаний, которые могут привести к разрушению конструкции. Оптимально подобранное расстояние позволит эффективно работать скользящему поясу, ограничивая чрезмерные горизонтальные смещения, снизить сейсмические нагрузки на надземные конструкции здания.

**Ключевые слова:** активная сейсмозащита, сейсмоизоляция, сейсмостойкое строительство, фторопластовые пластины, прямой динамический метод

**Заявление о конфликте интересов.** Авторы заявляют об отсутствии конфликта интересов.

**Вклад авторов.** *Мкртычев О.В.* — научное руководство, концепция исследования, развитие методологии, итоговые выводы. *Мингазова С.Р.* — проведение численных исследований, анализ результатов исследования, подготовка исходного текста, подготовка инфографиков, итоговые выводы.

**Для цитирования:** *Mkrtychev O.V., Mingazova S.R.* Behavior of reinforced concrete buildings with sliding belt seismic isolation and elastic limiter of horizontal displacements // *Строительная механика инженерных конструкций и сооружений*. 2024. Т. 20. № 4. С. 355–363. <http://doi.org/10.22363/1815-5235-2024-20-4-355-363>

## 1. Introduction

Seismic resistance of buildings and structures is an important aspect of engineering design and construction in earthquake-prone regions. With increasing urbanization and development of cities, involving construction in complex geological conditions, the problem of seismic resistance is becoming more and more relevant and important. Earthquakes can cause loss of life, destruction of infrastructure and significant economic losses, so it is important to ensure the safety and stability of buildings and structures against possible seismic impacts.

Many experts around the world are actively engaged in research and development of methods and technologies in the field of earthquake-resistant construction, contributing to this important field. The research papers of Ya.M. Eisenberg [1], O.V. Mkrtychev [2], I. Mirzaev [3], V.I. Smirnov [4], N. Maureira-Carsalade [5], M. Erdik [6], P.M. Calvi [7] and others [8–16] consider methods of increasing earthquake resistance of buildings and structures using various types of active seismic protection systems, including sliding belt

---

*Мкртычев Олег Вартанович*, доктор технических наук, профессор, заведующий кафедрой сопротивления материалов, Национальный исследовательский Московский государственный строительный университет (НИУ МГСУ), Москва, Россия; eLIBRARY SPIN-код: 9676-4986, ORCID: 0000-0002-2828-3693; e-mail: mkrtychev@yandex.ru

*Мингазова Салима Рафиловна*, аспирант кафедры сопротивления материалов, Национальный исследовательский Московский государственный строительный университет (НИУ МГСУ), Москва, Россия; eLIBRARY SPIN-код: 7506-5852, ORCID 0009-0009-3654-4038; e-mail: salima.mingazova@yandex.ru



base isolation. The authors of papers [17–19] investigated the sensitivity of seismic isolation systems under different parameters of the external seismic loading and the structure, as well as the influence of seismic isolation parameters under the optimal design of structures. In [20–22] the issues of seismic isolation of nuclear power plants are considered. In [23; 24], the influence of damping and its parameters on the performance of seismic isolation was studied.

The subject of this study is the performance of sliding belt base isolation with fluoroplastic plates (PTFE) during earthquake.

The purpose of the study is to analyze the influence of the elastic limiter of horizontal displacements on the efficiency of the sliding belt base isolation.

The main objectives of the study are:

- 1) development of a model of a cast-in-situ reinforced concrete building with sliding belt base isolation and an elastic limiter of horizontal displacements;
- 2) analysis of the cast-in-situ reinforced concrete building with sliding belt base isolation and an elastic limiter of horizontal displacements under an intense earthquake using the direct dynamic method;
- 3) examination of the results of the numerical study and evaluation of the influence of the elastic limiter on the efficiency of the sliding belt.

## 2. Method

The behavior of a cast-in-situ reinforced concrete building of different storeys (5, 9, 16 floors) with sliding belt seismic isolation and an elastic limiter of horizontal displacements on a rigid base has been investigated (Figures 1, 2).

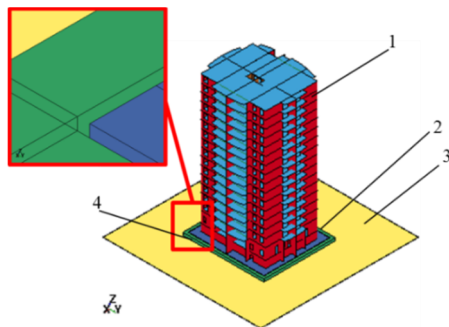


**Figure 1.** Model of a 16-storey building with a sliding belt and an elastic limiter of horizontal displacements:

- 1 — cast-in-situ reinforced concrete building with upper foundation;  
 2 — contact surface (PTFE+PTFE); 3 — lower foundation on rigid base;  
 4 — elastic limiter of horizontal displacements (sand)

Source: compiled by S.R. Mingazova in the LS-DYNA program

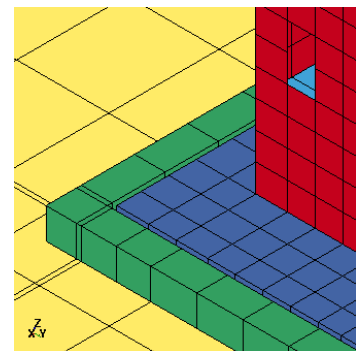


**Figure 2.** Fragment of the finite element model

Source: compiled by S.R. Mingazova in the LS-DYNA program

A material combination of PTFE over PTFE with a sliding friction coefficient of  $\mu = 0.05$  is used as the friction minimization component.

Compacted sand with the following mechanical characteristics is used as the elastic limiter of horizontal displacements:  $\rho = 1680 \text{ kg/m}^3$ ,  $E = 100 \text{ MPa}$ .

The elastic limiter is installed along the perimeter of the upper foundation at a particular distance. The value of the distance from the side edges of the upper foundation to the side edges of the sand should be selected in such a way as to ensure the efficiency of the sliding belt on one hand, and on the other hand, to prevent large residual displacements that may adversely affect the structure, including service lines. In the course of the study, the cases when the distance between the sand and the upper foundation is 5, 10, 15, 20 cm were considered.

The height and width of the sand is assumed to be 1 m. The concrete-sand sliding coefficient of friction is 0.3.

The initial data of the considered cast-in-situ reinforced concrete buildings are given in [25–27].

The analysis was performed by the direct dynamic method in *LS-DYNA* software using explicit schemes of direct integration of the equation of motion. The nonlinear behavior of concrete (*024 MAT PIECEWISE LINEAR PLASTICITY*) and elastic behavior of sand (*001 MAT ELASTIC*) were adopted in the analysis [28].

The intensity of the earthquake is 9 on the MSK-64 scale. A rigid base problem in a non-inertial reference frame is considered. The external seismic loading is specified using the accelerogram of the ground surface, which is the result of the combined ground motion due to the incoming waves from the interior of the earth (longitudinal, transverse and surface waves). The equation of motion of a system with a finite number of degrees of freedom in this case is written in the following form [29]:

$$[M]\ddot{\vec{U}} + [C]\dot{\vec{U}} + [K]\vec{U} = -[M] \cdot \vec{1} \cdot a_0(t),$$

where  $[M]$  is the mass matrix;  $[C]$  is the damping matrix;  $[K]$  is the stiffness matrix;  $\dot{\vec{U}}$  is the vector of velocities of the concentrated masses;  $\ddot{\vec{U}}$  is the vector of accelerations of the concentrated masses;  $\vec{U}$  is the vector of displacements of the concentrated masses;  $a_0(t)$  is the acceleration of seismic motion.

When analyzing a building with seismic isolation in the form of a sliding belt at the foundation level, it is necessary to take into account that, generally, the worst case for such structure is a low-frequency external seismic loading, which can, for example, lead to large residual displacements. Therefore, a two-component accelerogram with a dominant frequency of 1.04 Hz in the X-axis and 0.83 Hz in the Y-axis was considered as an external seismic load (Figures 3, 4).

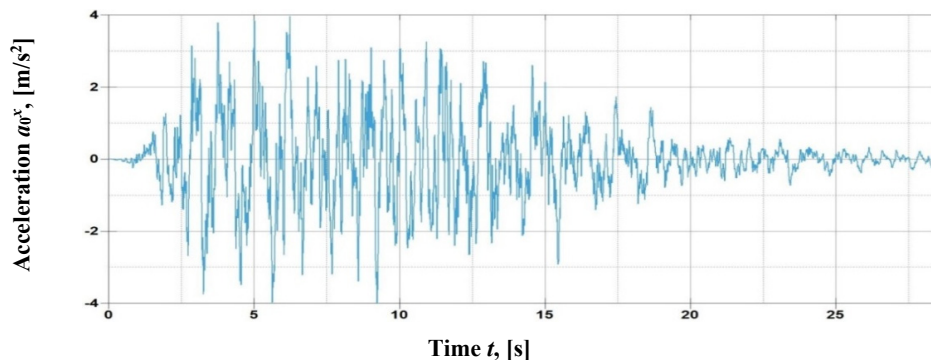


**Figure 3.** Single-component earthquake accelerogram in X direction for the 16-storey building  
Source: compiled by S.R. Mingazova in the LS-DYNA program

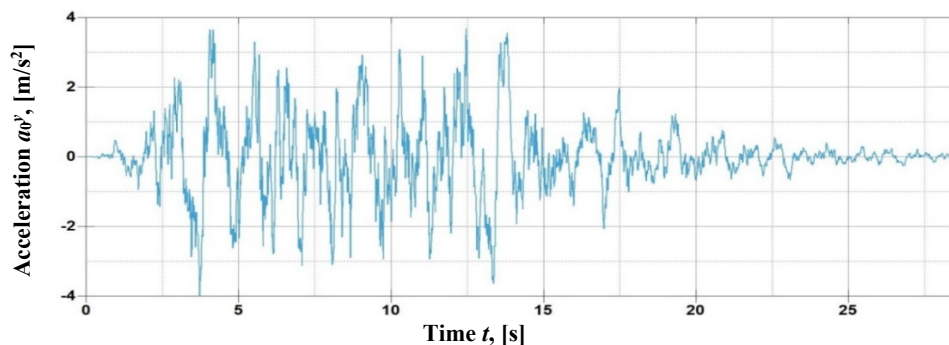


**Figure 4.** Single-component earthquake accelerogram in Y direction for the 16-storey building  
Source: compiled by S.R. Mingazova in the LS-DYNA program

### 3. Results and Discussion

Below are comparative graphs of relative displacements of the 1st floor of the 5-storey building along the  $X$  and  $Y$  axis without seismic isolation, with seismic isolation and without elastic limiter, with seismic isolation and with an elastic limiter of horizontal displacements located at a distance of 5, 10, 15 cm (Figures 5, 6).

It should be noted that in all figures for the 5-storey and 9-storey building there is no graph of relative displacement of the 1st floor in the case when the elastic limiter is installed at a distance of 20 cm from the side edges of the upper foundation, because the displacement of the upper foundation is less than this distance. This analysis case is similar to the case of a building with seismic isolation and without an elastic limiter.

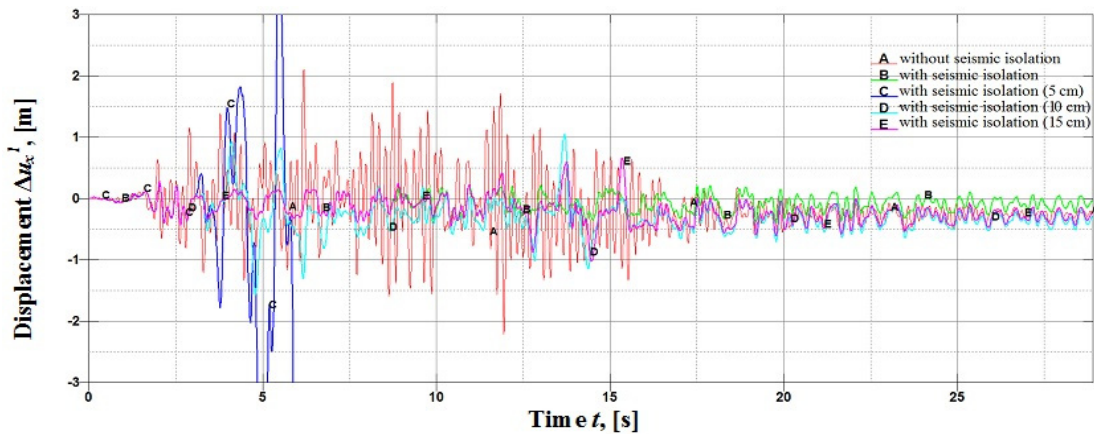


**Figure 5.** Displacement of the top of the 1st floor of the 5-storey building relative to its bottom along the  $X$  axis  
 Source: compiled by S.R. Mingazova in the LS-DYNA program

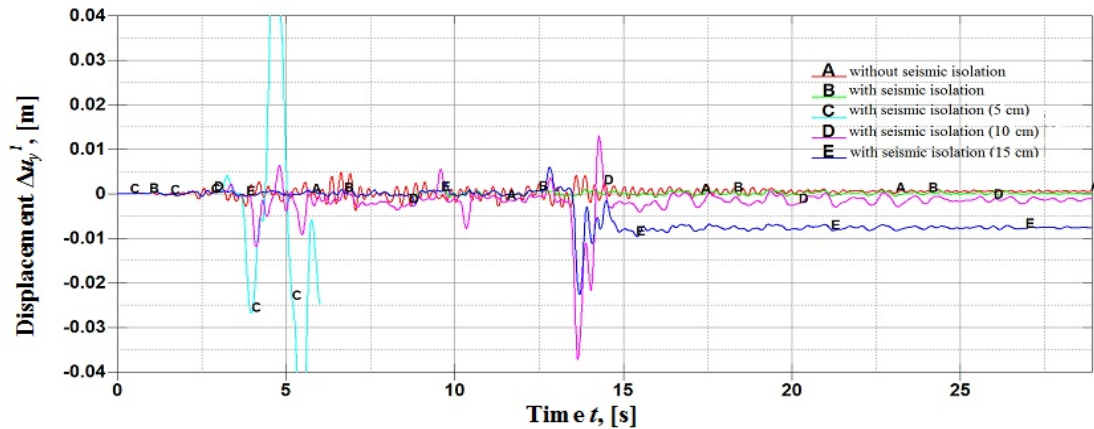


**Figure 6.** Displacement of the top of the 1st floor of the 5-storey building relative to its bottom along the  $Y$  axis  
 Source: compiled by S.R. Mingazova in the LS-DYNA program

Below are comparative graphs of relative displacements of the 1st floor of the 9-storey building along the  $X$  and  $Y$  axis without seismic isolation, with seismic isolation and without elastic limiter, with seismic isolation and with an elastic limiter at a distance of 5, 10, 15 cm (Figures 7, 8).

Below are comparative graphs of relative displacements of the 1st floor of the 16-storey building along the  $X$  and  $Y$  axis without seismic isolation, with seismic isolation and without elastic limiter, with seismic isolation and with an elastic limiter at a distance of 5, 10, 15 cm (Figures 9, 10).

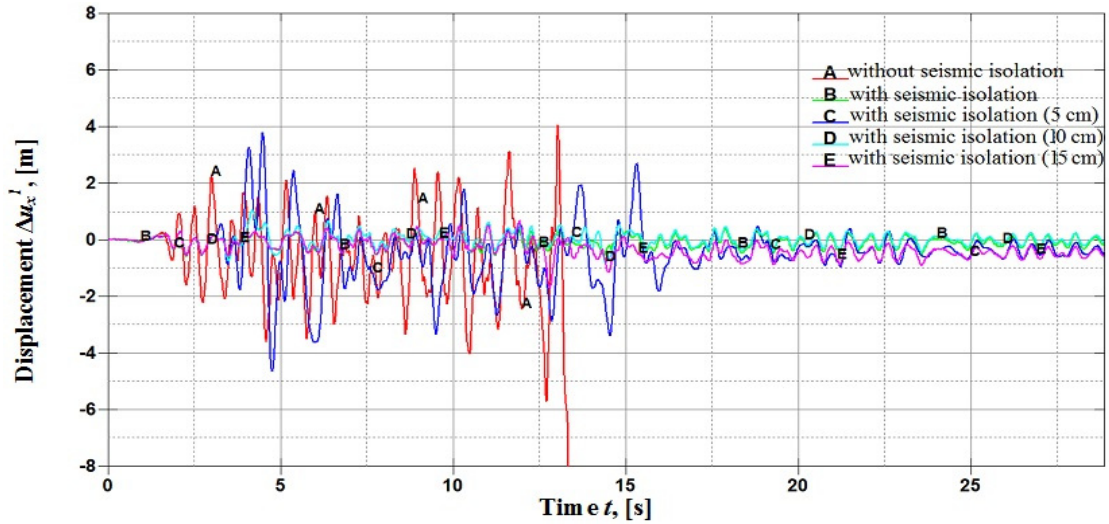


**Figure 7.** Displacement of the top of the 1st floor of the 9-storey building relative to its bottom along the  $X$  axis  
 Source: compiled by S.R. Mingazova in the LS-DYNA program

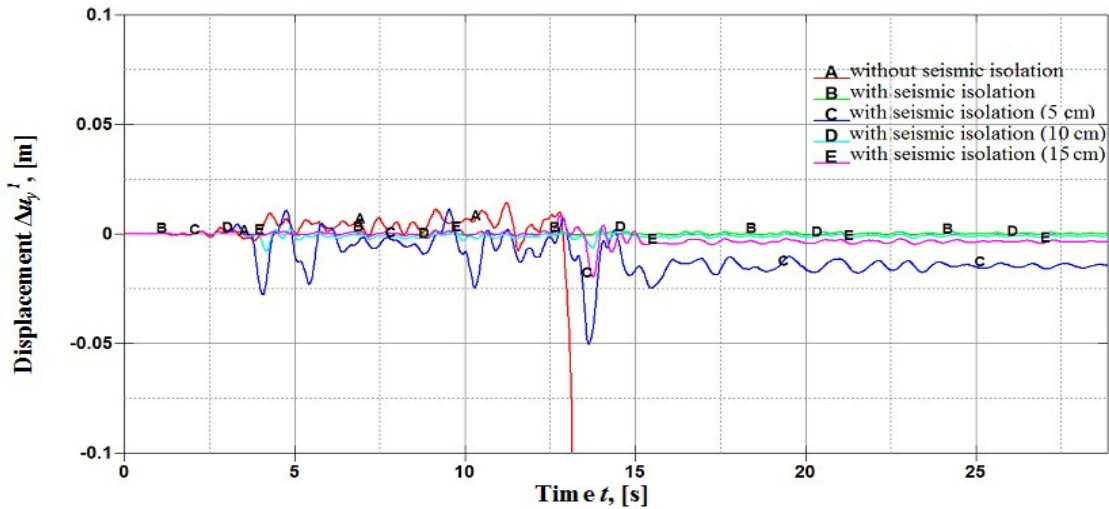


**Figure 8.** Displacement of the top of the 1st floor of the 9-storey building relative to its bottom along the  $Y$  axis  
 Source: compiled by S.R. Mingazova in the LS-DYNA program

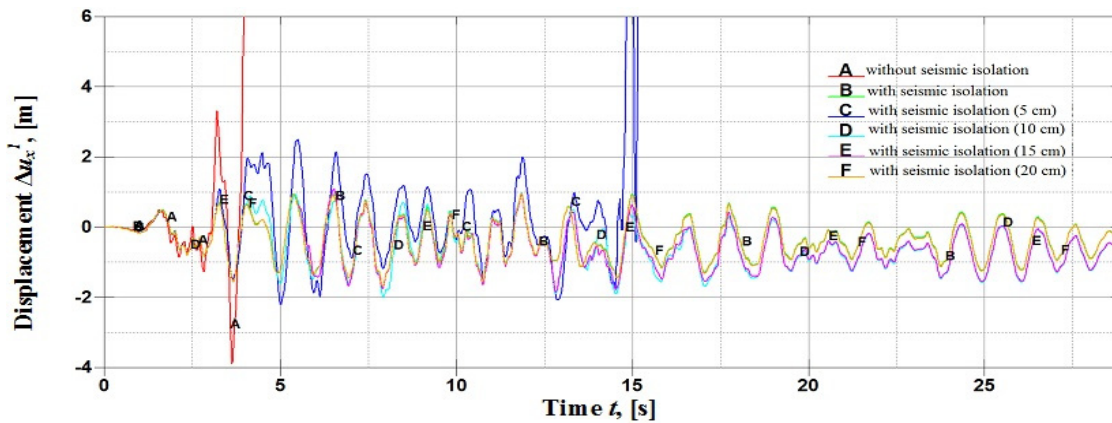


**Figure 9.** Displacement of the top of the 1st floor of the 16-storey building relative to its bottom along the  $X$  axis  
 Source: compiled by S.R. Mingazova in the LS-DYNA program

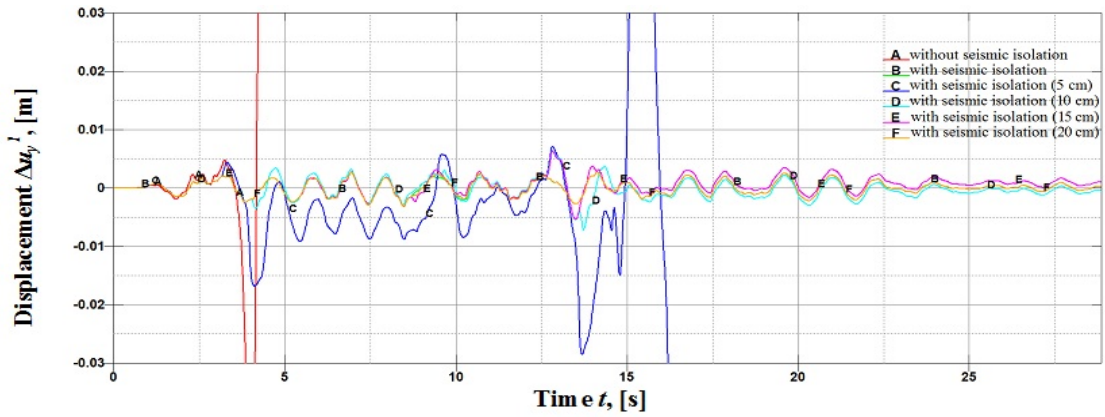


**Figure 10.** Displacement of the top of the 1st floor of the 16-storey building relative to its bottom along the  $X$  axis  
 Source: compiled by S.R. Mingazova in the LS-DYNA program

Figure 11 presents the stress intensity distributions for the 9-storey building with a PTFE sliding belt and an elastic limiter of horizontal displacements (at a distance of 5, 10, 15, 20 cm).

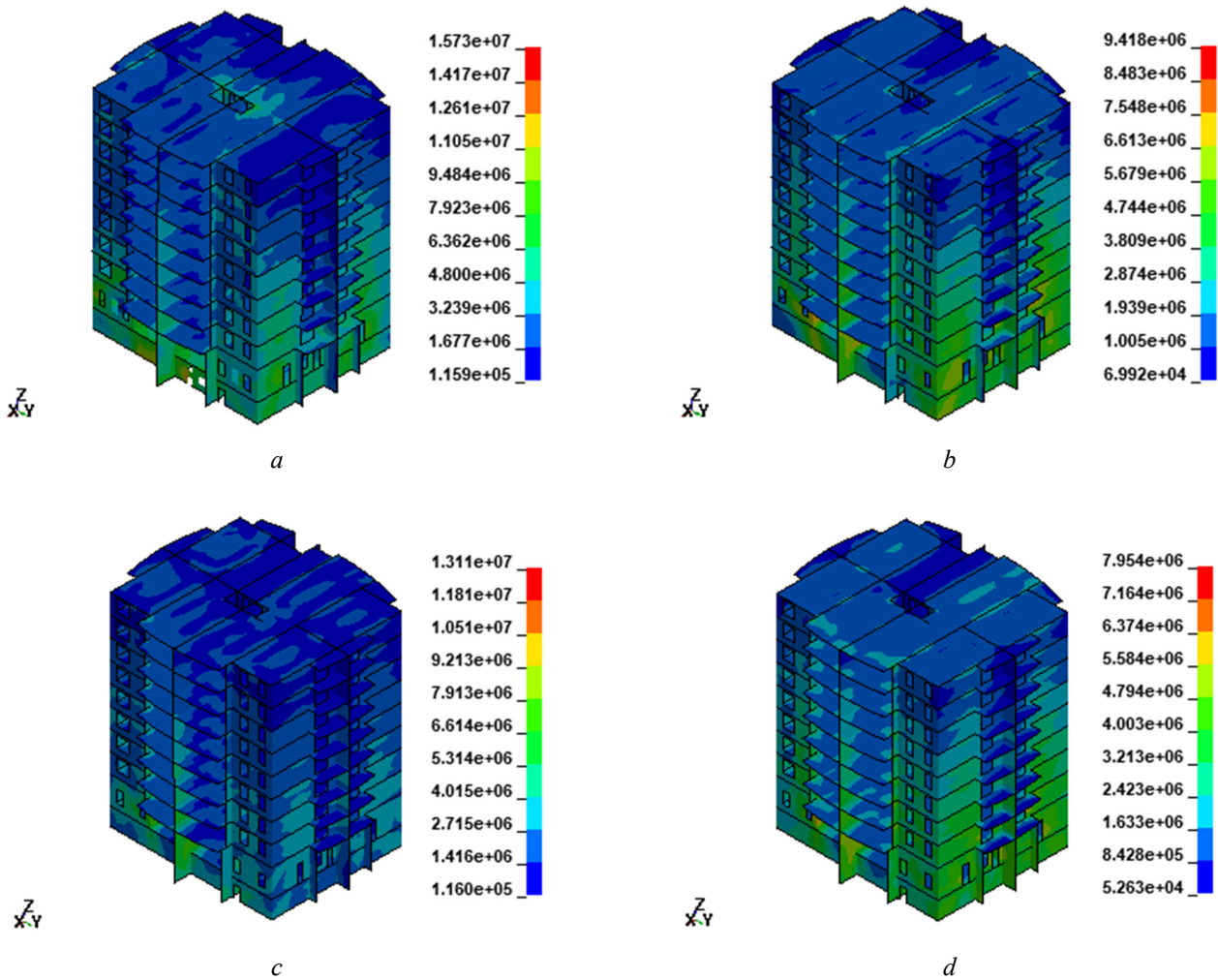


**Figure 11.** Stress intensity distribution (in units of Pa) at time  $t=13.20$  s of the 9-storey building with seismic isolation and elastic limiter of horizontal displacements at a distance of:  $a$  — 5 cm;  $b$  — 10 cm;  $c$  — 15 cm;  $d$  — 20 cm  
 Source: compiled by S.R. Mingazova in the LS-DYNA program

The analysis of the obtained results shows that at a distance of 5 cm between the sand and the upper foundation, the worst outcome — collapse — is observed for the 5- and 16-storey buildings. This is due to the fact that at the moment of impact of the upper foundation with the sand, strong vibrations of the building and large relative displacements occur.

As the distance between the upper foundation and the elastic limiter increases, the probability of collision decreases. The farther away the elastic limiter is located, the smaller the building vibrations and relative displacements will be, which is observed in the results of the 5, 9-storey and 16-storey buildings. The case where the distance between the upper foundation and the elastic limiter is 20 cm is similar to the case without the elastic limiter, where the lowest relative displacement of the storey is observed.

#### 4. Conclusion

The following conclusions are made based on the obtained results:

1. If the elastic limiter is close to the foundation (5 cm), the probability of impact increases, causing dangerous vibrations and structural damage.

2. When selecting the optimal gap size, it is necessary to ensure that this distance facilitates the performance of the sliding belt on one hand and is not too large on the other hand.

3. Despite of the fact that it is quite obvious that when the elastic limiter is close to the foundation, the probability of impact increases, causing dangerous vibrations and failure, the conducted studies allow to determine the value of the most optimal gap, which would ensure the efficiency of the sliding belt, limit excessive horizontal displacements and at the same time would not be too large.

4. The results of the numerical study show that the position of the elastic limiter of horizontal displacements critically affects the performance of the seismic isolation. With an optimally selected gap, this type of seismic isolation significantly reduces seismic loads on the superstructure, which allows to increase its stability and safety during earthquake.

The proposed analysis method of a cast-in-situ reinforced concrete building with seismic isolation by the direct dynamic method, based on explicit schemes of direct integration of the equation of motion, allows to obtain a solution in the time domain, taking into account the nonlinear behavior of the structure. The developed calculation method and research results can be used by design and research organizations in the construction of buildings and structures in earthquake-prone areas.

#### References / Список литературы

1. Eisenberg Ya.M., Smirnov V.I. Seismic safety of structures and settlements. Innovative solutions. *Urban planning*. 2013;(1):57–64. (In Russ.) EDN: PYWRPV  
*Айзенберг Я.М., Смирнов В.И.* Сейсмобезопасность сооружений и поселений. Инновационные решения // Градостроительство. 2013. № 1 (23). С. 57–64. EDN: PYWRPV
2. Mkrtychev O.V., Bubnov A.A. Features of calculating a seismically insulated building by displacement. *Vestnik MGSU*. 2014;(6):63–70. (In Russ.) EDN: SIJYDH  
*Мкртычев О.В., Бунов А.А.* Особенности расчета сейсмоизолированного здания по перемещениям // Вестник МГСУ. 2014. № 6. С. 63–70. EDN: SIJYDH
3. Mirzaev I., Turdiev M. Vibrations of buildings with sliding foundations under real seismic effects. *Construction of Unique Buildings and Structures*. 2021;1(94):9407. <https://doi.org/10.4123/CUBS.94.7>
4. Smirnov V.I. Application of innovative technologies of seismic isolation of buildings in seismic zone. *Earthquake engineering. Constructions safety*. 2009;(4):16–23. (In Russ.) EDN: QCLRRB  
*Смирнов В.И.* Применение инновационных технологий сейсмозащиты зданий в сейсмических районах // Сейсмостойкое строительство. Безопасность сооружений. 2009. № 4. С. 16–23. EDN: QCLRRB
5. Maureira-Carsalade N., Pardo E., Oyarzo-Vera C., Roco A. A roller type base isolation device with tensile strength. *Engineering structures*. 2020;221:111003. <https://doi.org/10.1016/j.engstruct.2020.111003>
6. Erdik M., Ulker O., Sadan B, Tuzun C. Seismic isolation code developments and significant applications in Turkey. *Soil dynamics and earthquake engineering*. 2018;115:413–437. <https://doi.org/10.1016/j.soildyn.2018.09.009>
7. Paolo M. Calvi, Gian Michele Calvi. Historical development of friction-based seismic isolation systems. *Soil dynamics and earthquake engineering*. 2018;106:14–30. <https://doi.org/10.1016/j.soildyn.2017.12.003>

8. Takafumi Fujita Dr. Seismic isolation of civil buildings in Japan. *Progress in structural engineering and materials*. 2005;1(3). <https://doi.org/10.1002/pse.2260010311>
  9. Zhou F.L. Seismic isolation of civil buildings in the People's Republic of China. *Progress in structural engineering and materials*. 2001;3(3):268–276. <https://doi.org/10.1002/pse.85>
  10. Avinash A.R., Krishnamoorthy A., Kamath K., Chaithra M. Sliding isolation systems: historical review, modeling techniques, and the contemporary trends. *Buildings*. 2022;12(11):8–23. <https://doi.org/10.3390/buildings12111997>
  11. Asaad R., Kaadan A. Retrofitting existing masonry structures by using seismic base isolation system. *Arabian journal for science and engineering*. 2023;49:5243–5254. <https://doi.org/10.1007/s13369-023-08381-9>
  12. Warn G.P., Ryan K.L. A Review of seismic isolation for buildings: historical development and research needs. *Buildings*. 2012;(2):300–325. <https://www.mdpi.com/2075-5309/2/3/300>
  13. Patil A.Y., Patil R.D. A review on seismic analysis of a multistoried steel building provided with different types of damper and base isolation. *Asian journal of civil engineering*. 2024;25:3277–3283. <https://doi.org/10.1007/s42107-023-00978-7>
  14. Cardone D., Flora A., Gesualdi G. Inelastic response of RC frame buildings with seismic isolation. *Earthquake engineering and structural dynamics*. 2013;42(6):871–889. <https://doi.org/10.1002/eqe.2250>
  15. Hou S., Chen Y., Wu H., Wang Z. Seismic isolation design and analysis of a complex medical building. *Structural concrete*. 2024;25(3):1495–1498. <https://doi.org/10.1002/suco.202300832>
  16. Banovic I., Radnic J., Grgic N., Matesan D. The use of limestone sand for the seismic base isolation of structures. *Advances in Civil Engineering*. 2018;(6):1–12 <https://doi.org/10.1155/2018/9734283>
  17. Dushimimana A., Dushimimana C., Mbereyaho L., Niyonsenga A.A. Effects of building height and seismic load on the optimal performance of base isolation system. *Arabian journal for science and engineering*. 2023;48:13283–13302. <https://doi.org/10.1007/s13369-023-07660-9>
  18. Leblouba M. Selection of seismic isolation system parameters for the near-optimal design of structures. *Scientific Reports*. 2022;12:14734. <https://doi.org/10.1038/s41598-022-19114-7>
  19. Politopoulos I., Pham H. Sensitivity of seismically isolated structures. *Earthquake engineering and structural dynamics*. 2009;38(8):989–1007. <https://doi.org/10.1002/eqe.879>
  20. Whittaker A.S., Sollogoub P., Kim M.K. Seismic isolation of nuclear power plants: past, present and future. *Nuclear Engineering and Design*. 2018;338:290–299. <https://doi.org/10.1016/j.nucengdes.2018.07.025>
  21. Yu C.-C., Bolisetti C., Coleman J.L., Kosbab B., Whittaker A.S. Using seismic isolation to reduce risk and capital cost of safety-related nuclear structures. *Nuclear engineering and design*. 2018;326:268–284. <https://doi.org/10.1016/j.nucengdes.2017.11.016>
  22. Lo Frano R. Benefits of seismic isolation for nuclear structures subjected to severe earthquake. *Science and technology of nuclear installations*. 2018;2018(1):8017394. <https://doi.org/10.1155/2018/8017394>
  23. Hall J.F. The role of damping in seismic isolation. *Earthquake engineering and structural dynamics*. 1999; 28(12):1717–1720. [https://doi.org/10.1002/\(SICI\)1096-9845\(199901\)28:1<3::AID-EQE801>3.0.CO;2-D](https://doi.org/10.1002/(SICI)1096-9845(199901)28:1<3::AID-EQE801>3.0.CO;2-D)
  24. Du Y., Li H., Spencer B.F. Effect of non-proportional damping on seismic isolation. *Journal of structural control*. 2002;9(3):205–236. <https://doi.org/10.1002/stc.13>
  25. Mkrtychev O., Mingazova S. Analysis of the reaction of reinforced concrete buildings with a varying number of stories with a seismic isolation sliding belt to an earthquake. *IOP Conference series: materials science and engineering*. 2020;869:052065. <https://doi.org/10.1088/1757-899X/869/5/052065>
  26. Mkrtychev O., Mingazova S. Numerical analysis of antiseismic sliding belt performance. *International Journal for Computational Civil and Structural Engineering*. 2023;19(2):161–171. <https://doi.org/10.22337/2587-9618-2023-19-2-161-171>
  27. Mkrtychev O., Mingazova S. Study of the seismic isolation sliding belt: The case of a monolithic reinforced concrete building. *Journal of Physics: Conference Series*. 2020;1425(1):012161. <https://doi.org/10.1088/1742-6596/1425/1/012161>
  28. LS-DYNA. KEYWORD users manual. Volume I, II. *Livermore Software Technology Corporation (LSTC)*. P. 3186.
  29. Mkrtychev O.V., Jinchvelashvili G.A. *Problems of accounting for nonlinearities in the theory of seismic resistance (hypotheses and misconceptions): monograph*. Moscow: MGSU; 2014. (In Russ.) ISBN 978-5-7264-0801-9
- Мкртычев О.В., Джинчвелашвили Г.А. Проблемы учета нелинейностей в теории сейсмостойкости (гипотезы и заблуждения): монография. Москва: МГСУ, 2014. 192 с. ISBN978-5-7264-0801-9

## ТЕОРИЯ ПЛАСТИЧНОСТИ THEORY OF PLASTICITY


DOI: 10.22363/1815-5235-2024-20-4-364-373

UDC 539.42

EDN: TCMXGL

Scientific review / Научный обзор

### Is It Possible to Determine the Whole Crack Path at Once?

Evgeny M. Morozov<sup>1</sup>, Arslan K. Kurbanmagomedov<sup>2</sup><sup>1</sup> National Research Nuclear University MEPhI, Moscow, Russia<sup>2</sup> RUDN University, Moscow, Russia kurbanmagomedov\_ak@pfur.ru

Received: April 14, 2024

Accepted: July 3, 2024

**Abstract.** A brief review of crack path calculation methods using integral principles of mechanics is presented. In two-dimensional setting, a crack is considered as a geodesic line on the surface of a body with a metric that depends on the initial stress state. The possibility of approximate determination of crack path on the basis of integral principles is illustrated on a number of problems. In particular, crack paths in a half-plane under uniformly distributed load applied on its edge are determined. The calculations include the stress state of the half-plane taken from the solution for a body without a crack. The fruitfulness of the representation of displacements of crack edges using the Winkler's hypothesis is shown. To study the subcritical behavior of the crack, the concept of cracon, a quasi-particle simulating the motion of the crack tip, can be introduced. The problem of determining the crack path on the basis of integral principles of mechanics is insufficiently investigated and requires further research.

**Keywords:** fracture mechanics, solid mechanics, cracks path, quasi-brittle fracture, fracture stress, composite material

**Conflicts of interest.** The authors declare that there is no conflict of interest.

**Authors' contribution.** *Morozov E.M.* — scientific guidance, research concept, development of methodology, final conclusions. *Kurbanmagomedov A.K.* — numerical analysis, evaluation of research results, preparation of text and infographics, final conclusions.

**For citation:** Morozov E.M., Kurbanmagomedov A.K. Is it possible to determine the whole crack path at once? *Structural Mechanics of Engineering Constructions and Buildings*. 2024;20(4):364–373. <http://doi.org/10.22363/1815-5235-2024-20-4-364-373>

---

**Evgeny M. Morozov**, Doctor of Technical Sciences, Professor Professor of the Department of Density Physics, National Research Nuclear University MEPhI (Moscow Engineering Physics Institute) Moscow, Russia; eLIBRARY SPIN-code: 3989-2934, ORCID: 0000-0002-4824-8481; e-mail: [evgeny.morozof@gmail.com](mailto:evgeny.morozof@gmail.com)

**Arslan K. Kurbanmagomedov**, Candidate of Physical and Mathematical Sciences, senior lecturer, Nikolskii Mathematical Institute, RUDN University, Moscow, Russia; eLIBRARY SPIN-code: 5262-5269, ORCID: 0000-0001-9158-0378; e-mail: [kurbanmagomedov\\_ak@pfur.ru](mailto:kurbanmagomedov_ak@pfur.ru)

© Morozov E.M., Kurbanmagomedov A.K., 2024

This work is licensed under a Creative Commons Attribution 4.0 International License  
<https://creativecommons.org/licenses/by-nc/4.0/legalcode>



## Возможно ли определение траектории трещины сразу и в целом?

Е.М. Морозов<sup>1</sup>, А.К. Курбанмагомедов<sup>2</sup>

<sup>1</sup> Национальный исследовательский ядерный университет МИФИ, Москва, Россия

<sup>2</sup> Российский университет дружбы народов, Москва, Россия

✉ kurbanmagomedov\_ak@pfur.ru

Поступила в редакцию: 14 апреля 2024 г.

Принята к публикации: 3 июля 2024 г.

**Аннотация.** Представлен краткий обзор методов расчета траектории трещины с использованием интегральных принципов механики. В двумерной постановке трещина рассматривается как геодезическая линия на поверхности тела с метрикой, которая зависит от начального напряженного состояния. Возможность приближенного определения траектории трещины на основе интегральных принципов проиллюстрирована на ряде задач. В частности, определены траектории трещины в полуплоскости под действием равномерно распределенной нагрузки на ее кромку. Расчеты включают напряженное состояние полуплоскости, взятое из решения для тела без трещины. Показана плодотворность представления смещений краев трещины с помощью гипотезы Винклера. Для изучения докритического поведения трещины может быть введено понятие *сгасоп* — квазичастицы, имитирующей движение вершины трещины. Проблема определения траектории трещины на основе интегральных принципов механики изучена недостаточно и требует дальнейших исследований.

**Ключевые слова:** фрактальная механика, механика твердого тела, траектория трещины, квазихрупкий фрактал, фрактальное напряжение, композиционный материал

**Заявление о конфликте интересов.** Авторы заявляют об отсутствии конфликта интересов.

**Вклад авторов.** *Морозов Е.М.* — научное руководство, концепция исследования, развитие методологии, итоговые выводы. *Курбанмагомедов А.К.* — проведение численных исследований, анализ результатов исследования, подготовка исходного текста, подготовка инфографиков, итоговые выводы.

**Для цитирования:** *Morozov E.M., Kurbanmagomedov A.K.* Is it possible to determine the whole crack path at once? // Строительная механика инженерных конструкций и сооружений. 2024. Т. 20. № 4. С. 364–373. <http://doi.org/10.22363/1815-5235-2024-20-4-364-373>

### 1. Introduction

In a three-dimensional setting, the path along which a crack propagates is the surface on which the front of the crack is located, limiting its area; in a two-dimensional setting, the line on which the tip (apex) of the crack is located is the point limiting the extent of the crack. The problem of calculating the crack path is not new. Moreover, it is completely solvable using numerical, step-by-step methods (at least in plane formulation). Finally, it is not among the primary ones, although it is possible to think of computational methods for determining a stronger or more durable body configuration based on the analysis of shape and length of cracks. Algorithms for finding the crack propagation path using the step-by-step method are clear because they rely on familiar mathematical operations. The specificity of fracture mechanics arises when choosing a criterion on the basis of which, at each step of the increase in the length of a crack (hereinafter, cracks in the form of a line are implied), the direction of this increase is established and, if the crack growth process is stable, then the load step or, conversely, the length of this increase at the selected load step as well. Each increment in crack length is accompanied by a final increment in load or stress intensity factor. Several such criteria are known [1–3]. For example in [4], a relationship for the crack growth rate under cyclic loading (such as the Paris formula) is used to calculate the increment in the length of subcritical crack

---

*Морозов Евгений Михайлович*, доктор технических наук, профессор, профессор кафедры физики прочности, Национальный исследовательский ядерный университет МИФИ, Москва, Россия; eLIBRARY SPIN-код: 3989-2934, ORCID: 0000-0002-4824-8481; e-mail: evgeny.morozov@gmail.com  
*Курбанмагомедов Арслан Курбанмагомедович*, кандидат физико-математических наук, старший преподаватель математического института С.М. Никольского, Российский университет дружбы народов, Москва, Россия; eLIBRARY SPIN-код: 5262-5269, ORCID 0000-0001-9158-0378; e-mail: kurbanmagomedov\_ak@pfur.ru

growth, implemented in [5; 6]. This addition to the step-by-step method, in contrast to the option with a constant crack increment, takes into account the “inertia” of crack propagation, determined by the crack speed (and therefore a crack growing at a higher speed is “straighter” than one growing at a low speed). In this regard, it would be interesting to compare the paths for materials with different mechanical properties of cyclic crack resistance. What follows is a plane problem (or a two-dimensional one on a curved surface of a body) for an isotropic material and, in addition, the slow subcritical growth of a crack due to cyclic loading, creep, etc. is not considered.

## 2. Methods

It is important that each state before the subsequent small increment in the crack length is a critical equilibrium state, in which the accepted failure criterion is met and this state is stable ( $W \frac{\partial p}{\partial l} > 0$ ,  $p$  is the load parameter,  $l$  is the crack length). In this case, there is no avalanche-like growth of a crack (or its jumps from one stable equilibrium state to another), since the step-by-step method is not able to describe the unstable, avalanche-like growth of a crack, which is dynamic in nature. At the same time, one can imagine a calculation algorithm with the necessary load drop per crack step, in order to try to take into account the unstable domain  $W \frac{\partial p}{\partial l} < 0$  of the critical equilibrium state. At the same time, however, the question remains open about the adequacy of the calculated path compared to the observation. A brief overview of some techniques for the numerical implementation of path calculations using finite element method can be found in [7]. However, let us discuss the question of whether there are any possibilities for determining crack paths in general. The well-known example of determining the entire crack path at once is based on the intuitive assumption that the crack coincides with the path of the smallest principal stress of the initial (without crack) stress field. This approach is confirmed by many particular cases of fracture, and is implemented in design, specifically, for diagnostic purposes using the “brittle coating method”. And yet there is no “theoretical” evidence of the validity of this approach. In addition to discrete (differential) methods for finding the path of a process, theoretical mechanics also considers integral methods that are interconnected with differential ones and describe the same process, but in a different mathematical implementation. Assuming that the propagation of a crack is a process of mechanical movement of its tip (as a material point) along an optimal path, in some sense in comparison with other possible paths, then one arrives at the variational problem

$$\delta L = 0, \quad L = \int_A^B \Phi(x, y, y') ds, \quad (1)$$

in which  $y = y(x)$  is the crack path equation, and the conditions at ends  $A$  and  $B$  may be different depending on the formulation of the problem. Condition (1) allows to interpret the crack propagation line as a generalized geodesic line with a metric depending on the stress state, namely  $ds^* = \Phi ds$ . The art of choosing the integral function  $\Phi$ , as well as the general choice of the Lagrange function in the integral variational principles of physics and mechanics [8], completely determines the success of the solution. Some simple specified relationships for function  $\Phi$  in the form of its proportionality to the greatest principal stress, deformation, and the product of stress and displacement, used in [9–11], gave acceptable forms of crack paths for the cases studied. The optimization condition can be the condition of the least cost of fracture work in comparison with the energy supplied to this process. Based on this, the shape of crack cells on the plane surface of a uniformly stressed body in the form of hexahedrons and rectangles was obtained [12]. Parts of these hexagonal cells in the form of three cracks converging at an angle of  $120^\circ$  can be observed on the surface of dried ground. The natural assumption of stress relaxation around the first crack formed and the sequential formation and growth of subsequent cracks, together with the analysis of

absorbed and available energies, made it possible to explain [13] various patterns of cracks in the Earth's crust on river floodplains, dried silt, on enamel dishes, on the surface of oil paintings etc. By the way, the idea of two types of energy required for the formation of cracks, allowed the authors together with Ya.B. Friedman, using the well-known analysis of fractures, introduce crack analysis into the mechanics of materials [14], which helps to draw useful conclusions about the mechanical behavior of a collapsing body. These representations, in accordance with the law of conservation of energy when varying the crack path, made it possible to write function  $\Phi$  in the form

$$\Phi = 2\gamma - \frac{1}{2} (p_i^+ u_i^+ + p_i^- u_i^-). \quad (2)$$

Here,  $2\gamma = \gamma^+ + \gamma^-$  is the specific work of fracture,  $p_i$  is the load acting on the surface of the crack  $p_i = -\sigma_{ji} n_j$ ,  $\sigma_{ji}$  is the stress in the solid body at the points where a crack is assumed (the principle of superposition is used to transform the external load to the load distributed over the surface of the crack),  $n_j$  is the normal line to the surface of the crack,  $u_i$  is the displacement on the surface of the crack due to load  $p_i$ . The superscripts “plus and minus” refer to the opposite edges of the crack along which integration is carried out.

From the definition of the intensity of the distributed load  $p_i$ , from the very meaning of the integral principles, it is clear that the crack path is determined by the initial stressed state of the body, i.e. without taking into account its distortion by the presence of a crack (which manifests itself and, therefore, can only be taken into account when analyzing the process of crack growth).

The use of expression (2) is associated with the difficulty of determining displacement  $u_i$  included in this expression. It is proposed to circumvent this complication by applying the Winkler hypothesis, used in foundation theory. According to this hypothesis, the movement of a point on the boundary of a half-plane is proportional to the load on this point. The Winkler hypothesis  $u_i = \beta p_i$  gives the greatest deviations from the solution of the theory of elasticity for the case of concentrated forces. Since in the present case a distributed load of intensity  $p_i$  acts on the edges of the crack, Winkler's hypothesis should give acceptable results. In addition, not a constant, but a variable bedding coefficient is proposed in the form  $\beta = \beta \sqrt{l^2 - s^2}$ , based on the elastic solution for a straight cut (in the Griffiths problem  $v = \left( \frac{2P}{E} \sqrt{l^2 - s^2} \right)$ ).

In this case, at the end of the crack (at  $s = l$ ) the displacement is always zero, according to the physical meaning in the elastic problem. The introduction of such assumption made it possible to obtain reasonable solutions to a number of problems with crack paths, for example, a spiral for a separation crack during torsion of a circular cylinder or gouging out an area around the point of application of a concentrated force in a plane [9].

In [15], the inhomogeneous distribution of the fracture work density was considered in the form  $\gamma = \gamma_0 + \gamma_1 \sin \frac{\pi x}{a} \sin \frac{\pi y}{b}$ , the accepted Winkler hypothesis for displacements on the desired path. The tensile stress on the plane is constant and satisfies the condition  $2\gamma_0 + p_y u_y = 0$ , which is obtained from (1) and (2) at  $l \rightarrow 0$ . As a result of the numerical calculation, a wavy crack path (bypassing the area of increased fracture resistance) across the tensile direction was obtained.

To be fair, there are negative opinions concerning the possibility of using integral principles to find crack paths [2; 16]. At the report of E.M. Morozov at the seminar of the Department of Mechanics of the Steklov Mathematical Institute, Professor G.P. Cherepanov stated that the crack path cannot be immediately determined as a whole, to which L.I. Sedov [2] remarked — “well, why not, it is an adequate formulation of the problem — among the multitude of lines passing through the predetermined points A and B, to find one that satisfies the condition of optimality in energies”. It was also pointed out in [16] that the path obtained

from the variational principle [17; 18] will depend on the external load as a parameter and will not “continue itself”. However, in the authors’ opinion, an additional condition (in the form of a fracture criterion) that crack growth along the desired path occurs at a critical load is omitted here, thereby eliminating the load parameter from the path equation.

The possibility of finding the path as a whole is also questionable in the case of combined loading, i.e. when in an unpredictable way, somewhere in the middle of the loading path, another load system is wedged in. In this case, the loading path must be foreseen in advance, divided into known simple ones, and the solution must be framed separately at each stage within which the loading is simple. This question is partly reminiscent of Poincaré’s judgment about the existence of non-analytic solutions to Lagrange’s equations of motion.

Let us consider the calculation of the path of crack motion under the action of a uniformly distributed load on a part of the half-plane boundary in more detail [18; 19]. The cracks enter from the ends of the loaded sections and have a form corresponding to the solution from the orthogonality of the crack to the lines of identical principal stresses [11; 18]. The determining equation is not the variational condition (1), but the assumption made that the stationary value of the functional  $L$  itself is equal to zero. This assumption was justified by the fact that the required and released energies are equal during the growth of a static stable crack, i.e.  $(p_i = pf_i(s))$ .

$$\int_0^l (2\gamma - \beta p^2 f_i^2(s) \sqrt{l^2 - s^2}) ds = 0.$$

The modified Winkler hypothesis was used for displacements. The load parameter  $p$ , as well as the specific work of fracture  $2\gamma$ , are excluded from the expression for  $L$  by the usual condition  $\frac{\partial L}{\partial l} = 0$ , which gives a connection between the load parameter and the crack length. The desired crack path  $y = y(x)$  is approximated by the expression  $x = a_0 + a_1 \exp(b_1 y) + a_2 \exp(b_2 y)$ , constants  $a_0, a_1, a_2, b_1, b_2$  in which are determined by the equation

$$\int_0^l \left[ 1 - \frac{f_i^2(s) \sqrt{l^2 - s^2}}{\int_0^l f_i^2(s) l (l^2 - s^2)^{\left(\frac{1}{2}\right)} ds} \right] ds = 0.$$

The length of the crack along its found path depends on the load parameter according to the formula

$$p^2 = \frac{2\gamma}{\int_0^l \beta f_i^2(s) l (l^2 - s^2)^{\frac{1}{2}} ds}.$$

The load parameter increases monotonically with increasing crack length, which indicates its stable growth.

In [20; 21], the same problem was solved for the crack equation in the form of polynomials of the fourth and fifth orders, obtaining approximately the same results. The calculated paths originated from the ends of the loaded area, going deeper and moving away from it in qualitative agreement with the experiments [22].

If in a material that is homogeneous and isotropic in terms of crack resistance properties, it is assumed that when the path is varied at a fixed length, the variation in the work of fracture is equal to zero and taking into account that,

$$\delta W + \delta A = \frac{1}{2} \delta \int_A^B \left[ (\sigma_{ij} n_j u_i)^+ + (\sigma_{ij} n_j u_i)^- \right] ds ,$$

then this expression can be used to formulate a variational condition in which the variation of the functional is caused by the variation of the crack path. Then condition (1) will be rewritten in the form

$$\delta \int_A^B (p_i^+ u_i^+ + p_i^- u_i^-) ds = 0 , \quad (3)$$

Considering the problem in [23]

$$\delta I = \delta \int_A^B \frac{1}{2} (p_i^+ u_i^+ + p_i^- u_i^-) ds = 0 \quad (4)$$

with isoparametric condition  $\int_0^l ds = \int_0^l \sqrt{1+y^2} dx = l - \text{const}$  , one obtains a problem for the unconditional

extremum of the functional  $L = \int_0^{x_B} \left[ \frac{1}{2} (p_i^+ u_i^+ + p_i^- u_i^-) + \Lambda \right] \sqrt{1+y^2} dx$  with boundary condition  $\frac{\partial M}{\partial y} = 0$

for  $x = x_B$  (since  $\delta y_B \neq 0$  ,  $M$  is the integrand of  $L$ ). Lagrange multiplier  $\Lambda$  in the isoparametric problem is the derivative of the extreme value of the original functional along the length of the crack,

$\Lambda = \frac{dI}{dl} = \frac{\partial I}{\partial l} + \frac{\partial I}{\partial p} \frac{dp}{dl}$ . For a crack growing in a subcritical state according to the law  $p = p(l)$  at the

critical moment one obtains  $\frac{dp}{dl} = 0$  and then from  $\Lambda = \frac{dI}{dl}$  we can find

$$I = \Lambda l - C . \quad (5)$$

At the same time, on a known path (in this case on the extremal), the load parameter  $p$  is related to the length of the crack by the relation  $\frac{\partial}{\partial l} (2\gamma l - I) = 0$  , from which  $2\gamma - \Lambda = 0$  . Now comparing (4) and (5), it can be concluded that at the extremal the energy functional takes on a constant value equal to zero.

$$\int_0^l \left[ 2\gamma - \frac{1}{2} (p_i^+ u_i^+ + p_i^- u_i^-) \right] ds = C . \quad (6)$$

It becomes possible to find the crack path based on the equality of functional (6) to zero. On the other hand, by immediately writing down the stationary condition of the functional in the form

$$\delta L = \delta \int_0^l \left[ 2\gamma - \frac{1}{2} (p_i^+ u_i^+ + p_i^- u_i^-) \right] ds = 0 , \quad (7)$$

with the same condition  $l = \text{const}$  , then assuming that the crack develops stationary, all the supplied energy is spent on fracture, and then with a slow increase or decrease in the external load, the crack also slowly and steadily spreads along the desired path. This means that the total derivative of functional  $L$  (but not  $I$ ) with respect to the length of the crack must be equal to zero. Consequently, in essence, both formulations of the problem gave the same result. An example of a combined solution method – step-by-step and integral ones — is given in the book [24], where the problem of stretching a plane with a crack, the line of which makes a specified angle with the direction of stretching, was solved. The displacements  $u_i$  were determined by mapping a plane with a broken crack onto a straight segment and then onto the exterior of a unit circle,

and the increment in length at each step was fixed. The use of a step-by-step method made it possible to take into account the change in stress state during crack growth. It was found that a growing crack, starting at the end of the initial crack, is curved and oriented along the direction of tension. This result is consistent with experiments and other calculations [1; 25].

It is known that catastrophic fracture of main gas pipelines is characterized by the propagation of a crack along a sawtooth path with rounded teeth. Between the teeth of the saw, the crack path is close to a spiral one. The sharp change in the direction of the crack in the tooth area is apparently explained by the fact that the asymmetry of the soil backpressure on the left and right wings of the crack becomes significant as the crack tip approaches the ends of the horizontal (parallel to the day surface) diameter of the pipe. In this regard, the problem was posed about the spiral propagation of a crack with a constant pre-Rayleigh velocity in a pipe under the influence of internal pressure and with a given axial stress [26]. The problem was solved as a plane one, to develop a cylindrical surface onto an infinite plane containing a number of parallel semi-infinite cracks. Using the integral [2], it was concluded that the spiral mode of crack propagation is possible only at negative values of the axial stress. The crack growth rate and the angle between its vector and the pipe axis are determined. The beginning of the discussion about the ability of integral variational principles to describe the whole mechanical or physical process at once for a certain period of time goes back to the times of formation of its formulations, which involved such names as Huygens, Maupertuis, Euler, Fermat, Hertz, Helmholtz, Ostrogradsky and others. The history of the creation of these principles can be found in [8]. It seemed impossible to find a process flowing over time, all at once, with a seeming violation of causality, bearing the character of foresight. For example, a ray of light according to Fermat's principle in an inhomogeneously refracting medium, leaving a point, follows the path of the shortest time; a material point (in the absence of external forces) moves along a surface along a geodesic line according to Hertz's principle; even Bernoulli's classical problem of the fastest movement of a material point from position A to position B is solved by the integral principle.

In mathematical terms, confusion is dispelled due to the equivalence of the variational formulation of the integral criteria to the corresponding Euler — Lagrange differential equations. However, philosophically, confusion remains. For example, Planck tried to explain the process (preliminary) of a ray of light finding its future path — at first (after switching on) the light goes arbitrarily, but on all other paths except the suitable one, it stalls, i.e. photons are scattered and their main flux, although not immediately (on the appropriate time scales), begins to follow the path predicted by the integral principle. Generally speaking, considering the growth of a crack as a process that occurs in time along the desired path, it should be recognized that the crack path satisfies variational principles (in the form of the variation of the functional being equal to zero) only in special cases. In general, one should require that the integral over time of the variation of the Lagrange function be equal to zero, as required by the Hamilton — Ostrogradsky principle for non-conservative systems (in which the operations of integration and variation are non-permutable), i.e.

$$\int_{t_A}^{t_B} \delta L dt = 0, \delta L = \delta \int_{x_A}^{x_B} \Phi ds, \quad (8)$$

where variations of the function  $y(x)$  describing the crack path are isochronous and not only the crack path must be found, but also the law of motion in time of its end  $x(t)$ ,  $y(t)$  (the position of which also varies) within a given time interval  $t_B - t_A$ . Here, the whole path is no longer determined at once, since it does not provide stationarity to any integral. Only in the case of explicit independence of  $L$  from time,  $\delta L = 0$ . This results in an equation in variations, to obtain which one can use the variational equation of L.I. Sedov [2], taking into account all possible associated effects.

Let us consider the case when the crack path is known. Then, when the position of the crack end is varied along path  $\delta L < 0$ , then  $\delta L$  is essentially dissipation ( $L$  is the difference between the required and available energy) and the crack grows spontaneously; if  $\delta L > 0$ , then  $\delta L$  is the increment of free energy and the crack does not grow spontaneously. Therefore, the condition  $\delta L = 0$  determines the critical state corresponding to the beginning of crack propagation.

Apparently, one can also imagine (by analogy with other quasiparticles introduced in physics, for example, phonon, hydron, etc.) the tip of a crack in the form of a material quasiparticle — cracon — a point with mass and moving under the action of the corresponding crack-driving forces according to the laws of mechanics [27]. The concept of cracon in combination with an additional optimality condition involving the Pontryagin maximum was quite successfully used to solve the problem of how the stress applied to a plane should change, so that the ends of a single rectilinear symmetric crack, starting to move at a critical moment, stop at specified points (the problem of speed). It turned out that for this purpose the initial tensile stress in the middle of the cracon path, i.e. the end of the crack, should change sign.

In a plane stress field, having written down and solved Newton's laws of motion for cracon, one can establish its law of motion and thereby find the crack path.

In addition, in the supercritical stage, the laws of cracon motion for a straight crack were obtained [28], which made it possible to establish the average growth rate in connection with the critical load. The result agrees satisfactorily with experiment. It has been shown that in the supercritical stage (in the Griffiths problem), the crack growth rate practically corresponds to the well-known Mott formula [29].

For a more adequate formulation of the problem, it is desirable to clarify the state and the following process not only from a mechanical, but also from a thermodynamic point of view, since fracture is the process of transition of one (initial) state of equilibrium to another (final), one type of energy to another (taking into account the accompanying conditions). An attempt at such a classification is presented in [10; 30], where, in particular, on this basis it is shown that for cases with irreversible processes occurring inside the volume of a body with a crack, on the actual path of fracture the amount of heat acquired by the body (ultimately dissipation) is stationary. To highlight the methodologically general cognitive usefulness of thermodynamic signs, let us consider the process of transition of a body from one mechanical and thermodynamic equilibrium to another using the example of a sample stretched by force. In the case of a thermodynamically closed system, the increment in internal energy consists of increments in free energy  $\delta F$  and unavailable energy  $T\delta S$  (at a constant temperature  $T$ , it cannot be separated). A decrease in free energy  $F$  is accompanied by a corresponding increase in entropy  $S$ . The sign of the increment  $\delta F$  indicates the possibility of a “spontaneous” process (fracture under constant external forces), and the absolute value of  $\delta F$  can serve as an indication of the rate of this process. Based on the second law of thermodynamics, the process cannot occur spontaneously without reducing the free energy of the system. In this case, since  $\delta F < 0$ , the equilibrium state of the system is unstable, but for instability to be realized, initial energy is required to activate this process.

Let us consider the process of deformation over time. First, while there is no external force, the body is in equilibrium and  $F = 0$ . Now (in a closed system that allows the exchange of energy, but not mass), an external force is applied, the mechanical work of which leads to an increase in internal energy, which in turn increases free energy (due to an increase in potential deformation energy). With increasing force, the excess free energy is supported by the work of this force, and the unavailable energy  $TS$  still remains approximately constant (although it may be due to elastic imperfections). If now the system at a certain achieved level of  $F$  (and force) is considered, then the energies can be redistributed towards an increase in entropy and a decrease in free energy. Then  $\delta F < 0$ , and all states at  $F > 0$  are unstable, but this is instability at rest, such as a supersaturated solution or a superheated liquid. In this case, the degree of nonequilibrium is proportional to the absolute value of the increase in free energy when the body is loaded with an external force. The system seems to be stable in small things: the higher  $F$ , the smaller “the hole in which the ball is located, and the steeper the hill on top of which this hole is located.” The system is unstable at large; but the initial energy is not yet enough to unbalance it. Finally, while  $F$  increases, an inevitable accident occurs – temperature fluctuations (apparently) provided the initial activation energy, which was sufficient to remove the system from unstable equilibrium (the system becomes unstable in small quantities) and fracture is a spontaneous irreversible process of transition to a new state of equilibrium — continues,  $\delta F < 0$ ,  $T\delta S > 0$ , and based on Prigogine's principle [18; 31]  $\frac{\delta S}{\delta t}$  is minimal and therefore

$\frac{F}{t}$  is maximum. From here there are two conclusions — with increasing temperature of the environment, the strength of the body decreases, and fracture occurs at the maximum possible (for given conditions) speed. In this case, the free energy comes down, but after complete fracture, when a new equilibrium state is reached, the value  $F > 0$  (i.e., is established at a new, higher level), since the new surface of the body has surface energy, which is part of the free energy.

### 3. Results

There are several ways to calculate the crack propagation path on the surface of a stressed body — the crack trajectory — at which the crack equation is immediately found. Eventually, it turned out that it will be possible using the mathematical apparatus of calculus of variations and the variational principles of mechanics. At the same time, in each specific case, among those considered, there are complicating circumstances, the overcoming of which should be sought in accordance with the formulation of this task. Several successfully solved tasks can be found in [33].

### 4. Conclusions

1. An analysis of possible options for determining the crack growth trajectory as a whole is given.
2. It is concluded that the equation of the crack trajectory can be obtained using the basis of the calculus of variations of mathematics and the variational principles of mechanics.

### References / Список литературы

1. Xu S., Reinhardt H.W. Determination of double-K criterion for crack propagation in quasi-brittle fracture, Part I: Experimental investigation of crack propagation. *International Journal of Fracture*. 1999;98(2):111–149. <https://doi.org/10.1023/A:1018668929989>
2. Sedov L.I. *Continuum mechanics*. St. Petersburg: Lan Publ.; 2004. (In Russ.) EDN: QJMTCB  
*Седов Л.И. Механика сплошной среды*. СПб.: Лань, 2004. EDN: QJMTCB
3. Elices M., Guinea G.V., Gomez J., Planas J. The cohesive zone model: advantages, limitations and challenges. *Engineering Fracture Mechanics*. 2002;69(2):137–163. EDN: ASFTOD
4. Schapery R.A. A theory of viscoelastic crack growth: revisited. *International Journal of Fracture*. 2022;233:1–16. <https://doi.org/10.1007/s10704-021-00605-z>
5. Dombrovskii Y.M., Stepanov M.S. Mechanisms of Intragrain Plastic Deformation in Steel Heating Process. *Metal Science and Heat Treatment*. 2024;65:747–750. <https://doi.org/10.1007/s11041-024-01000-w>
6. Komarov O.N., Sevastyanov G.M., Abashkin E.E., Khudyakova V.A. Shift of a Spherical Layer Under High Pressures. *Metallurgist*. 2023;67:801–813. <https://doi.org/10.1007/s11015-023-01568-3>
7. Lepikhin A.M., Morozov E.M., Makhutov N.A., Leschenko V.V. Possibilities of Estimation of Fracture Probabilities and Allowable Sizes of Defects of Structural Elements According to the Criteria of Fracture Mechanics. *Inorganic Materials*. 2023;59(15):1524–1531. <https://doi.org/10.1134/S0020168523150074>
8. Mahutov N.A., Morozov E.M., Gadenin M.M., Reznikov D.O., Yudina O.N. Coupled thermo-mechanical analysis of stress–strain response and limit states of structural materials taking into account the cyclic properties of steel and stress concentration. *Continuum Mechanics and Thermodynamics*. 2023;35:1535–1545. <https://doi.org/10.1007/s00161-022-01160-1>
9. Morozov E.M., Alymov M.I. Fracture Pressure in Microdefects of Consolidated Materials. *Doklady Physical Chemistry*. 2021;501:111–113. <https://doi.org/10.1134/S0012501621110026>
10. Matvienko Y.G., Morozov E.M. Two basic approaches in a search of the crack propagation angle. *Fatigue and Fracture of Engineering Materials and Structures*. 2017;40(8):1191–1200. <https://doi.org/10.1111/ffe.12583>
11. Pook L.P. The linear elastic analysis of cracked bodies, crack paths and some practical crack path examples. *Engineering Fracture Mechanics*. 2016;167:2–19. <https://doi.org/10.1016/j.engfracmech.2016.02.055>
12. Morozov E.M., Alymov M.I. Fracture Pressure in Microdefects of Consolidated Materials. *Doklady Physical Chemistry*. 2021;501(1):111–113. <https://doi.org/10.1134/S0012501621110026>
13. Kurbanmagomedov A.K. Crack of the normal gap in the elastic layer. *Bulletin of the Yakovlev chuvash state pedagogical university series: Mechanics of limit state*. 2017;(1):96–104. (In Russ.) EDN: ZGIEKB



- Курбанмагомедов А.К. Трещина нормального разрыва в упругом слое // Вестник ЧПУ им. И.Я. Яковлева. Серия: Механика предельного состояния. 2017. № 1. С. 96–104. EDN: ZGIEKB
14. Kolesnikov Yu.V., Morozov E.M. *Mechanics of contact failure*. Moscow: Nauka Publ.; 2012. (In Russ.)
- Колесников Ю.В., Морозов Е.М. Механика контактного разрушения. М.: Наука, 2012. 224 с.
15. Gordeeva G.V., Kurbanmagomedov A.K., Spitsov D.V. Strength control of concrete structures during the assessment of the residual life of buildings and structures of a hazardous production facility in the field of thermal power engineering. *The System technologies*. 2022;(4):73–86. (In Russ.) [https://doi.org/10.55287/22275398\\_2022\\_4\\_73](https://doi.org/10.55287/22275398_2022_4_73)
- Гордеева Г.В., Курбанмагомедов А.К., Спицов Д.В. Контроль прочности бетонных конструкций при проведении оценки остаточного ресурса зданий и сооружений опасного производственного объекта в сфере теплоэнергетики // Системные технологии. 2022. № 4. С. 73–86. [https://doi.org/10.55287/22275398\\_2022\\_4\\_73](https://doi.org/10.55287/22275398_2022_4_73)
16. Kurbanmagomedov A., Radzhabov Z., Okolnikova G. Investigation of Normal Fracture Cracks in an Infinite Elastic Medium. In: Guda, A. (eds) *Networked Control Systems for Connected and Automated Vehicles. NN 2022. Lecture Notes in Networks and Systems*. Springer, Cham. 2022;509. [https://doi.org/10.1007/978-3-031-11058-0\\_142](https://doi.org/10.1007/978-3-031-11058-0_142)
17. Nikhamkin M., Ilinykh A. Low cycle fatigue and crack grow in powder nickel alloy under turbine disk wave form loading: Validation of damage accumulation model. *Applied Mechanics and Materials*. 2014;467:312–316. <https://doi.org/10.4028/www.scientific.net/AMM.467.312>
18. Yablonsky A.A., Nikiforova V.M. Course of theoretical mechanics. Moscow: KnoRus Publ.; 2011. (In Russ.) EDN: QJYXKR
- Яблонский А.А., Никифорова В.М. Курс теоретической механики. М.: Изд-во КноРус, 2011. 603 с. EDN: QJYXKR
19. Hou J.-P., Wang Q., Yang H.-J., Wu X.-M., Li Ch.H., Zhang Zh.-F., Li X.W. Fatigue and Fracture behavior of a Cold-Drawn Commercially pure aluminum wire. *Materials*. 2016;9(9):764. <https://doi.org/10.3390/ma9090764>
20. Wang Q., Ren J.Q., Wu Y.K., Jiang P., Sun Z.J., Liu X.T. Comparative study of crack growth behaviors of fully-lamellar and bi-lamellar Ti-6Al-3Nb-2Zr-1Mo alloy. *Journal of Alloys and Compounds*. 2019;789:249–255. <https://doi.org/10.1016/j.jallcom.2019.02.302>
21. Sadananda K., Babu M.N., Vasudevan A.K. A review of fatigue crack growth resistance in the short crack growth regime. *Materials Science and Engineering: A*. 2019;754:674–701. <https://doi.org/10.1016/j.msea.2019.03.102>
22. Mall S., Perel V.Y. Crack growth behavior under biaxial fatigue with phase difference. *International Journal of Fatigue*. 2015;74:166–172. <https://doi.org/10.1016/j.ijfatigue.2015.01.005>
23. Berto F., Ayatollahi M.R., Borsato T., Ferro P. Local strain energy density to predict size-dependent brittle fracture of cracked specimens under mixed mode loading. *Theoretical and Applied Fracture Mechanics*. 2016;86(Part B): 217–224. <https://doi.org/10.1016/j.tafmec.2016.07.004>
24. Kaminsky A.A., Kurchakov E.E. Fracture Process Zone at the Tip of a Mode I Crack in a Nonlinear Elastic Orthotropic Material. *International Applied Mechanics*. 2019;55(1):23–40. <https://doi.org/10.1007/s10778-019-00931-9>
25. Tumanov A.V., Shlyannikov V.N., Zakharov A.P. Crack growth rate prediction based on damage accumulation functions for creep-fatigue interaction. *Fracture and Structural Integrity*. 2020;14(52):299–309. <https://doi.org/10.3221/IGF-ESIS.52.23>
26. Ghelichi R., Kamrin K. Modeling growth paths of interacting crack pairs in elastic media. *Soft Matter*. 2015;(11): 7995–8012. <https://doi.org/10.1039/c5sm01376c>
27. Musayev V.K. Mathematical Modeling of Stresses Under Unsteady Wave Action in Geo-Objects. *Power Technology and Engineering*. 2023;57(3):351–364. <https://doi.org/10.1007/s10749-023-01668-9>
28. Stepanova L.V., Roslyakov P.S. Multi-parameter description of the crack-tip stress field: analytic determination of coefficients of crack-tip stress expansions in the vicinity of the crack tips of two finite cracks in an infinite plane medium. *International Journal of Solids and Structures*. 2016;100–101:11–28. <https://doi.org/10.1016/j.ijsolstr.2016.06.032>
29. Xu S., Xiong L., Deng Q., McDowell D.L. Mesh refinement schemes for the concurrent atomistic-continuum method. *International Journal of Solids and Structure*. 2016;90:144–152. <https://doi.org/10.1016/j.ijsolstr.2016.03.030>
30. Carpinteri A., Brighenti R., Spagnoli A. Part-through cracks in pipes under cyclic bending. *Nuclear Engineering and Design*. 1998;185(1):1–14. [https://doi.org/10.1016/S0029-5493\(98\)00189-7](https://doi.org/10.1016/S0029-5493(98)00189-7)
31. Carpinteri A., Brighenti R., Spagnoli A. Fatigue growth simulation of part-through flaws in thick-walled pipes under rotary bending. *International Journal of Fatigue*. 2000;22(1):1–9. [https://doi.org/10.1016/S0142-1123\(99\)00115-2](https://doi.org/10.1016/S0142-1123(99)00115-2)
32. Musayev V.K. Mathematical Modeling of Explosive and Seismic Impacts on an Underground Structure. *Power Technology and Engineering*. 2024;57(6):875–881. <https://doi.org/10.1007/s10749-024-01751-9>
33. Astafyev V.I., Radaev Yu.N., Stepanova L.V. *Nonlinear mechanics of destruction*. Samara: Samara National Research University named after Academician S.P. Kirov. 2001. (In Russ.) EDN: XDVQPF
- Астафьев В.И., Радаев Ю.Н., Степанова Л.В. Нелинейная механика разрушения Сам. гос. ун-т. Самара: Сам. ун-т, 2001. 630 с. EDN: XDVQPF

# ДИНАМИКА КОНСТРУКЦИЙ И СООРУЖЕНИЙ DYNAMICS OF STRUCTURES AND BUILDINGS


DOI: 10.22363/1815-5235-2024-20-4-374-387

УДК 624.04

EDN: LWBXNO

Научная статья / Research article

## Расчет виброизолирующей системы здания с нелинейными характеристиками при кинематическом воздействии (смещении основания)

Д. Кбейли<sup>1</sup>  , Ю.Т. Чернов<sup>2</sup> <sup>1</sup> ИнжГеоСервис, Москва, Россия<sup>2</sup> Национальный исследовательский московский государственный строительный университет, Москва, Россия jaafarqbaily@gmail.com

Поступила в редакцию: 14 мая 2024 г.

Принята к публикации: 17 июля 2024 г.

**Аннотация.** Виброизолирующие системы играют важную роль в защите зданий от сейсмических повреждений. Так как они состоят из элементов с нелинейными характеристиками, расчетные модели виброизолирующих систем требуют разработки методов с учетом изменения динамических характеристик сооружения (матрицы жесткости или податливости), частот и форм собственных колебаний. В исследовании предложен алгоритм и зависимости, основанные на возможности выключения или разрушения дополнительных связей (элементы с нелинейными характеристиками) при определении сейсмических сил и перемещений сооружений при сейсмическом воздействии. Результаты тестовых расчетов показали, что амплитудно-частотная характеристика, перемещение и поперечная сила в основании сооружения уменьшились при выключении или разрушении дополнительных связей. Таким образом, предлагаемая методика, учитывающая работу виброизолирующих систем с нелинейными связями, позволяет снизить материальный, экономический и человеческий ущерб при сейсмическом воздействии. Полученные результаты показали, что зависимости алгоритма расчета, разработанные в работе, можно использовать в инженерной практике при оценке динамического поведения виброизолированной системы здания (амплитудно-частотная характеристика) в процессе колебаний при сейсмическом воздействии.

**Ключевые слова:** динамические характеристики, сейсмические воздействия, сейсмоизоляция здания, амплитудно-частотная характеристика

**Заявление о конфликте интересов.** Авторы заявляют об отсутствии конфликта интересов.

**Вклад авторов.** Нераздельное соавторство

**Для цитирования.** Кбейли Д., Чернов Ю.Т. Расчет виброизолирующей системы здания с нелинейными характеристиками при кинематическом воздействии (смещении основания) // Строительная механика инженерных конструкций и сооружений. 2024. Т. 20. № 4. С. 374–387. <http://doi.org/10.22363/1815-5235-2024-20-4-374-387>




**Кбейли Джаафар**, кандидат технических наук, инженер-конструктор проектного сектора ПИО, ООО «ИнжГеоСервис», Москва, Россия; eLIBRARY SPIN-код: 8790-7877, ORCID: 0000-0002-3875-9413; e-mail: jaafarqbaily@gmail.com

**Чернов Юрий Тихонович**, доктор технических наук, профессор кафедры строительной и теоретической механики, Национальный исследовательский московский государственный строительный университет, Москва, Россия; eLIBRARY SPIN-код: 2375-6712, ORCID: 0000-0002-0808-9981; e-mail: chernovyt@mgsu.ru

© Кбейли Д., Чернов Ю.Т., 2024

This work is licensed under a Creative Commons Attribution 4.0 International License  
<https://creativecommons.org/licenses/by-nc/4.0/legalcode>

# Calculation of a Vibration-Isolated Building System with Non-Linear Characteristics Under Kinematic Action (Base Displacement)

Jaafar Qbaily<sup>1</sup>  , Yury T. Chernov<sup>2</sup> 

<sup>1</sup> Inggeoservice, Moscow, Russia

<sup>2</sup> Moscow State University of Civil Engineering (National Research University), Moscow, Russia

✉ jaafarqbaily@gmail.com

Received: May 14, 2024

Accepted: July 17, 2024

**Abstract.** Vibration isolation systems play a major role in protecting buildings from seismic damage. Since they consist of elements with non-linear characteristics, the calculation models of the vibration isolation system require taking into account changes in the dynamic characteristics of the structure (stiffness or compliance matrix), frequencies and forms of natural vibrations. The study proposes an algorithm and dependencies which are based on the possibility of the disconnection or the destruction of the additional connections (elements with non-linear characteristics) due to certain seismic forces and displacement of structures under seismic impact. The results showed that the amplitude-frequency response, displacement, and shear force at the base of the structure decreased when additional connections were disconnected or destroyed. Thus, the proposed method, which takes into account the operation of vibration isolation systems with nonlinear connections, allows reducing the material, economic and human damage during seismic action. The obtained results of the example show that the dependences of the calculation algorithm developed in the work can be used in engineering practice when evaluating the dynamic behavior of a vibration-insulated building system (amplitude-frequency response) during vibrations under seismic influence.

**Keywords:** dynamic impacts, seismic impacts, building seismic isolation, amplitude-frequency response

**Conflicts of interest.** The authors declare that there is no conflict of interest.

**Authors' contribution.** Undivided co-authorship.

**For citation:** Qbaily J., Chernov Yu.T. Calculation of a vibration-isolated building system with non-linear characteristics under kinematic action (base displacement). *Structural Mechanics of Engineering Constructions and Buildings*. 2024; 20(4):374–387. (In Russ.) <http://doi.org/10.22363/1815-5235-2024-20-4-374-387>

## 1. Введение

Значительное число систем виброизоляции для повышения эффективности виброзащиты включает в себя отдельные нелинейные элементы. Эти элементы могут быть либо включены в систему конструктивно (виброизоляция, динамические гасители и т.п.), либо возникать в процессе деформирования конструкций при интенсивных динамических воздействиях как выключающиеся или разрушающиеся элементы [1–3].

Системы сейсмической защиты достаточно многочисленны, разнообразны и направлены на защиту гражданских конструкций и их неструктурных компонентов при сейсмических воздействиях [4; 5].

Во многих случаях виброизоляция обеспечивается в основном за счет введения между надземной частью конструкции и фундаментом гибкого горизонтального интерфейса с высоким внутренним демпфированием [6–8].

В настоящее время наиболее часто используются следующие варианты для сейсмоизоляции.

1. Устройство бетонного слоя с демпфирующими характеристиками вокруг фундамента с целью изоляции зданий от вибраций во время землетрясения — такой бетон готовится с использованием различного процентного содержания резиновой крошки и стального шлака в качестве заполнителя [9].

---

*Jaafar Qbaily*, Candidate of Technical Sciences, Design Engineer of the Design Sector PIO, LLC “Inggeoservice”, Moscow, Russia; eLIBRARY SPIN-code: 8790-7877, ORCID: 0000-0002-3875-9413; e-mail: jaafarqbaily@gmail.com

*Yury T. Chernov*, Doctor of Technical Sciences, Professor of the Structural Mechanics Department, Moscow State University of Civil Engineering (National Research University), Moscow, Russia; eLIBRARY SPIN-code: 2375-6712, ORCID: 0000-0002-0808-9981; e-mail: chernovyt@mgsu.ru

2. Цилиндрические резиновые опоры с высоким демпфированием (рис. 1), установленные между надземной несущей системой и фундаментами здания [10].



**Рис. 1.** Цилиндрические резиновые опоры

И с т о ч н и к: Mike Renlund: Base\_isolators\_under\_the\_Utah\_State\_Capitol.jpg

**Figure 1.** Cylindrical rubber supports

S o u r c e: Mike Renlund: Base\_isolators\_under\_the\_Utah\_State\_Capitol.jpg

3. Роликовая система нейтрализации колебаний при сейсмических воздействиях. Это система, которая обеспечивает возможность сейсмоизоляции здания от основания и дает возможность после землетрясения возвращать эту систему в исходное состояние (рис. 2) [11];

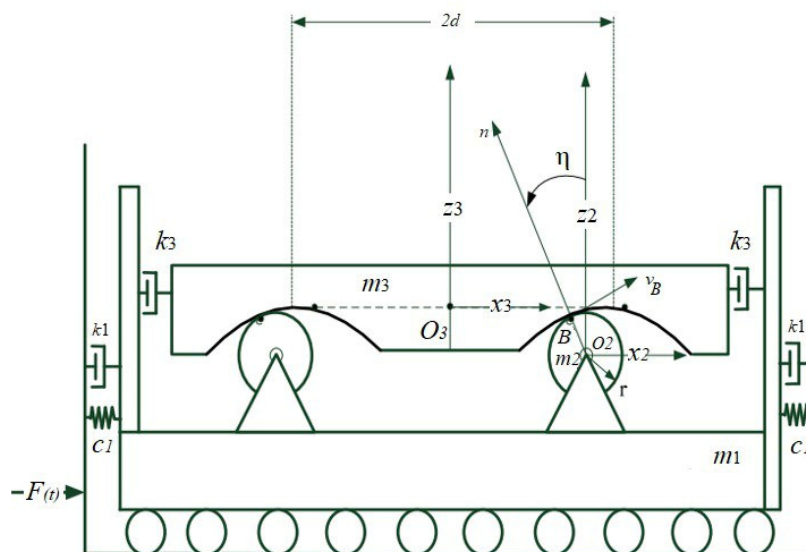


**Рис. 2.** Роликовая система нейтрализации колебаний сейсмического воздействия

И с т о ч н и к: О.А. Бурцева, С.А. Чипко, Н.Р. Абуладзе [12]

**Figure 2.** Roller system for neutralizing seismic vibrations

S o u r c e: О.А. Burtseva, S.A. Chipko, N.R. Abuladze [12]

4. Здание с системой геотехнической сейсмоизоляции (рис. 3). Геотехническая сейсмоизоляция (ГСИ) считается инновационной системой изоляции основания, размещенной ниже фундамента надстройки для защиты от повреждений при землетрясении. Эта система состоит из слоя материалов с низким модулем сдвига и высокими демпфирующими свойствами, такими как смесь песка и резины, используемая для слоя ГСИ [13].

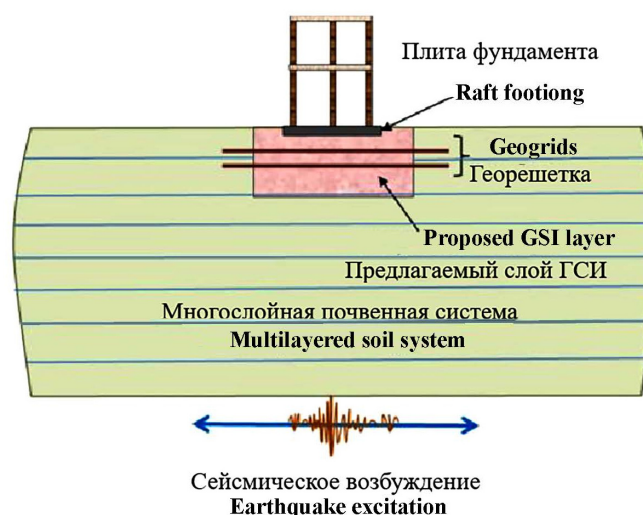


**Рис. 3.** Здание с системой геотехнической сейсмоизоляции  
И с т о ч н и к: А. Boominathathan [14]

**Figure 3.** Building with geotechnical seismic isolation system  
S o u r c e: A. Boominathathan [14]

5. Здания с вязкими демпферами. Вязкостной демпфер, считается пассивным устройством рассеивания энергии. Применяется в гражданских конструкциях для изменения динамических характеристик конструкций, подверженных землетрясению или ветровым воздействиям (рис. 4).



**Рис. 4.** Вязкостный демпфер  
И с т о ч н и к: <https://www.taylordevices.com/direct-acting-damping/>

**Figure 4.** Viscous damper  
S o u r c e: <https://www.taylordevices.com/direct-acting-damping/>

Данный тип сейсмоизоляции показывает хорошие характеристики по уменьшению значений реакции конструкции, перемещений, смещения между этажами и воздействия на основание соответственно. Суть метода основана на оценке отключения или разрушения дополнительных связей, которые находятся между несущей системой и фундаментами во время колебаний. Отключение или разрушение дополнительных связей приводит к изменениям конструктивной схемы в процессе колебаний, в том числе динамических характеристик сооружения (матрицы жесткости или податливости), собственных частот и форм колебаний [15].

Собственные частоты виброизолированной системы приблизительно снижают уровень колебаний (значения амплитудно-частотных характеристик). Подобные системы виброизоляции можно оценить с помощью коэффициента динамичности:

$$A = \frac{1}{1 - \frac{\omega^2}{\rho^2}},$$

где  $\omega$  — частота вынужденных колебаний;  $\rho$  — частота собственных колебаний.

## 2. Алгоритмы расчета

### 2.1. Алгоритм расчета системы с одной степенью свободы с выключенными связями при кинематическом воздействии (смещении основания)

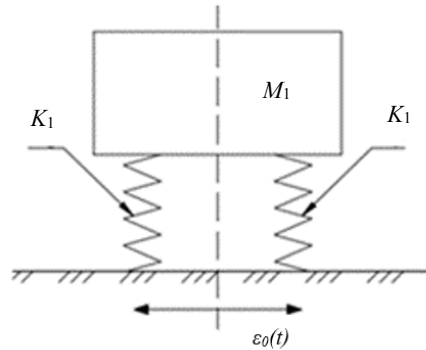


**Рис. 5.** Система с одной степенью свободы с выключенными связями:

$K_1$  — жесткость системы;  $K_2$  — жесткости виброизоляторов;  $\epsilon_0(t)$  — закон смещения основания.

И с т о ч н и к: выполнено Д. Кбейли

**Figure 5.** A one level of freedom system with disconnected constraints

$K_1$  — stiffness of the system;  $K_2$  — stiffness of vibration isolators;  $\epsilon_0(t)$  — base displacement function.

S o u r c e: made by J. Qbaily

Уравнение движения нелинейной системы (рис. 5) (активная виброизоляция) имеет вид

$$My + \left(1 + 2\nu \frac{d}{dt}\right) C(y) y = -M\epsilon_0. \quad (1)$$

Для принятого типа нелинейности зависимость «реакции — перемещения»

$$C(y) y = K_1 y \quad \text{при } y \leq y_0,$$

$$C(y) y = K_1 y - K_2 (y - y_0) \quad \text{при } y > y_0, \quad (2)$$

где  $y_0$  — перемещение системы при выключении связи.

При построении алгоритма уравнение (1) следует преобразовать, а именно перенести нелинейные составляющие в правую часть и добавить к обеим частям уравнения

$$\begin{aligned} & \left(1 + 2\nu \frac{d}{dt}\right) p_1^2 y; \\ \ddot{y} + \left(1 + 2\nu \frac{d}{dt}\right) p_1^2 y &= -\ddot{\epsilon}_0 + \left(1 + 2\nu \frac{d}{dt}\right) p_1^2 y - \left(1 + 2\nu \frac{d}{dt}\right) C(y) y, \end{aligned} \quad (3)$$

где  $p_1^2 = \frac{M_1}{K_1}$ .

Для зависимости вида (2) уравнения движения системы с одной степенью свободы с нелинейной связью (3) примет вид

$$\ddot{y} + \left(1 + 2\nu \frac{d}{dt}\right) p_1^2 y = -\ddot{\epsilon}_0 + \left(1 + 2\nu \frac{d}{dt}\right) \frac{K_2(y - y_0)}{m}. \quad (4)$$

Решение уравнения (4) представляется в виде двух решений: линейной системы на смещения основания и на фиктивную нагрузку, которая зависит от вида нелинейности  $\left(1 + 2\nu \frac{d}{dt}\right) K_2 - y_0$ ,

$$y = y_{\text{л}} - y_{\text{нл}}. \quad (5)$$

Решение уравнения от смещения основания где

$$\begin{aligned} y_{\text{л}} &= \frac{-1}{p_1^* M} \int_0^t \ddot{\epsilon}_0(\tau) e^{-n_1(t-\tau)} \sin p_1^*(t-\tau) d(\tau); \\ y_{\text{л}} &= \frac{-1}{p_1^* M} \int_0^t \ddot{\epsilon}_0(\tau) e^{-n_1(t-\tau)} [\sin p_1^* t \cos p_1^* \tau - \sin p_1^* \tau \cos p_1^* t] d(\tau) = \\ &= \frac{-1}{p_1^* M} [d_1(t) F_2(t) - d_2(t) F_1(t)], \end{aligned} \quad (6)$$

где  $2n_1 = 2\nu p_1^2$ ,  $p_1^* = \sqrt{p_1^2 - n_1^2}$ .

$$d_1(t) = e^{-n_1 t} \sin p_1 t; \quad d_2(t) = e^{-n_1 t} \cos p_1 t, \quad (7)$$

$$F_1 = \int_0^t \ddot{\epsilon}_0(\tau) e^{-n_1 \tau} \sin p_1^* \tau d(\tau); \quad F_{12} = \int_0^t \ddot{\epsilon}_0(\tau) e^{-n_1 \tau} \cos p_1^* \tau d(\tau). \quad (8)$$

Нелинейная составляющая решения определяется из интегрального уравнения

$$y_{\text{нл}} = \frac{-1}{p_1^* M} \int_{t_0}^t \left(1 + 2\nu \frac{d}{dt}\right) K_2(y - y_0) e^{-n_1(t-\tau)} \sin p_1^*(t-\tau) d(\tau), \quad (9)$$

где  $t_0$  — время первого включения дополнительной связи в процессе колебаний.

Следуя (7), (8) можно записать следующим образом:

$$\begin{aligned} y_{\text{нл}} &= \frac{K_2}{p_1^* M} \int_{t_0}^t (y - y_0) e^{-n_1(t-\tau)} [\sin p_1^* t \cos p_1^* \tau - \sin p_1^* \tau \cos p_1^* t] d(\tau); \\ y_{\text{нл}} &= \frac{K_2}{p_1^* M} [d_1(t) F_2(t_0, t) - d_2(t) F_1(t_0, t)] d(\tau), \end{aligned} \quad (10)$$

где  $F_1(t_0, t) = \int_{t_0}^t \lambda_1(y \pm y_0) \cos p_1^* \tau d(\tau)$ .

Полное перемещение вычисляется по формуле (6).

Знак ((+)) в (10) при  $y(t) \leq 0$

$\lambda_1 = 0$  при  $y \leq y_0$ ,  $\lambda_1 = 1$  при  $y > y_0$ .

### 2.2. Алгоритм расчета виброизолированной системы здания с нелинейными характеристиками при кинематическом воздействии

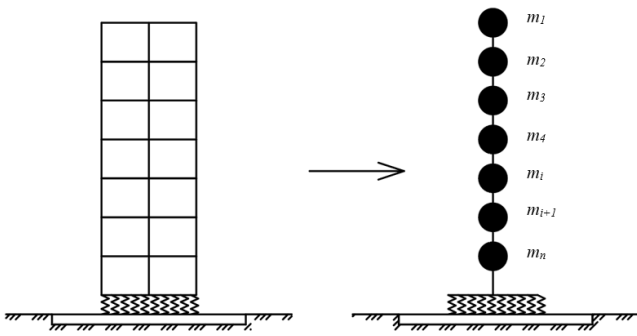


**Рис 6.** Расчетная динамическая схема виброизолированной системы здания  
И с т о ч н и к : выполнено Д. Кбейли

**Figure 6.** The calculated dynamic scheme of the vibration-insulated building system  
S o u r c e : made by J. Qbaily

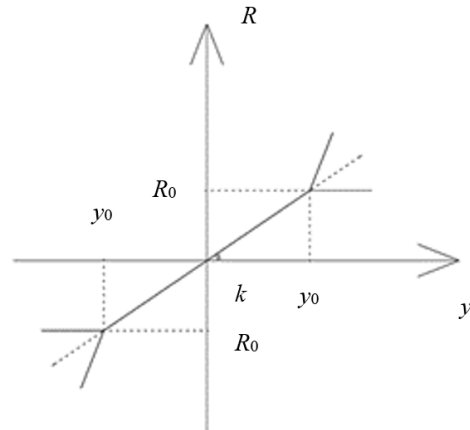


**Рис 7.** Нелинейная зависимость «смещение — реакция»  
И с т о ч н и к : выполнено Д. Кбейли

**Figure 7.** Nonlinear dependence of “displacement — reaction”  
S o u r c e : made by J. Qbaily

Уравнения движения системы (рис. 6):

$$\begin{aligned} m_1 \ddot{y}_1 + k_{11} y_1 + k_{12} y_2 + \dots + k_{1n} y_n &= m_1 \ddot{\xi}_{50} \\ m_2 \ddot{y}_2 + k_{21} y_1 + k_{22} y_2 + \dots + k_{2n} y_n &= m_2 \ddot{\xi}_{50} \\ \dots & \\ m_n \ddot{y}_n + k_{n1} y_1 + k_{n2} y_2 + \dots + k_{nn} y_n &= m_n \ddot{\xi}_{50}, \end{aligned} \tag{11}$$

где  $m_i, k_{ij} (i, j = 1, 2, \dots, n)$  соответственно, характеристики масс и жесткости системы,  $y_i (i = 1, 2, 3) —$  перемещения масс системы.

Из диаграммы реакции в системах виброизоляции, расположенных под зданием (рис. 7), реакцию системы можно записаться в виде

$$k_{nn} y_n = R_n = k_m y_n \quad \text{при } y < y_0, \tag{12}$$

$$R_n = k_{n1} y_n \pm y_n (k_{n1} + k_{n2}) \quad \text{при } |y| \geq y_0 \tag{13}$$

где

$$R_{n1} = \sum_{i=1}^n k_{nn} y_n = \sum_{i=1}^n k_{ni} y_i, \tag{14}$$

$$R_2 = R_2 - \sum_{i=1}^n k_{ni} (y_i - y_{0i}). \tag{15}$$

Разрешающую систему уравнений удобно записать в виде

$$m_n y_{n1} y_1 + k_{n1} y_1 + k_{n2} y_2 + \dots + k_{nn} y_n = m_n \ddot{\xi}_{50} + k_{mn}, \tag{16}$$



Учитывая (16), разрешающую систему уравнений можно записать в виде системы линейных уравнений (17) и дополнительной системы (18), которая учитывает нелинейную составляющую

$$M\ddot{Y} + K\bar{Y} = M\ddot{\xi}_0 \quad (17)$$

можно записать

$$M\ddot{Y} + k\bar{Y} = \bar{\beta}_i, \quad (18)$$

где

$$\bar{\beta}_i = \begin{pmatrix} 0 \\ 0 \\ 0 \\ \vdots \\ \beta_n \end{pmatrix}, \text{ где } \beta_n = R_n - \sum_{i=1}^n k_{ni}(y_i - y_{0i}) = R_{\text{доп}}. \quad (19)$$

Решение для основной системы удобно представить в виде разложения по собственным формам в виде

$$\Phi M \Phi \ddot{Y} + \Phi K \Phi \bar{Y} = \bar{\beta}_i, \quad (20)$$

где  $\bar{\beta}_i = \Phi M \xi_0^2$  для дополнительной системы

$$\bar{\beta}_d = \Phi \beta_d \quad \text{или} \quad \begin{pmatrix} Y_{11} & Y_{21} & \dots & Y_{n1} \\ Y_{21} & Y_{22} & \dots & Y_{n2} \\ \dots & \dots & \dots & \dots \\ Y_{n1} & Y_{n1} & \dots & Y_{nn} \end{pmatrix} \begin{pmatrix} 0 \\ 0 \\ \dots \\ R_d \end{pmatrix} = \begin{pmatrix} Y_{n1} \\ Y_{n2} \\ \dots \\ Y_{nn} \end{pmatrix} * R_d. \quad (21)$$

Жесткости виброизоляторов на первом шаге расчета  $K_{\text{сум}} = M_{\text{зд}} (2\pi\rho)^2$ , где  $M_{\text{зд}}$  — масса всего здания.

### 3. Пример расчета

Рассмотрено 3-этажное виброизолированное железобетонное здание, симметричное в схеме, с высотой этажа 3,5 м, свойства и характеристики материалов и элементов конструкций приняты в соответствии с нормами РФ (рис. 8–10).

Составив уравнения движения (системы виброизоляторов выключены), определим частоты, периоды, матрицу жесткости  $k$  и матрицу масс  $M$  (т),

$$T = \begin{pmatrix} 0,095 \\ 0,17 \\ 0,555 \end{pmatrix} \text{ (с)} \quad \omega = \begin{pmatrix} 10,6 \\ 5,88 \\ 1,8 \end{pmatrix} \text{ (Гц)}$$

$$M = \begin{pmatrix} 67,31 & 0 & 0 \\ 0 & 67,31 & 0 \\ 0 & 0 & 60,61 \end{pmatrix} \text{ (т)} \quad k = \begin{pmatrix} 175424,843 & -107559,047 & 21531,282 \\ -107559,047 & 159578,255 & -75159,107 \\ 21531,282 & -75159,107 & 56528,263 \end{pmatrix} \text{ (т/м)}$$

Матрица масс Матрица жесткости

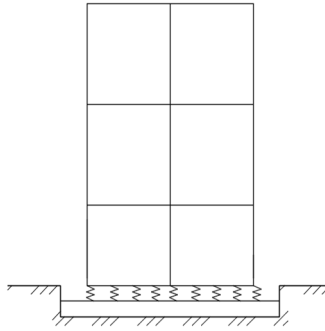


**Рис. 8.** Разрез здания  
И с т о ч н и к: выполнено Д. Кбейли  
**Figure 8.** Building section  
S o u r c e: made by J. Qbaily

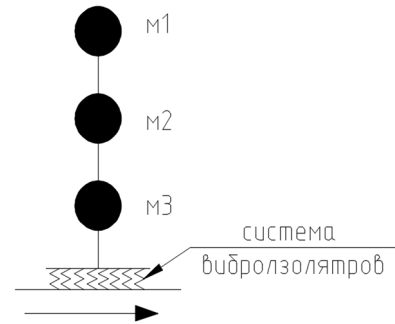


**Рис. 9.** Расчетная динамическая схема здания  
И с т о ч н и к: выполнено Д. Кбейли  
**Figure 9.** Estimated dynamic scheme of the building  
S o u r c e: made by J. Qbaily

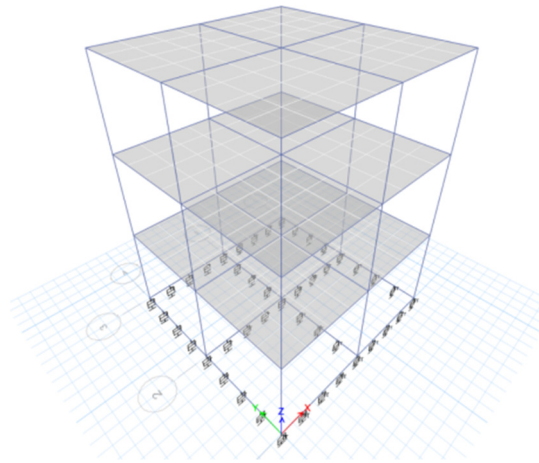


**Рис. 10.** Расчетная динамическая схема в расчетной программе  
И с т о ч н и к: выполнено Д. Кбейли  
**Figure 10.** Dynamic calculation scheme in the calculation program  
S o u r c e: made by J. Qbaily

Количество виброизоляторов определяется в соответствии с несущей способностью при  $\rho = 10 \text{ Гц}$ .  $K_{\text{сум}} = M_{\text{зд}} (2 \cdot \pi \cdot \rho)^2 = 770737,14 \text{ кН/м}$ .

На первом шаге определяем жесткость здания, сейсмические силы и перемещения верхнего этажа при жесткости виброизоляторов:  $K_{\text{сум}} = K_1$ , на втором шаге  $K_2 = 0,95K_1$ , и т.д., а также амплитудно-частотную характеристик  $A = \frac{1}{1 - \frac{\omega^2}{\rho^2}}$ .

$$A = \frac{1}{1 - \frac{\omega^2}{\rho^2}}$$

При расчете использовались системы компьютерной математики MATHCAD и программный комплекс ETABS.

Здание находится в сейсмической зоне (8 баллов), категория грунта I, спектр реакции для этой области согласно нормам СП 14.13330.2018<sup>1</sup> показан на рис. 11.

На рис. 12 показаны перемещения верхнего этажа здания.

<sup>1</sup> СП 14.13330.2018. Строительство в сейсмических районах. М.: Стандартинформ, 2018. 114 с.

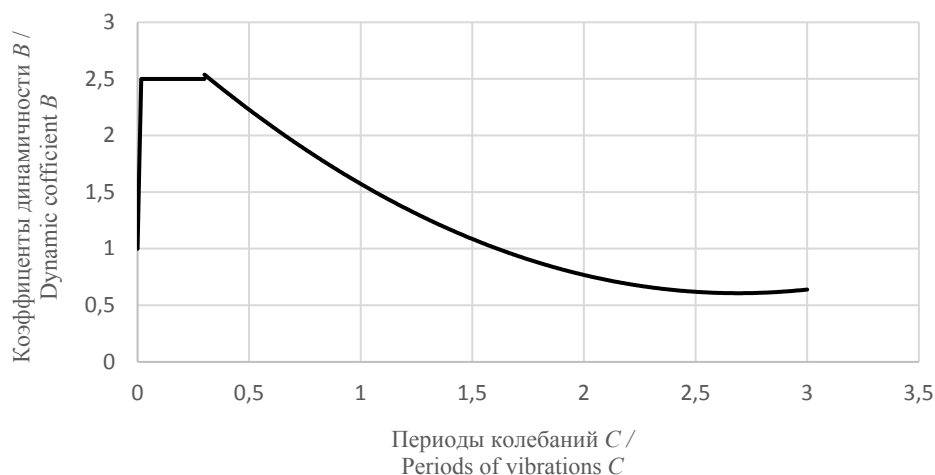


**Рис. 11.** Значение коэффициента динамичности  
И с т о ч н и к: СП 14 13330 2018<sup>1</sup>

**Figure 11.** The value of the dynamic coefficient  
S o u r c e: СП 14 13330 2018<sup>1</sup>

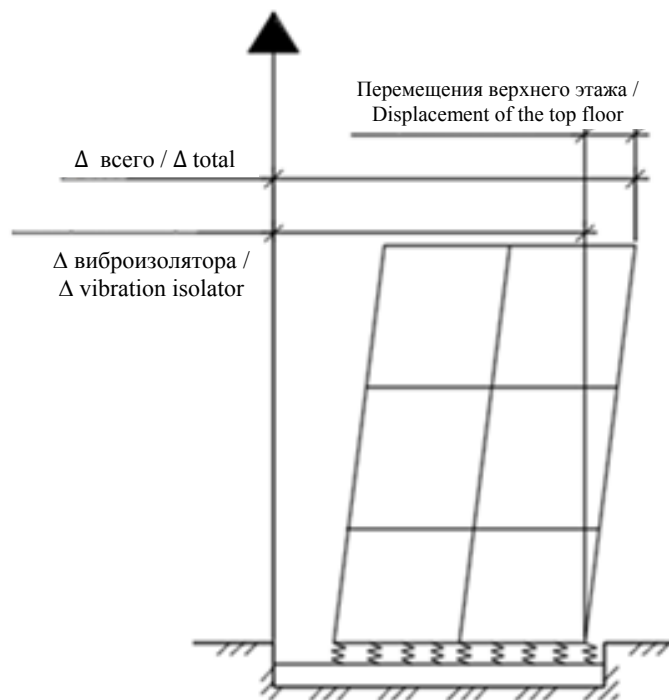


**Рис. 12.** Перемещения верхнего этажа  
И с т о ч н и к: выполнено Д. Кбейли

**Figure 12.** Displacement of the top floor  
S o u r c e: made by J. Qbaily

#### 4. Результаты и обсуждение

После завершения расчетов были получены сейсмические силы, частоты, периоды и матрица жесткости (табл. 1).

С помощью данных табл. 1 были построены графики, представленные на рис. 13 и 14.

Таблица 1

Результаты численного моделирования

% $K_1$	Жесткости виброизоляторов $K_1$ , кН/м	Поперечная сила в основании $S$ , кН	Перемещение верха сооружения $\Delta_{top}$ , мм	$\rho$ , Гц	Амплитудно-частотная характеристика $A$	$\omega/\rho$
0,95	732195	247,49	12	9,75	5,180722	1,113191
0,9	693000	243,98	11,9	9,48	4,233316	1,144238
0,85	655200	240,49	11,7	9,22	3,598649	1,176782
0,8	616500	237,17	11,58	8,94	3,119788	1,213155
0,75	577800	233,5	11,4	8,66	2,753401	1,253124
0,7	539100	229,5	11,2	8,36	2,464027	1,297323
0,65	500400	224,6	10,96	8,06	2,229692	1,346555
0,6	462420	221	10,78	7,75	2,039354	1,400763
0,55	423900	216	10,5	7,42	1,876857	1,463023
0,5	385200	208,2	10,1	7,07	1,737746	1,534757

Источники: выполнено Д. Кбейли

Table 1

Results of numerical modeling

% $K_1$	Stiffness of vibration isolators $K_1$ , kN/m	Shear force at the base $S$ , kN	Displacement of the top of the structure $\Delta_{top}$ , mm	$\rho$ , GHz	Amplitude frequency response $A$	$\omega/\rho$
0.95	732195	247.49	12	9.75	5.180722	1.113191
0.9	693000	243.98	11.9	9.48	4.233316	1.144238
0.85	655200	240.49	11.7	9.22	3.598649	1.176782
0.8	616500	237.17	11.58	8.94	3.119788	1.213155
0.75	577800	233.5	11.4	8.66	2.753401	1.253124
0.7	539100	229.5	11.2	8.36	2.464027	1.297323
0.65	500400	224.6	10.96	8.06	2.229692	1.346555
0.6	462420	221	10.78	7.75	2.039354	1.400763
0.55	423900	216	10.5	7.42	1.876857	1.463023
0.5	385200	208.2	10.1	7.07	1.737746	1.534757

Source: made by J. Qbaily

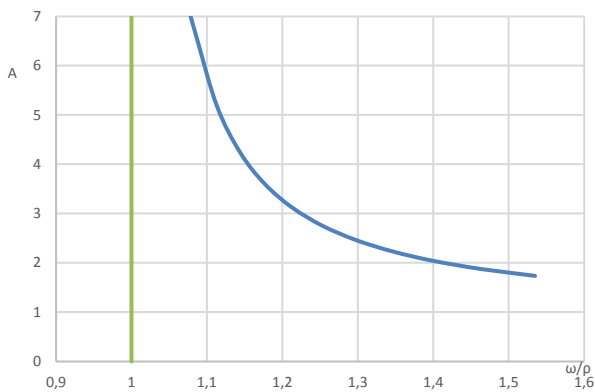


Рис. 13. Амплитудно-частотная характеристика

Источники: выполнено Д. Кбейли

Figure 13. Amplitude-frequency response

Source: made by J. Qbaily

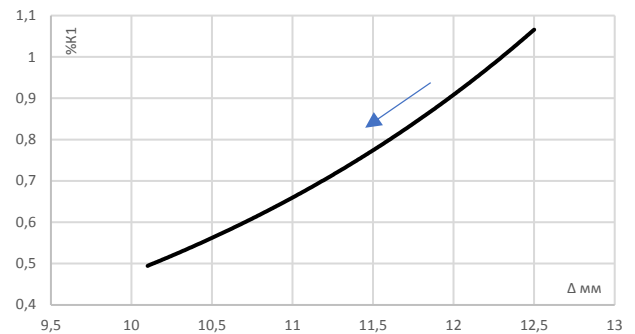


Рис. 14. Отношение поперечной силы в основании с жесткостью виброизоляторов

Источники: выполнено Д. Кбейли

Figure 14. The ration of base shear force to the Stiffness of vibration isolators

Source: made by J. Qbaily

Изменения частот и периодов здания при изменении жесткости виброизоляторов:

$$K = 0,95K_1;$$

$$T = \begin{pmatrix} 0,102 \\ 0,247 \\ 3,288 \end{pmatrix} \text{ (с);} \quad \omega = \begin{pmatrix} 9,75 \\ 4,053 \\ 0,304 \end{pmatrix} \text{ (Гц);}$$

$$K = \begin{bmatrix} 189360,448 & -108900,678 & 15915,119 \\ -108900,678 & 131889,184 & -50397,878 \\ 15915,119 & -50397,878 & 37135,2793 \end{bmatrix};$$

$$K = 0,85K_1;$$

$$T = \begin{pmatrix} 0,108 \\ 0,25 \\ 3,471 \end{pmatrix} \text{ (с);} \quad \omega = \begin{pmatrix} 9,22 \\ 4 \\ 0,288 \end{pmatrix} \text{ (Гц);}$$

$$K = \begin{bmatrix} 59514,092 & -77177,317 & 18489,505 \\ -77177,317 & 153907,564 & -76929,832 \\ 18489,505 & -76929,832 & 58462,282 \end{bmatrix};$$

$$K = 0,7K_1;$$

$$T = \begin{pmatrix} 0,119 \\ 0,247 \\ 3,818 \end{pmatrix} \text{ (с);} \quad \omega = \begin{pmatrix} 8,36 \\ 4,05 \\ 0,261 \end{pmatrix} \text{ (Гц);}$$

$$K = \begin{bmatrix} 63070,908 & -81997,426 & 19650,426 \\ -81997,426 & 1460221,439 & -78444,333 \\ 19650,426 & -78444,333 & 58825,381 \end{bmatrix};$$

$$K = 0,5K_1;$$

$$T = \begin{pmatrix} 0,141 \\ 0,248 \\ 4,658 \end{pmatrix} \text{ (с);} \quad \omega = \begin{pmatrix} 7,07 \\ 4,03 \\ 0,214 \end{pmatrix} \text{ (Гц);}$$

$$K = \begin{bmatrix} 62747,122 & -81898,883 & 19636,348 \\ -81898,883 & 160191,447 & -78440,048 \\ 19636,348 & -78440,048 & 58824,769 \end{bmatrix}.$$

Результаты расчета, когда система виброизоляторов выключена, отображены в табл. 2.

**Результаты численного моделирования при выключении системы виброизоляторов**  
**The results of numerical modeling studies when the vibration isolator system is turned off**

$\% K_1$	Поперечная сила в основании $S$ , кН / Shear force at the base $S$ , kN	Перемещение верха сооружения $\Delta_{top}$ , мм / Displacement of the top of the structure $\Delta_{top}$ , mm
Без связи / Without connection	420	24,68

Источник: выполнено Д. Кбейли  
Source: made by J. Qbaily

Отключение или разрушение дополнительных связей в процессе колебаний могут вызвать значительные изменения динамических свойств здания и, как следствие, изменения значений и распределения сейсмических сил.

Включающиеся связи могут уменьшать перемещение до 40 % и поперечную силу в основании до 49 % при значении жесткости 50 %  $K_1$ .

### 5. Заключение

1. Разработан алгоритм расчета виброизолирующей системы с учетом изменения динамических характеристик конструкции (матрицы жесткости или податливости), собственных частот и форм колебаний во время колебаний.

2. Полученные зависимости и алгоритмы основаны на оценке отключения или разрушения дополнительных связей (элементы с нелинейными характеристиками) при определении сейсмических сил и перемещений сооружений при сейсмическом воздействии.

3. Рассмотрена виброизолированная система здания с нелинейными характеристиками при кинематическом воздействии. Результаты расчета показали, что амплитудно-частотная характеристика снизилась на 30 %, поперечная сила в основании снизилась на 49 % при значении жесткости виброизоляторов 50 %  $K_1$ .

### References / Список литературы

- Chernov Yu.T. *Vibrations of building structures*. 2nd ed. Moscow: ACB Publ.; 2011. (In Russ.) EDN: QNPJJR  
Чернов Ю.Т. Вибрации строительных конструкций. 2-е изд. М.: Изд-во АСВ, 2011. 384 с. EDN: QNPJJR
- Moroni M., Sarrazin M., Soto P. Behavior of instrumented base-isolated structures during the 27 February 2010 Chile Earthquake. *Earthquake Spectra*. 2012;28(1):407–427. <https://doi.org/10.1193/1.4000041>
- Nimmy T., Sruthy S., Mini K.M. Vibration isolation at the level of footing using modified concrete. *Materials Today: Proceedings. International Conference AMMA 2018, India*, 2020;24(2):1090–1099. <https://doi.org/10.1016/j.matpr.2020.04.422>
- Astroza R., Conte J.P., Restrepo J.I., Ebrahimian H., Hutchinson T. Seismic response analysis and modal identification of a full-scale five-story base-isolated building tested on the NEES@UCSD shake table. *Engineering Structures*. 2021; 238(9):112087. <https://doi.org/10.1016/j.engstruct.2021.112087>
- Burtseva J.A., Tkachev A.N., Chipko S.A. Roller seismic impact oscillation neutralization system for high-rise buildings. *Procedia Engineering*. 2015;129:259–265. <https://doi.org/10.1016/j.proeng.2015.12.046>
- Dhanya J.S., Boominathan A., Banerjee S. Response of low-rise building with geotechnical seismic isolation system. *Soil Dynamics and Earthquake Engineering*. 2020;136:106187. <https://doi.org/10.1016/j.soildyn.2020.106187>
- Chernov Yu.T., Qbaily J. Accounting for horizontal torsional vibrations of foundations when calculating seismic load. *Bulletin of the Scientific Research Center "Construction"*. 2021;31(4):66–78. (In Russ.) [https://doi.org/10.37538/2224-9494-2021-4\(31\)-66-78](https://doi.org/10.37538/2224-9494-2021-4(31)-66-78)  
Чернов Ю.Т., Кбейли Д. Учет горизонтально-вращательных колебаний фундаментов при вычислении сейсмических сил // Вестник НИЦ «Строительство». 2021. Т. 31. № 4. С. 66–78. [https://doi.org/10.37538/2224-9494-2021-4\(31\)-66-78](https://doi.org/10.37538/2224-9494-2021-4(31)-66-78)
- Chernov Yu.T., Qbaily J. Evaluation of seismic forces under modified structural schemes in the process of vibrations. *Structural Mechanics of Engineering Constructions and Buildings*. 2021;17(4):391–403. (In Russ.) <http://doi.org/10.22363/1815-5235-2021-17-4-391-40>

Чернов Ю.Т., Кбейли Д. Оценка сейсмических сил при измененных в процессе колебаний конструктивных схемах // Строительная механика инженерных конструкций и сооружений. 2021. Т. 17. № 4. С. 391–403. <https://doi.org/10.22363/1815-5235-2021-17-4-391-403>

9. Qbaily J., Jazzan M., Chernov Y., Markovich A.S. Evaluation of the Changes in the Structure's Dynamic Properties on the Seismic Forces During the Vibration Process. *Proceedings of the International conference on engineering research (ICER 2021), Moscow, Russia*. 2022;2559(1):050015. <https://doi.org/10.1063/5.0099028>

10. Moroni M., Sarrazin M., Soto P. Behavior of instrumented base-isolated structures during the 27 February 2010 Chile Earthquake. *Earthquake Spectra*. 2012;28(1):407–427. <https://doi.org/10.1193/1.4000041>

11. Celebi M. Successful performance of a base-isolated hospital building during the 17 January 1994 Northridge earthquake. *Structural Design of Tall Buildings*. 1996;5(2):95–109 [https://doi.org/10.1002/\(SICI\)1099-1794\(199606\)5:2<95::AID-TAL71>3.0.CO;2-7](https://doi.org/10.1002/(SICI)1099-1794(199606)5:2<95::AID-TAL71>3.0.CO;2-7)

12. Burtseva O., Chipko S., Abuladze N. Passiv system of high-rise building vibrocompensation. *Earthquake engineering. Constructions safety*. 2017;(5):59–63. (In Russ.) EDN: ZWOONL

Бурцева О.А., Чипко С.А., Абуладзе Н.Р. Пассивная система виброкомпенсации высотного сооружения // Сейсмостойкое строительство. Безопасность сооружений. 2017. № 5. С. 59–63. EDN: ZWOONL

13. Kasai K., Mita A., Kitamura H., Matsuda K., Morgan T.A., Taylor A.W. Performance of seismic protection technologies during the 2011 Tohoku-Oki Earthquake. *Earthquake Spectra*. 2013;29(1):265–293. <https://doi.org/10.1193/1.4000131>

14. Boominathan A. Innovative Geotechnical Solutions for Base Isolation of Buildings. *Indian Geotechnical Journal*. 2014;54:3–39. <https://doi.org/10.1007/s40098-023-00771-y>

15. Chernov Yu.T., Qbaily J.A. The analysis of a structure subjected to seismic action, taking into account the change in the structure's design in the vibration process. *Earthquake engineering. Constructions safety*. 2020;(3):19–30. (In Russ.) <https://doi.org/10.37153/2618-9283-2020-3-19-30>

Чернов Ю.Т., Кбейли Д.А. К расчету конструкций на сейсмические воздействия с учетом изменений конструктивной схемы в процессе колебаний // Сейсмостойкое строительство. Безопасность сооружений. 2020. № 3. С. 19–30. <https://doi.org/10.37153/2618-9283-2020-3-19-30>

